

Experimental Design for Three Vibration Experiments

A Project Presented to
The Faculty of the Department of Aerospace Engineering
San José State University

In Partial Fulfillment of the Requirements for the Degree
Master of Engineering in Aerospace Engineering

By
Rahul Sharma
December 2021

Approved by
Dr. Maria Chierichetti
Faculty Advisor



San José State
UNIVERSITY

© 2021
Rahul Sharma
ALL RIGHTS RESERVED

ABSTRACT

Experimental Design for Three Vibration Experiments

Rahul Sharma

This paper details the design of three vibration experiments. These experiments are all designed to be added into a course curriculum of a vibrations class. The three experiments covered are conducting a drop calibration experiment, finding the frequencies and modes of a beam, and building a vibration absorber. The drop calibration experiment involves mounting an accelerometer inside an apparatus to conduct the drop. The beam experiment involves mounting several accelerometers on a beam and striking the beam with an impact hammer. The vibration absorber experiment involves creating a system of two masses attached to each other by a spring. Then that system is mounted to an apparatus where the vibration of the system can be observed visually. Each experiment has a detailed procedure and error analysis so that they can be replicated fairly easily. The results of research papers covering similar experiments are also provided to give context for how reasonable the results of the experiments covered in the paper are. The tools and design choices for each experiment are covered in detail, and the results of each experiment are provided.

ACKNOWLEDGEMENTS

I would like to thank my family and friends for their unwavering belief in me and their continuous encouragement. I would especially like to thank my advisor, Dr. Chierichetti for her mentorship over the course of this project.

TABLE OF CONTENTS

1.0 Introduction and Literature Review	1
1.1 Introduction	1
1.2 Literature Review	2
1.2.1 Importance of Experiments	2
1.2.2 Experimental Design.....	3
1.2.3 Vibration Experiments	6
1.3 Project Objective	9
1.4 Methodology.....	10
2.0 Equipment and Experiment Description	11
2.1 Equipment.....	11
2.1.1 Acquisition System	11
2.1.2 Actuators	12
2.1.3 Sensors	16
2.1.4 Other Important Equipment	23
2.2 Signal Processing.....	24
3.0 Drop Calibration Experiment	28
3.1 Calibration	28
3.2 Drop Calibration Experiments	34
3.3 Design of Drop Calibration Experiment.....	37
3.3.1 Procedure	37
3.4 Results	40
3.5 Error.....	41
4.0 Determining Frequencies and Modes of a Beam	42
4.1 Modal Testing	42

4.2 Modal Testing Experiments.....	44
4.3 Design of Modal Testing of Beam Experiment.....	46
4.3.1 Procedure	46
4.4 Results	47
4.5 Error.....	60
5.0 Building a Vibration Absorber.....	62
5.1 Vibration Absorber	62
5.2 Vibration Absorber Designs	63
5.3 Procedure.....	65
5.4 Results	67
5.5 Error.....	69
6.0 Conclusion.....	70
6.1 Summary.....	70
6.2 Future Work.....	70
6.3 Lab Guidelines and Procedure.....	71
6.3.1 Drop Calibration	71
6.3.2 Obtaining Frequencies and Modes of a Beam Experimentally	72
6.3.3 Building a Vibration Absorber.....	73
References	75

TABLE OF FIGURES

Figure 1.1: Schematic of accelerometer drop calibration experiment [2].....	4
Figure 1.2: Experimental setup with steel cantilever beam [4].....	5
Figure 1.3: Experimental setup of vibration absorber [3].....	6
Figure 1.4: Sample schematic of a vibration test experiment [12, pp. 619]	7
Figure 2.1: Hardware schematic of a data acquisition system [12, pp. 587].....	12
Figure 2.2: Schematic of a shaker [25]	12
Figure 2.3: Schematic of an electromagnetic shaker [26].....	13
Figure 2.4: Schematic of impact hammer [27]	14
Figure 2.5: Schematic of a speaker-driven actuator [28].....	15
Figure 2.6: Stack actuator [29].....	15
Figure 2.7: Stripe actuator [29].....	16
Figure 2.8: Schematic of piezoelectric accelerometer [30].....	17
Figure 2.9: Schematic of a strain gauge [31]	17
Figure 2.10: Circuit diagram of Wheatstone bridge circuit [31].....	18
Figure 2.11: Rosette strain gauge schematic [33]	18
Figure 2.12: Circuit diagram of quarter-bridge circuit [34].....	19
Figure 2.13: Circuit diagram of half-bridge circuit [34].....	19
Figure 2.14: Circuit diagram of full-bridge circuit [34].....	19
Figure 2.15: Schematic of a strain gauge load cell [36].....	20
Figure 2.16: DIC example image [38]	21
Figure 2.17: Image of 1-D laser-scanning vibrometer [41]	22
Figure 2.18: Image and schematic of 3-D laser-scanning vibrometer [42].....	23
Figure 2.19: Time signal and respective Fourier spectrum and digital record [12, pp. 593]	25
Figure 2.20: Leakage example [12, pp. 596]	27
Figure 2.21: The effect of a window function on leakage [12, pp. 596].....	27
Figure 3.1: Inversion calibration [46].....	29
Figure 3.2: Graph of inversion calibration [46]	29
Figure 3.3: Accelerometers and anvil setup [47]	30
Figure 3.4: Full calibration setup [47]	30
Figure 3.5: Output signal comparison [47]	31
Figure 3.6: Setup of shakers [47].....	32
Figure 3.7: Frequency response of an accelerometer [47]	32
Figure 3.8: Air bearing shaker [47].....	33
Figure 3.9: Setup of a drop calibration test [46]	34
Figure 3.10: Signal of accelerometer during free fall [46].....	34
Figure 3.11: Results of first setup drop calibration [2]	36
Figure 3.12: Top (left), front (center), and isometric (right) views of metal frame	37
Figure 3.13: Top (left), front (center), and isometric (right) views of metal plate and springs	38
Figure 3.14: Bottom (left), front (center), and isometric (right) views of completed experimental setup	38
Figure 3.15: Drop calibration final setup.....	39
Figure 3.16: Time vs signal graph after drop.....	40
Figure 3.17: Free-fall portion of graph	41

Figure 4.1: General setup of a modal testing experiment [48].....	42
Figure 4.2: Different shaker placement in modal testing [48]	43
Figure 4.3: Impact hammer modal testing [48].....	44
Figure 4.4: Experimental setup with steel cantilever beam [4].....	45
Figure 4.5: Accelerometer results, top left: impact at node 3, top right: impact at node 6, bottom: impact at node 10 [4]	46
Figure 4.6: Example of setup of beam with marked nodes [4]	47
Figure 4.7: First vertical bending mode.....	48
Figure 4.8: Second vertical bending mode	48
Figure 4.9: First axial bending mode	48
Figure 4.10: Third vertical bending mode	48
Figure 4.11: First torsional mode.....	49
Figure 4.12: Fourth vertical bending mode.....	49
Figure 4.13: Graphs of accelerometer 1; Strike at node 4 (top), strike at node 7 (center), strike at node 11 (bottom).....	50
Figure 4.14: Graphs of accelerometer 2; Strike at node 4 (top), strike at node 7 (center), strike at node 11 (bottom).....	51
Figure 4.15: Graphs of accelerometer 3; Strike at node 4 (top), strike at node 7 (center), strike at node 11 (bottom).....	52
Figure 4.16: Frequency vs acceleration graphs of accelerometer 1; Strike at node 4 (top),strike at node 7 (center), strike at node 11 (bottom).....	54
Figure 4.17: Frequency vs acceleration graphs of accelerometer 2; Strike at node 4 (top),strike at node 7 (center), strike at node 11 (bottom).....	55
Figure 4.18: Frequency vs acceleration graphs of accelerometer 3; Strike at node 4 (top),strike at node 7 (center), strike at node 11 (bottom).....	56
Figure 4.19: Modal shape at first vertical bending mode	57
Figure 4.20: Modal shape at second vertical bending mode.....	58
Figure 4.21: Modal shape at third vertical bending mode	59
Figure 4.22: Modal shape at torsional mode.....	59
Figure 4.23: Modal shape at fourth vertical bending mode	60
Figure 5.1: System without vibration absorber (top), System with vibration absorber (bottom)..	63
Figure 5.2: Taipei 101 vibration absorber [49]	63
Figure 5.3: Power line vibration absorber [49].....	64
Figure 5.4: Experimental setup of vibration absorber [3]	65
Figure 5.5: Front (left), and two isometric (center, right) views of completed experimental setup	66
Figure 5.6: Vibration absorber experiment final setup	67
Figure 5.7: Acceleration of primary mass before vibration absorber	68
Figure 5.8: Acceleration of primary mass with vibration absorber	68
Figure 5.9: Acceleration of vibration absorber	69

TABLE OF TABLES

Table 4.1: Theoretical vs experimental natural frequency comparison	53
Table 4.2: Distance from fixed end vs acceleration at first vertical bending mode.....	57
Table 4.3: Distance from fixed end vs acceleration at second vertical bending mode	58
Table 4.4: Distance from fixed end vs acceleration at third vertical bending mode.....	58
Table 4.5: Distance from fixed end vs acceleration at torsional mode	59
Table 4.6: Distance from fixed end vs acceleration at fourth vertical bending mode	60

SYMBOLS

Symbol	Definition	Units
N	Number of Samples	
T	Time Period	s
a_0	Digital Spectral Coefficient	
a_i	Digital Spectral Coefficient	
b_i	Digital Spectral Coefficient	
C	Matrix of Coefficients	
a	Vector of Spectral Coefficients	
x	Vector of Digital Records	
S	Sensitivity	mV/m/s ²
V_{peak}	Peak Voltage	mV
g	Acceleration Due to Gravity of Earth	m/s ²
a_1	Acceleration	m/s ²
a_{ref}	Reference Acceleration (1e-6)	m/s ²
dB	Decibels	dB
R	Resistance	Ohms (Ω)
m	Mass of Primary Mass	kg
m_a	Mass of Vibration Absorber	kg
SUT	Sensor Under Test	

1.0 Introduction and Literature Review

1.1 Introduction

Due to the Covid-19 pandemic, labs have been closed at SJSU for the last year. When campus begins to open again, and the school begins to operate like normal, it is important that students have new experiments to complete. Experiments are vital for students to do as it helps supplement the theoretical aspect of their learning and helps them apply skills that they have developed in real world situations.

Experiments are defined as a procedure designed to test a hypothesis or demonstrate a known fact. Therefore, experiments are the ultimate way of testing one's technical knowledge. In classrooms, most knowledge is passed on in a theoretical way, however in engineering this is not enough as students must be taught to apply this knowledge in a practical sense. The best way one can accomplish this is to supplement classroom learning with experiments in the lab.

There are several different types of experiments that one can do in the field of vibrations. The goal of this project is to design and build the following experiments:

- I. Calibrating Accelerometers using Drop Calibration
- II. Measuring Frequencies and Modes of a Beam
- III. Building a Vibration Absorber

Some important sensors that students will be introduced to in these experiments are strain gauges, accelerometers, and load cells. Strain gauges measure strain on a structure [1]. This gauge works because its electrical resistance varies when force is applied to it, therefore it is good at measuring the stress and strain on a structure. Accelerometers measure the acceleration of an object [2], as such they can be used to measure the dynamic response at different points in a structure and be used to identify how a structure moves when vibrations are imposed on it. Finally, load cells measure mechanical force and convert it into a measurable electrical output. As a result, they are extremely good at measuring the weight of an object. All these sensors are important to use in testing vibrations and will give students a better understanding of how structures vibrate in the real world.

Some tools that students will use include actuators, such as a shaker and an impact hammer. Actuators are tools that are used to impose vibrations on a structure. Shakers are a very common actuator used in several forms of testing including aircraft and spacecraft vibration testing. They are used to shake structures which then cause the structures to vibrate [3]. An impact hammer is an actuator that is being used more recently due to it being easier to use than a shaker. It is a hammer with a force sensor built into its head which is used to strike a structure and impose vibration on it [4].

1.2 Literature Review

1.2.1 Importance of Experiments

In today's day and age, a big aspect of education deals with theoretical learning. Theoretical learning is vital in order for students to be successful in abstract thinking. It helps students develop a non-rigid mindset for applying their learning, and how to apply their skills to solve various problems. It also provides a strong base for students to be able to apply their knowledge later in life. However, recent studies have shown that problem-solving skills in humans are generally stronger than theoretically optimum problem-solving methodology [5]. In other words, humans will perform better once they are given a chance to actually solve a problem as opposed to when they are simply taught how to solve a problem. Giving students a chance to actually implement the theory they have learned is vital because it will give them a chance to truly apply methodology that they have learned and add new wrinkles to it as well.

Moreover, it is also important to not just give students demonstrations of experiments, as even though this can help them further understand the theory, it prevents them from being able to draw their own conclusions [6]. This in turn prevents students from understanding the variations between theory and what happens in the real world. They begin to idealize theory, instead of realizing that in some cases there are limits to the theory they were presented with. Allowing students to conduct experiments by themselves with limited supervision gives them a chance to explore the theory they have learned and see where its limits lie [6]. It also gives students a chance to be creative by letting them use several different methods to reach a conclusion. Well-designed experiments should be able to change students' understanding of theory, rather than simply enhance it.

Another key reason that experimentation is important in education is that it helps increase student involvement in a classroom [7]. A major downside to theoretical learning is that a student has very little to do while being taught. All they can do is listen and take notes. This can lead to students being disinterested and unengaged during class time. Adding experiments to a curriculum can change this, as students have to be actively involved in the process of learning. Experiments are also useful in active involvement after they are completed. If students are asked to critically analyze their past experiments and determine one thing they would change in it, they will be forced to use problem solving skills which will help reinforce their knowledge around the subject in which the experiment is being conducted. Experiments also help students feel more passionate about the subject they are learning [8]. This passion will not only help students stay more involved during class time but will also help them in the future if they choose to work in the same field. Having experiments that are focused on topics that many students may be familiar with already can also help students appreciate the learning more, which in turn will help involvement.

Experiments are also important as they give insight into real world situations [9]. It is very important to introduce real world situations into learning because it helps students understand that what they are learning is not an abstract concept, but a key part of their field and something that impacts their life. Experiments that tie into real world situations also help students develop skills that are directly translatable to industry work, as they will have to deal with specific problem solving techniques, tools, and software. This helps set students up for the

future as they have less to learn in the transition from school to the industry.

A particularly relevant reason that experiments are important in the current world is the fact that hands-on learning has been at a standstill due to the pandemic. Currently the education gap worldwide is being widened due to remote learning [10]. Not every student has the same access to the technology they need to attend classes. Another issue is that some students need more outside help than the current online learning format can provide. These gaps can be felt even more in fields such as engineering, where labs and other forms of hands-on are an important part of learning. These forms of instruction have been halted completely so students who do not have access to machines or lab equipment at home are being left behind. However, with the vaccine rollout and reduction of nationwide cases in the United States, labs will soon begin to open once more. As a result of this it is more important than ever to design experiments that net the maximum amount of involvement, creativity, and real world application to get students caught up with the hands-on learning that they have been missing. Experiments are vital in helping students develop key problem solving skills that will prepare them for the future, therefore, it is vital that the experiments be designed in a way that even students who have never worked with any machines or tools before can complete them and learn from them.

1.2.2 Experimental Design

In order for an experiment to help facilitate student learning it must be designed correctly. Without proper experiment design the experiment as a whole will be useless to the student.

Experimental design is an important part of an experiment as without it the result is meaningless [11]. The experiment must be planned a certain way so that the result provided is interesting and meaningful. The most important step of proper experimental design is to set an aim or end goal for the experiment. Defining the aim of the experiment is made easier by identifying the important variables in an experiment. To identify these variables, one must first note the knowns and unknowns of the system on which the experiment is being conducted. From this information independent and dependent variables can be defined. Analyzing the knowns and unknowns of the system also helps to determine which responses can and should be measured. Once this information is determined one can set an aim for the experiment. The aim should be an overarching question that every step of the experiment works towards answering. Without an aim the experiment would be disjointed, and its steps would be muddled. It would lead to several results that have no value, thus making it difficult to decipher which result is actually meaningful. After determining the aim of the experiment, it is necessary to screen the variables. Not all variables are actually meaningful to the experiment, some have no value at all. It is important to identify and disregard these variables before beginning the experiment. Finally, it is also necessary to optimize the experiment. The goal of proper experimental design is to obtain the maximum number of valuable information with the minimum number of necessary steps. To accomplish this each step of the procedure must be reviewed to ensure that each step is relevant.

In this paper there are three experiments that will be designed, as discussed previously in the introduction section. Each experiment will need to be meticulously designed to provide interesting and relevant results.

The first experiment that will be designed in this project involves drop calibration of

accelerometers. Drop calibration is a process that involves dropping an accelerometer from a high place so that it undergoes free fall in Earth’s gravity. This helps determine the sensitivity of the accelerometers as it is known that at free fall the acceleration due to gravity from the Earth is 9.81 m/s^2 . Calibration of accelerometers, and of sensors in general, is important as it helps determine the sensitivity of the instrument, so the readings taken from it make sense, and it also helps ensure that the sensor is working properly. An article by Krelle [2] discusses using drop calibration to calibrate accelerometers. There are two different kinds of accelerometers: piezoelectric and piezoresistive. Piezoelectric accelerometers use a piezoelectric component, such as a quartz crystal, which produces an electric charge when force is applied to it, while piezoresistive accelerometers use piezoresistive components, such as a silicon resistor, which change their electrical resistivity when a force is applied to them. In drop calibration, the accelerometers are attached to drop weights. The data recorded from the drops is recorded and graphed. After the completion of all the drops, the data is used to determine the sensitivity of the accelerometers. In this experiment there are several sources of possible error. The primary source of error in this experiment is the accelerometer itself. There is uncertainty in the standard of the accelerometer, which can lead to significant error in the measurements taken from it. Other sources of error include the uncertainty of voltage measurements and the signal amplifier that was used. A schematic of the setup of this experiment is provided in Figure 1.1.

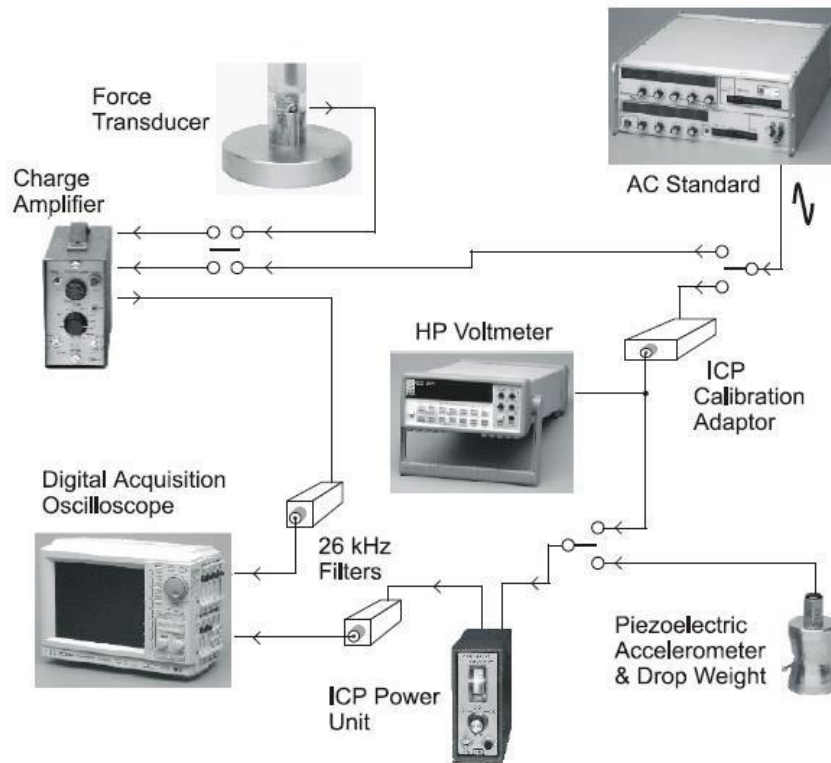


Figure 1.1: Schematic of accelerometer drop calibration experiment [2]

The second experiment focuses on modal analysis of a beam, in which frequencies and modes are measured using an impact hammer excitation. It is important to be able to determine the frequencies and mode shapes of structures through experimentation. If frequencies and mode shapes are determined solely through theory, it is not enough because there can be flaws in the

material or design of the structure. It is necessary to verify the theoretical frequencies and mode shapes through experimentation because experimentation provides a more accurate look at the true frequencies and mode shapes of the structure. Mao et al. [4] discuss a possible experimental design to measure the frequencies of a beam. The experiment was done using a steel cantilever beam, an impact hammer, and accelerometers. The beam was 88.5 cm in length, with a cross section of 7.5 cm in width and 1.2 cm in height. The steel beam was first clamped on one side, while the other side was left free. The beam was then divided into 11 elements and the 12 nodes were marked down, 0 being the mode at the fixed side and 11 being the node at the free end. Accelerometers were then attached to nodes 5, 9, and 11 to measure the acceleration signals of the beam. The impact hammer was then used to strike the beam first at node 3, then at node 6, and finally at node 10. The results from the accelerometers at nodes 5, 9, and 11 were then analyzed from each test and used to determine the mode shapes and frequencies of the beam. Possible sources of error in this experiment include uncalibrated accelerometers, improper labeling of nodes, and human error in striking the nodes. All of these errors can lead to improper readings taken, which can impact the final measurements of the frequencies. Figure 1.2 shows the experimental setup of the test where node 10 was struck with an impact hammer. The black boxes represent the accelerometers, and the arrow represents the spot where the impact hammer was used to strike the beam.

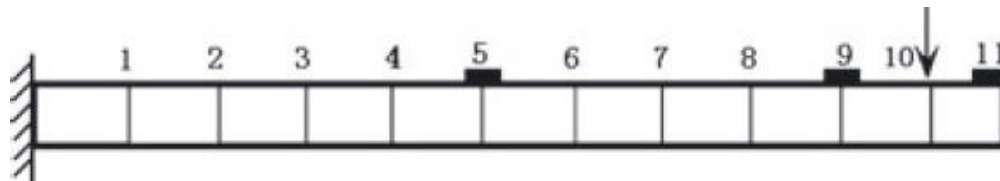


Figure 1.2: Experimental setup with steel cantilever beam [4]

The third experiment discussed in the paper is building a vibration absorber. A vibration absorber is a device that is attached to a main body to prevent that body from vibrating. Rather, the vibration absorber absorbs the vibration from the main body and vibrates instead of it. Vibration absorbers are a key part of many vehicles and buildings. They are used in buildings to prevent structural damage from large amounts of vibrations caused by large gusts of wind, and they are used in vehicles to prevent shaking from affecting passengers. As a result of the many applications of a vibration absorber, it is important for students to learn how they work through the process of building one. An article by Bobrovnikii et al. [3] discusses an experiment in which a mass is used as a vibration absorber. The experiment is done using two masses, a shaker, accelerometers, and a force sensor. The two masses and the shaker were placed on a rubber gasket. Accelerometers were attached to each mass, and a force sensor was attached to the second mass. The masses were then connected in tandem, and the second mass was made to act like a vibration absorber. The first mass was then excited by the shaker, and the accelerometers and force sensor were then used to see how efficient the second mass was at being a vibration absorber. In this experiment the biggest source of error is the potential human error in incorrectly designing the absorber. Another source of error is incorrectly calibrating the sensors. This can lead to inaccurate readings. Figure 1.3 shows a diagram of the experimental setup of the vibration absorber. 1 is referring to the oscillatory system with its source, 2 is referring to the absorber, 3 is referring to the rubber

gaskets, 4 is the shaker, 5 is the accelerometers, and 6 is the force sensor.

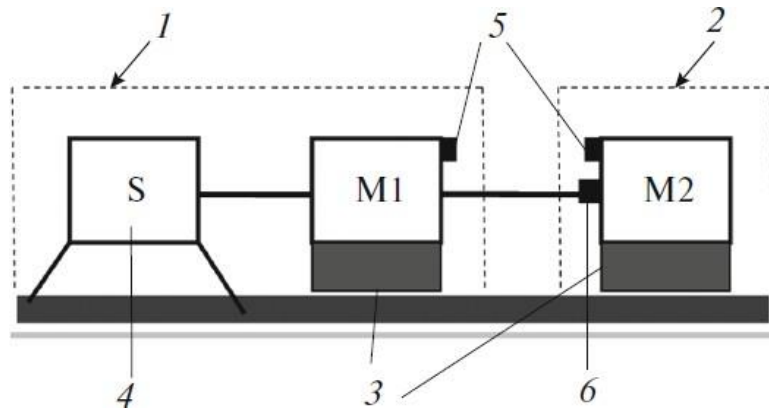


Figure 1.3: Experimental setup of vibration absorber [3]

These experiments serve as good guides to proper experimental design. The articles discussed will be used later in this paper to design the experiments discussed in the introduction section of this paper.

1.2.3 Vibration Experiments

The field of vibrations is a very broad field, experiments involving vibration suppression, and vibrational testing both fit into this field.

Vibration suppression experiments are founded on the principle that any structure will undergo vibration and these vibrations need to be suppressed [12, pp. 448]. Vibration can lead to several undesirable circumstances, for example unsuppressed vibration can cause discomfort to car drivers and leave them sore and tired, or it can also cause cracks and other structural compromise in skyscrapers. Two ways to ensure that the vibration in a system does not go above acceptable levels of vibration are to use vibration isolation or to use a vibration absorber. Vibration isolation involves isolating the part of the system that is dealing with intense vibrations from the rest of the system [12, pp. 454]. The other way to reduce vibration on a body is by using a vibration absorber, which has been previously discussed. Experiments involving suppression are necessary, as different systems require different methods of vibration suppression. Without intensive experiments on each system, it is impossible to determine which method will work for the system. Oftentimes, it is necessary to use multiple methods of vibration suppression on one system. For example, in an airplane it would be necessary to use vibration isolation to reduce vibrations within the engines, but vibration absorbers would be needed to prevent vibrations from damaging the wings or body of the airplane. Without undergoing extensive experimentation, one cannot be sure if vibrations will not damage a system, therefore vibration suppression experiments are necessary.

In experiments dealing with vibration testing more often than not the experiment will involve modal analysis, because frequencies and mode shapes of the structure being tested will need to be calculated. These types of experiments are important because they help determine frequencies, modal shapes, and damping ratios [12, pp. 586]. Many tools are required to do an

experimental modal analysis of a structure. The most common tools used to impose vibrations on a system are an impact hammer and a shaker. To measure the vibrations of the system a sensor is needed. A sensor converts the mechanical motion of the structure into an electrical signal. As a result, the most common sensors are made of piezoelectric crystals, which produce an electric charge when experiencing strain [13]. Strain gauges, devices that measure deformations in a precise manner [1], are the most common sensor used to pick up vibrational responses. Finally, signal conditioners match and amplify signals which are then represented in the time domain. To convert these readings to the frequency domain, they are analyzed by a digital Fourier analyzer, also called a Fast Fourier Transform analyzer [12, pp. 590-591]. The Fourier Transform Analysis is a tool used to reconstruct a periodic wave with series harmonics [14]. After the signal is analyzed, it is possible to extract modal data from the signal. This data is then used to calculate modal shapes and frequencies. Vibration testing is very important in every kind of structure because mode shapes and frequencies calculated by hand need to be verified by experimentation to ensure that the model is correct and can be used in design and response prediction with confidence [12, pp. 588]. Vibration testing can also be used to determine the durability of a device [12, pp. 586]. This can be done by subjecting the device to intense vibrations for a period of time. After the vibrations have been stopped the device can be checked to see if it still performs its task. This is important because it is possible that the structure of the device can withstand intense vibrations, but the inside of the device cannot. Vibration testing can also be used in machinery diagnostics for maintenance. This is done for continuously monitoring the frequencies of a structure or machine. A shift in frequency can indicate pending problems or a need for maintenance. This is an important art of vibration testing, as eventually any structure or machine will degrade and require maintenance. Continuously monitoring the structure will help prevent any failures from occurring due to unexpected problems. Figure 4 shows an example experimental setup of a vibration test experiment.

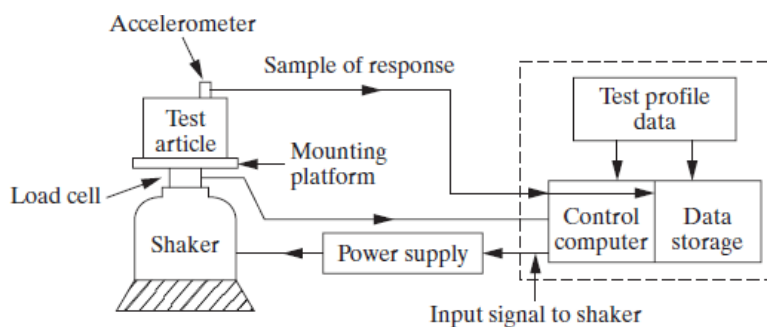


Figure 1.4: Sample schematic of a vibration test experiment [12, pp. 619]

Vibrational testing is also key to the success of aircraft and spacecraft. Testing for these distinct crafts is done in different ways.

Testing of aircraft is done through a process called Ground Vibrational Testing (GVT) [15]. This process requires the use of a phase-resonance method. To implement this method the

shaker's location and phase relation is carefully chosen to cause the aircraft to behave as a single-degree-of-freedom system. This method is then complemented by phase separation techniques which find the aircraft's modes using frequency response functions. The GVT is used primarily to obtain vibrational data of the entire aircraft to validate and improve its structural models. This process is generally done late in the aircraft development phase but is arguably the most important part of it. Testing the aircraft as a whole system before approving it is very important as this process tests for potential design flaws. If even one component of an aircraft is affected by the vibrations given to the entire system, the test is a failure, the entire structure of the aircraft needs to be restructured. Despite flaws in the GVT, it is still the safest way of testing aircraft to ensure maximum safety. A supplement to the GVT is creating a finite element model of the aircraft. This model allows for fast updating, as it condenses the model to have only a few DOF [16]. Due to the fast updating model, the parameters can be changed with relative ease to match the experimental values more appropriately. This process gives a model that can be used to predict what the results of an experiment should look like. This fast updating model is an important supplement to the GVT, as it can give accurate predictions of what the craft should look like while undergoing testing, and it also allows for additional factors to be tested that cannot always be tested at ground level. This model also allows for shorter testing times, which allows for faster rollout of safe new aircraft. Despite the key role that the GVT and a fast updating model play in the testing of aircraft, currently testing engineers are looking for new ways to revolutionize these methods. A current challenge with the GVT is its long implementation times, and the limited amount of availability of aircraft to test on. Due to a high number of configurations that need to be tested the GVT is currently too slow to keep up with deadlines at the industry level [15]. For this reason, new methods that increase testing and analysis speeds are being researched and implemented. One method that may begin to be more widely implemented in the future is the Taxi Vibration Test (TVT). This method uses natural excitation as the aircraft rolls on pavement [17]. Accelerometers are attached to the frame of the aircraft, and a data acquisition system is placed within the aircraft. This makes it so the dynamic response of aircraft can be used in an output-only modal analysis scheme to determine frequencies, mode shapes, and damping ratios of the aircraft. The TVT allows for much faster analysis and testing than the GVT does, which makes it a superior way of obtaining modal parameters on the ground. In addition to this, it can also be used in combination with a Flight Vibration Test (FVT), which makes it a more versatile process. However, there are certain issues it has yet to sort out. The biggest drawback to this method is that the landing gear shock absorbers cause deviations in damping ratio and frequency calculations. This has led to major concerns with this test because accuracy is very important in testing. Despite the method still needing more development before it can be fully implemented, it is a promising step in making aircraft testing faster.

Testing a spacecraft before a launch and testing a model of it to see how it holds up after it is inserted into space is very important. Most spacecraft can cost millions, if not billions, of dollars to launch, and only one chance is provided for the launch to be successful. If testing is not done extensively, minor structural errors can cause the loss of the spacecraft, as well as the failure of an entire mission. Spacecraft vibration testing is performed differently than aircraft testing. Two types of shakers are used to vibration test a spacecraft, stinger-drive shakers, and base-drive shakers [18]. Stinger vibration tests are conducted with the test craft in a free-free or fixed-interface configuration. These tests are mainly used to verify or update a current mathematical model. On the other hand, base vibration tests are done with a craft mounted to a

moving platform that is driven by an electro-dynamic shaker. These tests are mainly used to screen workmanship and to qualify flight hardware and launch dynamic environments. The purpose of these shaker tests is to test workmanship of the completed craft and ensure that it will survive the mission dynamics and load environments. The benefits of shaker testing include the fact that it is the only verification of the mechanical integrity of the flight subsystems. It also is the most important dynamics test, which helps prepare the spacecraft for launch. A pitfall of the shaker test is that the dynamics of the shaker and shaker head expander must be included in the finite element model or else the modal information can be misleading. It is also important to ensure that the shaker equipment is not too old, or else testing errors can occur. In addition to testing the spacecraft in a facility before its launch, it must also be tested to ensure that it can handle the vigor of space. This cannot be tested prior to launch, so models must be developed to ensure that the spacecraft will be successful in space. A way to construct a model that can predict how a spacecraft will handle vibrations imposed on it in space is by decomposing measured responses of the structure into modal coordinates [19]. This model can be applied to a free response or a forced response. It is important to build a model such as this to test what would happen should a small asteroid collide with the spacecraft, or how the spacecraft deals with vibrations from its engines.

As the space industry moves into the future, new forms of propulsion are being introduced. These propulsion systems affect the vibration of the spacecraft in different ways than traditional propulsion systems. An example of such a propulsion system is green propulsion. This propulsion system aims to offer a significant reduction in personnel hazards, shorter payload processing, and low toxicity green propellants [20]. Currently, these propulsion systems are being tested using an air cooled electrodynamic shaker. Sine vibration was used to test workmanship and to simulate launch vehicle loading conditions, and random vibration was used to test workmanship and to simulate launch vehicle aerodynamic environmental levels. Despite the differences in vibration due to the changing propulsion system and the drawbacks to shaker testing mentioned in the previous paragraph, it is still the primary way to test modern propulsion systems. This is where spacecraft vibration testing differs greatly from aircraft vibration testing. As the industry evolves, the vibration testing stays the same, whereas the aircraft industry needs to evolve the way they test as their industry progresses into the future.

1.3 Project Objective

As discussed in the introduction, the goal of this project is to design and build three experiments. The first experiment will teach students how to calibrate accelerometers using drop calibration. This involves dropping the accelerometer from a height which causes it to reach free-fall. During this period of time the acceleration of the accelerometer is known as it will be equal to the acceleration due to gravity of Earth. The second experiment deals with experimentally measuring the frequencies and modal shapes of a beam. This will be done by striking structures with an impact hammer and using the vibrations to find the frequency of the structure, as well as its mode shapes. This will help students transition from the theoretical aspect of vibration, calculating the frequencies and mode shapes of theoretical structures, to a more practical application of their knowledge. In the final experiment students will create a vibration absorber, similar to ones that are used in skyscrapers or on telephone wires. This absorber will help the main structure not vibrate, as the vibrations will be moved to the absorber.

These are not the only experiments that can be used to experiment in the field of vibrations, but they are highly applicable to real life. For example, calibrated accelerometers were used to test the dynamic response of a bridge in Islamabad, Pakistan [21]. Furthermore, vibration absorbers are used to dampen vibrations for a wide range of structures. For example, they can be used in tall buildings to reduce the swaying of the building due to wind [22], and they can also be used in airplanes to reduce cabin noise during flight [23]. Finally, performing modal analysis on a wing to determine its modes and frequencies is vital, as aircraft wings end up being slender and flexible, which in turn makes them vulnerable to vibrations [24]. As a result, modal analysis is vital to ensure there will be no problems during flight. From the aforementioned examples, it is clear that these experiments are being selected for this project because they provide students with the chance to work on experiments that have a wide range of applications to real world engineering problems.

1.4 Methodology

To achieve the goals that this project has set forth to accomplish, a strict procedure must be followed. The first step for all three experiments will be to create an experimental procedure for all three experiments. The next step in the experiment involving drop calibration of an accelerometer will be to explain why drop calibration is the correct form of calibration to use. Other forms of calibration will also be discussed, and reasons will be given for why these are not ideal in terms of this experiment. These calibration types will include shock calibration, resonance calibration, and handheld calibration. After the choice of drop calibration is properly explained the experiment will be designed and built. For the experiment involving finding the frequencies and modes of a beam the next step will be to design the experiment. Then a detailed description of the setup for the experiment will be given. This will include going in depth about why sensors are placed where they are and why the impact hammer is used. Finally, for the vibration absorber experiment the next step will be to choose a design for the experiment. This process will involve looking through many different designs of a vibration absorber and selecting one that is the easiest to recreate and will also provide the clearest results. After this, the experiment will be built. The design of the experiments will be continually modified and updated based on how well the tests go. To design each experiment so that it returns results that are relevant and interesting, the articles discussed in the literature review will be used to create a basic layout of how the experiment should work.

2.0 Equipment and Experiment Description

2.1 Equipment

To successfully perform the accelerometer calibration experiment, modal shapes, and frequencies of a beam experiment, and designing a vibration absorber experiment, it is first important to know which equipment is needed. The following section will discuss equipment utilized in vibration experiments. This equipment includes an acquisition system, actuators, sensors, signal conditioner, and cables.

2.1.1 Acquisition System

A vital part of any vibration experiment is a data acquisition system. This is a system composed of a combination between hardware and software that allows measurements of real world events and convertsthem into digital signals that can be analyzed by a computer. The basic hardware components required in an acquisition system are actuators, sensors, signal conditioning amplifiers, and an analysis system [12, pp. 587]. Actuators are a component that provides a known or controlled input force to a structure. Oftentimes a signal generator and power amplifier are also attached to an actuator. The signal generated is used to generate electronic signals with certain fixed properties, such as amplitude, frequency, and wave shape. The power amplifier is used to drive the power of an input signal higher. It is necessary for actuators that need to deliver a large amount of power, such as shakers. These components are used in tandem to sweep the excitation signal into a form that meets the requirement of the structure being tested, whether that be sinusoidal, random, or another appropriate system. A sinusoidal input consists of applying a harmonic forceof constant magnitude at multiple different frequencies in a specific range, while a random signal consists of random forces at random times. Sensors are necessary to convert the mechanical motion of a structure into an electrical signal. Signal conditioning amplifiers help to match the characteristics of the sensor to theinput electronics of the digital data acquisition system, which is important because it feeds the computer data in a form that the computer can actually analyze. The final component of a data acquisition system is an analysis system in which the modal analysis and signal processing computer programs reside. Figure 2.1 shows a schematic of a data acquisition system. In this schematic the exciter is interchangeable with actuatorand the transducer is interchangeable with sensor.

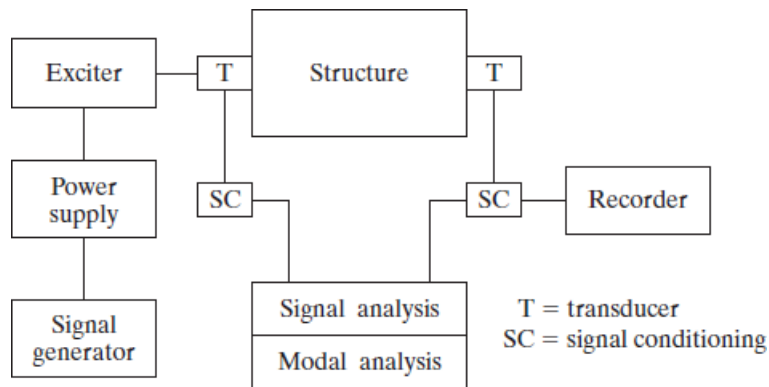


Figure 2.1: Hardware schematic of a data acquisition system [12, pp. 587]

2.1.2 Actuators

Actuators are devices that are used to send a driving force to a system to cause vibrations. There are several types of actuators that can be used. The most common types are shakers, impulse hammer, andspeakers.

Shakers are a type of actuator commonly used to vibration test structures. As discussed previously, the shaker is a device that shakes structures to impose a force on them. Figure 2.2 shows a schematic of ashaker.

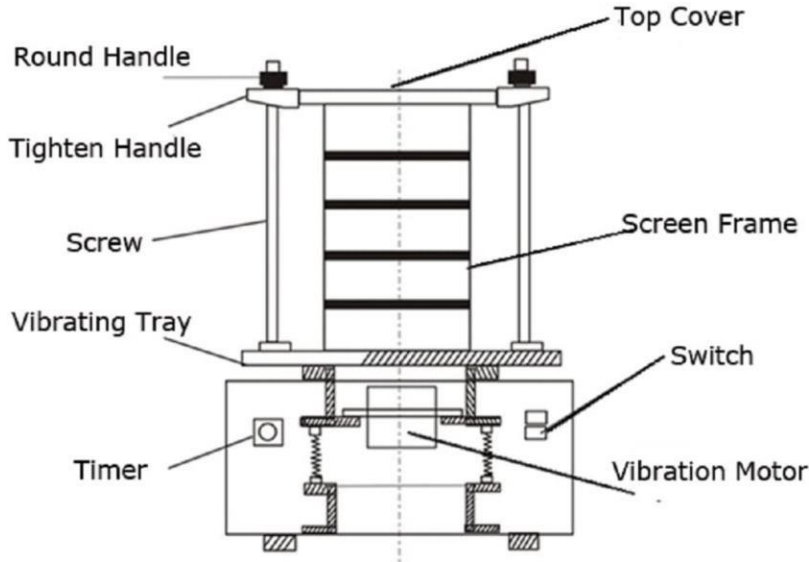


Figure 2.2: Schematic of a shaker [25]

The most commonly used shaker is the electromagnetic shaker. This shaker is a linear electric motor consisting of coils of wire surrounding a shaft in a magnetic field [12, pp. 588]. An alternating current is provided to the coil which then causes a force to be applied to the shaft, which then applies force to the structure. The electromagnetic shaker is very easily controlled through a signal generator, as it applies forceproportional to the voltage it receives. Therefore, as

a result of the signal generator's ability to provide several different input signals, a variety of different forces can be applied on the structure using the electromagnetic shaker. Figure 2.3 shows a schematic of an electromagnetic shaker. A downside to shakers is that they generally have significant mass. If proper care is not taken to separate the mass of the shaker from the test mass the apparent frequency measured will be significantly lower than the true frequency of the structure. This is a process called mass loading. To avoid mass loading a stinger can be attached to the shaker. The stinger is a short thin rod running from the driving point of the shaker to a force sensor mounted directly on the structure. This isolates the mass of the shaker from the structure, thus reducing the added mass to the structure. The stinger also serves to transmit the force axially through it, which allows for more control in the direction of the applied force. Shakers are a very versatile actuator and can be used on small structures, such as beams, or very large structures, such as spacecraft. Due to this versatility, they are the most commonly used actuator in vibration testing.

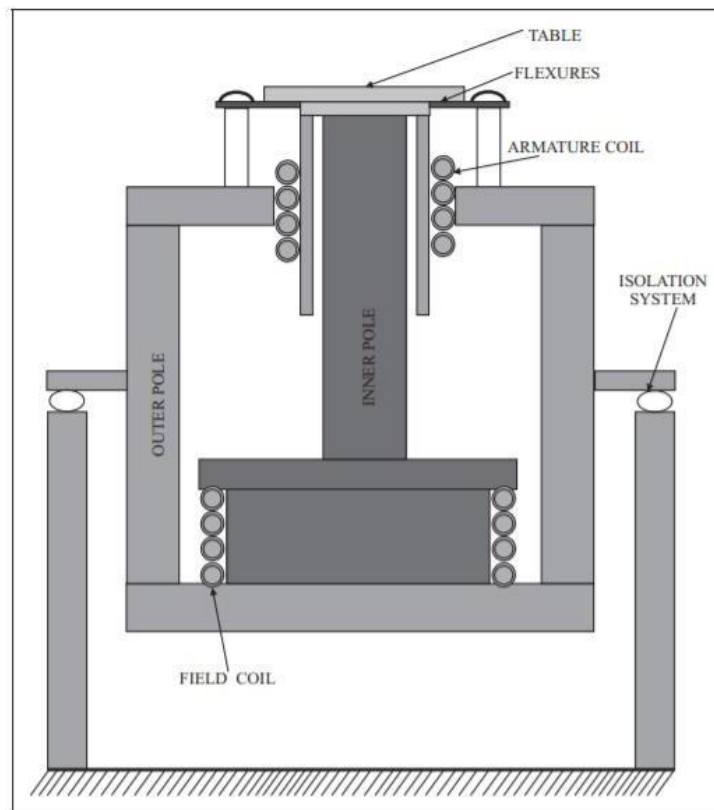


Figure 2.3: Schematic of an electromagnetic shaker [26]

Recently, an actuator known as an impact hammer has become increasingly popular. This actuator consists of a hammer with a force sensor built into its head [12, pp. 588]. Unlike the shaker it has a very simple design and simple method of use. Figure 2.4 shows a schematic of an impact hammer. To use this actuator to apply force to a system, one simply strikes the structure with it. The impulse provided by the hammer excites a broad range of frequencies in the structure. The impulse response in the structure contains excitations at each of the system's natural frequencies, and the peak impact force is nearly proportional to the hammerhead's mass and impact velocity. The force sensor in the hammerhead provides a measurement of the impact

force. The duration of the force and frequency response of the structure is based on the mass and stiffness of both the structure and hammer. If a small hammer is used on a hard structure, such as metal, the shape of the response and the highest excited frequency depend on the stiffness of the hammer tip. The heavier the hammer is and the stiffer the tip is, the lower the maximum excited frequency will be. The hammer is less effective at exciting modes above the maximum excited frequency than it is below this frequency. Some benefits of using the impact hammer are they are fairly inexpensive, are portable, are faster to use than shakers, and most importantly do not cause mass loading. Despite these pros, there are also several cons of an impact hammer including the fact that it is often incapable of transferring enough energy to the structure to cause a frequency response in the range of interest. Also, peak impact loads can damage the structure, and the direction of the applied load is difficult to control.

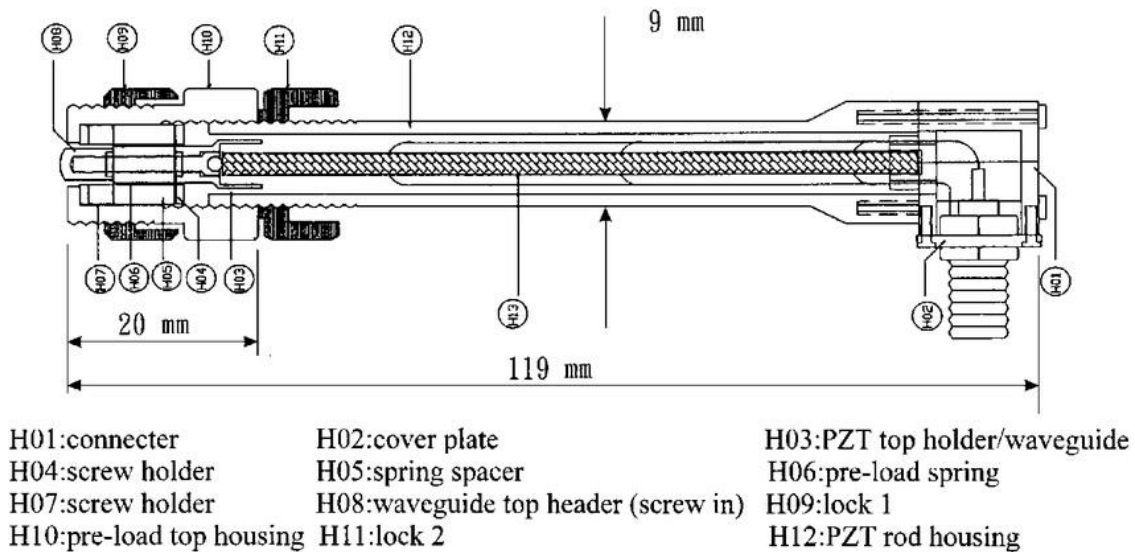


Figure 2.4: Schematic of impact hammer [27]

Another actuator that can be used is a speaker. This is a relatively new form of actuator that uses the vibrations caused by a speaker as a driving force. A design for a speaker-driven actuator is shown in Figure 2.5. As is evident from the design the actuator needs a lot more than just the speaker to work [28]. The actuator is composed of a diaphragm, and plexiglass. First a diaphragm is mounted on the speaker. Next a plexiglass sheet with a hole drilled into the center is bolted down to the other side of the diaphragm. The hole in the plexiglass needs to be aligned with the center of the speaker. This will completely seal the head of the speaker on every side. The only way for air to get out will be through the hole in the plexiglass. This hole is important as when the speaker moves up and down to produce vibrations it will cause air to be sucked down through the hole and then pushed back out. This repeated motion will cause a ring of air to be pushed out, which will in turn cause the driving force. This actuator is very uncommon and is not an ideal choice over a shaker or impact hammer. It is uncommon due to the fact that it can only provide a weak amplitude of vibration. As a result, it can only vibrate very light structures. One thing this actuator can be used for is to vibrate a Chladni plate. This is a thin metal plate which is placed over the speaker-driven actuator on which sand is sprinkled. When the speaker-driven actuator vibrates the plate at one of its natural frequencies the sand on the plate will show the

standing waves moving through the plate.

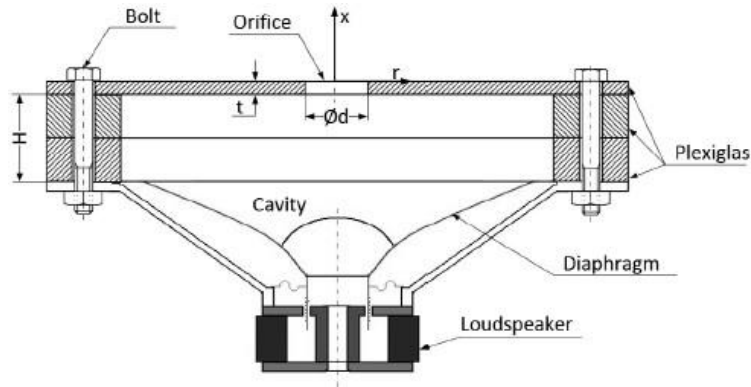


Figure 2.5: Schematic of a speaker-driven actuator [28]

The final actuator that will be discussed in this paper is a piezoelectric element. Piezoelectric elements are characterized by their propensity to change shape when a force or voltage is applied [29]. There are two distinct types of piezoelectric actuators, stack and stripe actuators. Stack actuators are made by stacking separate actuators on top of each other and sealing them with either an insulating coating seal or a stainless-steel case, depending on the environmental factors they need to be protected from. The stack of piezoelectric elements is held together by high temperature sintering. Stripe actuators are made from bonding two layers of piezoelectric ceramic. These layers have a coinciding direction of polarization and are electrically connected in parallel to each other. When electrical input is provided, one layer contracts and the other expands. This causes the actuator to flex. The stack actuator provides limited motion, but high force to a structure, while the strip actuator causes a large deflection in the structure which results in high motion but low force. Figure 2.6 shows an image of a stack actuator, while figure 2.7 shows an image of a stripe actuator.



Figure 2.6: Stack actuator [29]



Figure 2.7: Stripe actuator [29]

2.1.3 Sensors

There are several different types of sensors used to accurately measure relevant data. The type of sensor used depends primarily on the type of data needed.

A prominent sensor that is used in many vibration experiments is an accelerometer. An accelerometer is a device that measures acceleration. It consists of two masses, one of which is attached to the structure and the other is separated from it by a piezoelectric material, which is a type of material that generates an electrical charge when strained [12, pp. 590]. The piezoelectric material acts like a stiff spring, which causes the sensor to have a resonant frequency. The maximum measurable frequency is only a fraction of the accelerometer's measurable frequency, which means accelerometers do not break easily. Since the accelerometer is mounted to a structure when the structure undergoes vibrations, the piezoelectric material inside the accelerometer will undergo a similar force, which will move the masses with respect to each other. This will then cause the piezoelectric material to generate a charge that can be passed through a signal conditioner and then be analyzed. Figure 2.8 shows a schematic of a piezoelectric accelerometer. This makes accelerometers very useful for experiments involving detecting how a structure moves when experiencing vibration. Thus, accelerometers are used to measure vibration on cars, buildings, machines, control systems, and safety installations. They can also be used to detect seismic activity, to determine the rate at which an animal is expending its energy in the wild, and to monitor machine health.

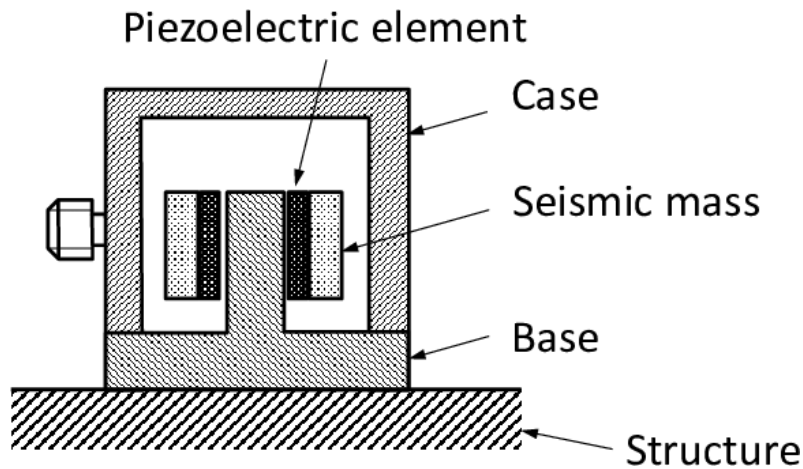


Figure 2.8: Schematic of piezoelectric accelerometer [30]

Another sensor that is used often in vibration experiments is a strain gauge. There are two types of strain gauges, a linear strain gauge, and a rosette strain gauge. A linear strain gauge is a type of sensor that exhibits a change in electrical resistance when subjected to strain [12, pp. 590]. They are generally built using metallic or semiconductor material and are constructed by bending a conducting wire back and forth over a small surface. This is then attached to the structure which is being tested. When the structure undergoes strain, the electrical resistance of the wire changes. The gauge is made a part of a Wheatstone bridge circuit which measures the change of resistance of the wire, and therefore is able to determine the strain on the structure. A Wheatstone bridge circuit is a type of circuit that is used to measure unknown electrical resistance. It accomplishes this by balancing two legs of a bridge circuit, a circuit in which two branches of the circuit are connected by a third branch, or bridge. Due to the way the wire is coiled it can only measure the strain in one direction. Figure 2.9 shows a schematic of a strain gauge. A circuit diagram of a Wheatstone circuit is shown in figure 2.10.

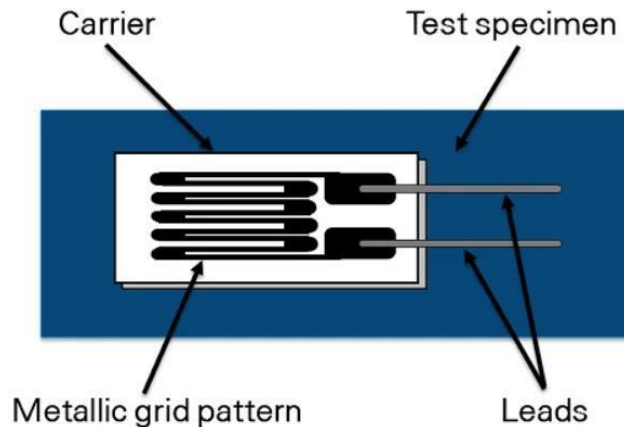


Figure 2.9: Schematic of a strain gauge [31]

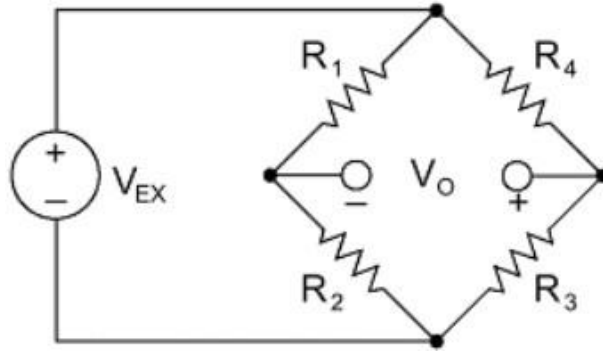


Figure 2.10: Circuit diagram of Wheatstone bridge circuit [31]

A rosette strain gauge is a type of strain gauge that is made up of two or more linear strain gauges [32]. These gauges are positioned closely but aligned differently to effectively measure the strain in multiple directions. This allows more precise measurement of strain on a surface, as the gauge accounts for strain in multiple directions. Figure 2.11 shows a rosette strain gauge.

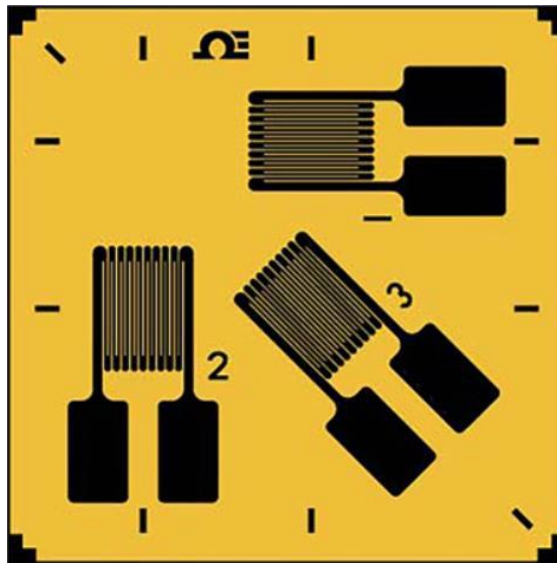


Figure 2.11: Rosette strain gauge schematic [33]

There are three different kinds of circuits involving strain gauges: quarter-bridge, half-bridge, and full-bridge circuit [31]. The difference in these types of circuits is determined by the number of strain gauges in the Wheatstone bridge circuit.

The first type of circuit is the quarter-bridge strain gauge circuit. In this circuit one of the four resistors shown in figure 2.10 is replaced by a strain gauge [34]. Due to the fact that only one out of four resistors are changed to a strain gauge this circuit is referred to as a quarter-bridge circuit. This circuit is the least sensitive to strain, and only provides a signal that is approximately proportional to the applied strain. Therefore, this is not the ideal circuit to use. Figure 2.12 shows a circuit diagram of the quarter- bridge circuit.

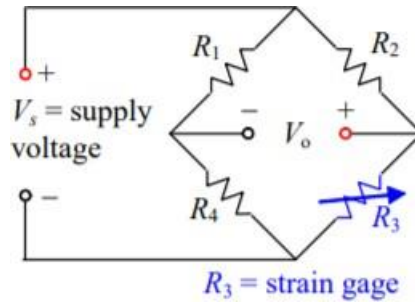


Figure 2.12: Circuit diagram of quarter-bridge circuit [34]

The next circuit is the half-bridge circuit. This circuit is referred to as “half-bridge”, because two of the four resistors in the circuit are replaced with strain gauges. The strain gauges cannot replace two resistors on the same branch, instead they must replace resistors on different branches. The output voltage of the half-bridge circuit is twice that of the quarter-bridge circuit, thus it can be said that the sensitivity of the half-bridge circuit is twice that of the quarter-bridge circuit. This makes the half-bridge circuit a better choice than the quarter-bridge circuit. Figure 2.13 shows a circuit diagram of the half-bridge circuit.

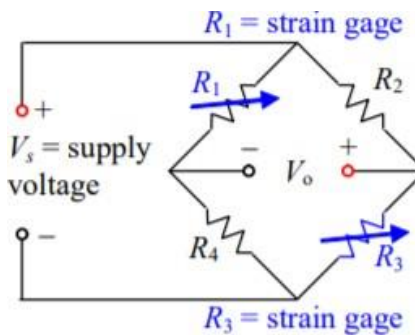


Figure 2.13: Circuit diagram of half-bridge circuit [34]

The final circuit configuration is referred to as a full-bridge circuit. This circuit replaces all resistors in a Wheatstone bridge circuit with strain gauges, which is why it is called “full-bridge”. This is the most sensitive bridge, with four times the sensitivity of a quarter-bridge circuit. The high sensitivity makes this circuit configuration superior, as it is the most accurate of all the configurations. Figure 2.14 shows a circuit diagram of the full-bridge circuit.

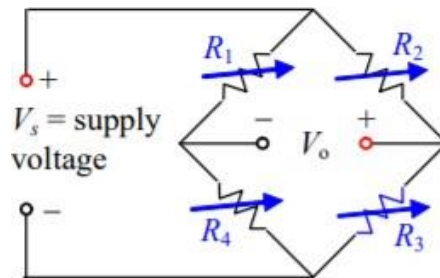


Figure 2.14: Circuit diagram of full-bridge circuit [34]

Load cells are another sensor that are commonly used in vibration experiments. These sensors convert mechanical force into digital values that can be read and recorded [35]. The most common type of load cell is comprised of strain gauges. For a strain gauge load cell to work, an assembly of strain gauges is placed within the load cell. The gauges are bonded to a beam or other structural member that deforms when weight is placed on the load cell. Most of these load cells have four strain gauges inside them to ensure maximum accuracy of measurements. Two of these gauges are in compression, and two are in tension. This is done by mounting two gauges in a horizontal orientation and the other two in a vertical orientation. When there is load on the load cell, the output voltage of the strain gauges will be changed. This change in voltage is converted into readable values using a digital meter. Figure 2.15 shows a schematic of a strain gauge load cell.

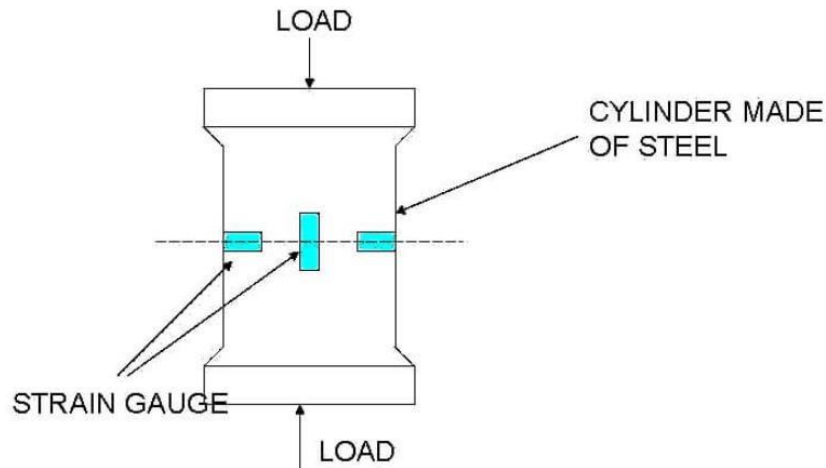


Figure 2.15: Schematic of a strain gauge load cell [36]

Recently, a new method of measuring vibrations through a structure has come into play. This method is called Digital Image Correlation (DIC) [37]. DIC is not a physical sensor and does not involve the use of any physical sensors, yet it still performs the task of a sensor as it measures the deformation of a structure due to vibrations. It is accomplished by taking digital images of a high-contrast, random speckle pattern on the face of a surface. As the surface is deformed by vibrations, the pattern is as well. By photographing the changes in this pattern, the strain that the structure undergoes can be measured and quantified. This method has many advantages over the traditional sensors. The first advantage comes from the ability of DIC to measure the strain of the structure simultaneously at hundreds of points. This would be nearly impossible with sensors because there would be too much experimental setup required to accomplish this. Another advantage DIC has over sensors is that it is not physical. All sensors have some mass, which can cause slight errors in the measurement of modes and frequencies, as mass loading can shift these frequencies. The added mass can also introduce extraneous damping. These problems are especially prevalent when measuring light-weight, lightly damped structures. DIC can measure modes and frequencies of a structure without introducing effects of sensor mounting on the structure. Despite these positives, DIC has many drawbacks as well. The biggest drawback so far is the lack of a temporal aliasing filter for high-speed image acquisition. Temporal aliasing is caused when the frames per second of the images taken are lower than the process occurring in real life. This causes jumps and skips in time. Other issues in DIC include

noise caused by the cooling systems located inside the cameras. Due to these problems DIC is currently not ready to overtake physical sensors as the primary vibration measuring tool, but it provides an intriguing look at what the future could hold for vibration testing. Figure 2.16 shows a sample image of how DIC works.

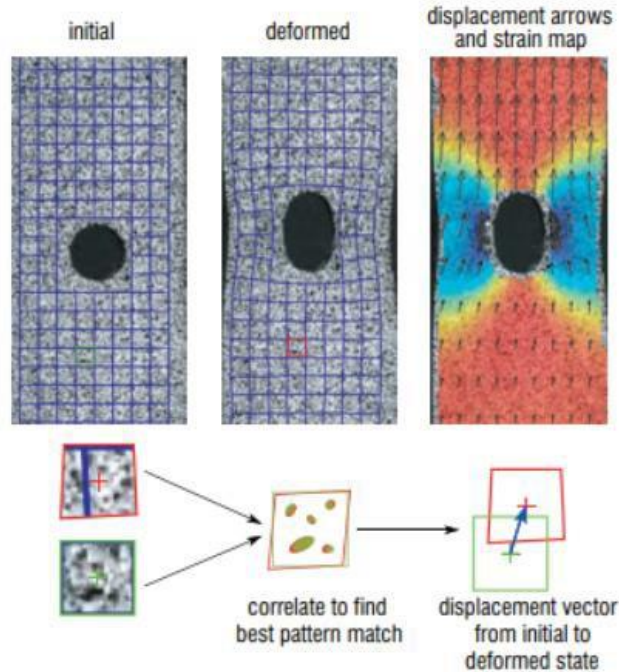


Figure 2.16: DIC example image [38]

Another tool used to measure vibrations in a structure without placing sensors on it is a laser- scanning vibrometer. The vibrometer is a machine which emits a laser that is directed onto a vibrating surface [39]. When the laser hits a vibrating surface, some of it is reflected back into the machine. Based on doppler's effect this light will have been affected by the vibrating surface and will have a shift in wavelength or frequency. From this shift in the light's properties, velocity of points on the structure can be determined. From this data a deformation profile of the structure can be constructed. There are two types of laser-scanning vibrometers, 1-D and 3-D [40]. A 1-D vibrometer only has one head. Therefore, the surface it is pointed at appears as a 2-D shape. As a result, the 1-D laser-scanning vibrometer is unable to detect motion that is perpendicular to it. To combat this a 3-D laser-scanning vibrometer must be used. A 3-D vibrometer has three heads that it uses to measure motion due to vibration in all three directions. This is much harder to use than a 1-D vibrometer as calibration times are very long and alignment of the lasers is much more complicated. In the vibrometers the laser, or lasers, is programmed to measure the vibrations at all mesh points of the structure and display it as time responses, Fourier transforms, frequency response functions, spectral densities, coherence functions, or operational deflection shapes [12, pp. 591]. There are two methods of collecting this data [39]. The first method involves keeping the laser fixed at one point on the structure for an extended period of time. This enables the machine to gather a lot of information about that point on the structure, but it is a very slow process as this needs to be repeated for several spots. The second method involves continuously moving the laser around the structure. From this method there is not a great deal of information

obtained about singular points, however the velocity response and deflection shape of the structure become clear. For this reason, the second method is much better than the first. Advantages of this method of measuring vibrations in a structure are similar to the advantages listed for the DIC, it offers a contactless way of determining how vibration affects a structure, thus not causing error that comes from mass loading. However, these scanners are also much more expensive than the simple sensors such as accelerometers and strain gauges and require longer calibration time [40]. Figure 2.17 provides an image of a 1-D laser-scanning vibrometer. Figure 2.18 provides an image of a 3-D laser-scanning vibrometer.



Figure 2.17: Image of 1-D laser-scanning vibrometer [41]

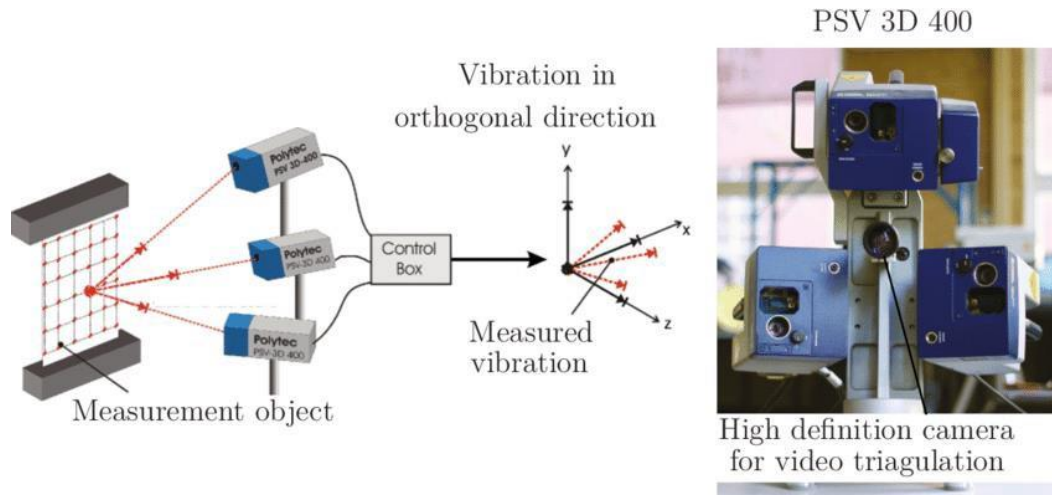


Figure 2.18: Image and schematic of 3-D laser-scanning vibrometer [42]

2.1.4 Other Important Equipment

An important tool used in correlation with sensors is a signal amplifier. This tool is a necessity as most sensors do not have a suitable output impedance for direct input into signal analysis equipment [12, pp. 590]. As a result, a signal conditioner is used to match and amplify signals prior to analysis. In order for a signal conditioner to function properly, the sensors need to be properly calibrated in terms of magnitude and phase over the frequency range of interest. Signal conditioning is particularly important for accelerometers. This is because when accelerometers are exposed to low-frequency vibrations they provide very weak signals. This is because, even when the low-frequency vibration displacement is substantial, the acceleration can still be very small. For this reason, it is important to use a signal conditioner with an accelerometer, as these smaller signals can be lost otherwise.

Other key pieces of equipment include the cables used in the setup of the acquisition system. When conducting vibration experiments, it is vital to get a good output signal. Without a clear output signal, the data retrieved from the experiment can be flawed or inaccurate. As a result, it is important to do everything possible to reduce any noise that may enter the system. Signal conditioning already helps to eliminate noise from the sensors in the system, however there are still other sources of noise that can arise. The most prevalent noise sources after sensors are the cables used in the acquisition system. When cables are exposed to mechanical stress, which can be imposed through bending or dropping of the cable, the layers of the cable move relative to each other, for example the conductors will move relative to the cable shield [43]. In regular cables this causes the insulation to gain a charge, creating a charged capacitor that creates a voltage difference between conductors or a conductor and the cable shield. This process is referred to as charging. The voltage difference then causes noise to appear in the signal analysis, which can slightly alter the output signal from the sensors and lead to inaccuracies in the results. This process is even more prevalent in coaxial cables, which are the cables used to connect to signal generators and analyzers. When these cables undergo mechanical stress, they generate an even larger voltage difference within the cable than normal multi-conductor cables. To prevent cable noise from interfering with the results of an experiment, low-noise cables must be used. Low-noise cables prevent charging by adding a layer of conductive material to the surface of the

insulation of the cable. This layer is then bonded to the insulation to prevent movement of the two layers with respect to one another. The conductive layer makes it so any voltage difference that builds between layers is immediately dissipated. A low-noise cable helps to reduce noise in the cable anywhere from 15 to 250 microwatts. Even though this seems like a relatively small number, the signals from the sensors are not all that strong, and even a very small amount of noise can lead to a big change in the output signal. To ensure that the cables are not impacting results of the experiments in any way, it is necessary to use low-noise cable in the setup of the acquisition system, especially because of how drastically charging affects coaxial cables.

2.2 Signal Processing

Most of the analysis done in modal testing is performed in the frequency domain inside the analyzer [12, pp. 591]. The analyzer must convert time-domain analog signals into frequency-domain digital signals and then perform the required computations on the transformed signals. To change the signal from time-domain to frequency-domain a Fourier transform must be used. However, before a signal can pass through an analyzer it must first be filtered.

Oftentimes in signal processing a signal can get affected by noise or even get distorted. To combat this and restore the original signal filters need to be put into the acquisition filter. Filters are a device or process that strips away unwanted components of a signal. Filters have two uses in signal processing, one is signal separation, and the other is signal restoration [44]. Signal separation involves removing noise, interference, or other signals to obtain the signal of interest. Signal restoration deals with restoring a signal that has become distorted in some way. Filters can either be digital or analog. Though analog filters are much cheaper than digital filters, digital filters perform at a much higher level, in fact digital filters can provide thousands of times better performance than analog filters. Filters have an input and output signal in the time-domain so no conversion to the frequency-domain is required at this step of signal processing. The most common types of digital filters are the low-pass, high-pass, band-pass, and band-reject filters. Low-pass filters only allow frequencies below a certain cut-off frequency to pass. High-pass filters only allow frequencies above a certain cut-off frequency to pass. A band-pass filter allows frequencies within a certain frequency band to pass. A band-reject filter allows only frequencies not in a certain frequency band to pass. In all of these cases the frequencies that do not meet the criteria of the filter are attenuated.

Next, the analyzer first converts the analog signal to digital records. The first step of this process is to perform a process known as sampling. Sampling is done by taking samples of the analog signal, referred to in this paper by $x(t)$, at several equally spaced values. This value is referred to as sampling time. Next, an analog-to-digital (A/D) converter is used to produce a digital record from the analog signal. The process it uses to accomplish this is called quantization. Quantization is a process of mapping input values from a continuous set to output values in a smaller, discrete set. The set of numbers produced by the A/D converter is referred to in this paper by $x(t_k)$, where k is an integer denoting the number of samples and t_k is a discrete time value. Each t_k is separated by the sampling time chosen earlier in this process. Figure 2.19 shows several time-domain signals and their respective Fourier representations and digital records. To perform this Fourier transform, one must take care in choosing the sampling time. If improper sampling time is chosen an error known as aliasing may occur. Aliasing refers to the misrepresentation of

the analog signal by the digital record. If the sampling rate is too slow to catch the details of the analog signal, the high frequencies appear as low frequencies in the digital record. To avoid aliasing the sampling interval must be small enough to provide two samples per cycle of the highest frequency to be calculated. In other words, the signal has to be sampled at a rate at least twice the highest frequency in the signal. In fact, 2.5 samples per cycle is the ideal rate. The best way to prevent aliasing from occurring is to use an antialiasing filter. This is essentially a low-pass filter that cuts off all frequencies higher than half of the maximum frequency of interest. This maximum frequency of interest is referred to as the Nyquist frequency.

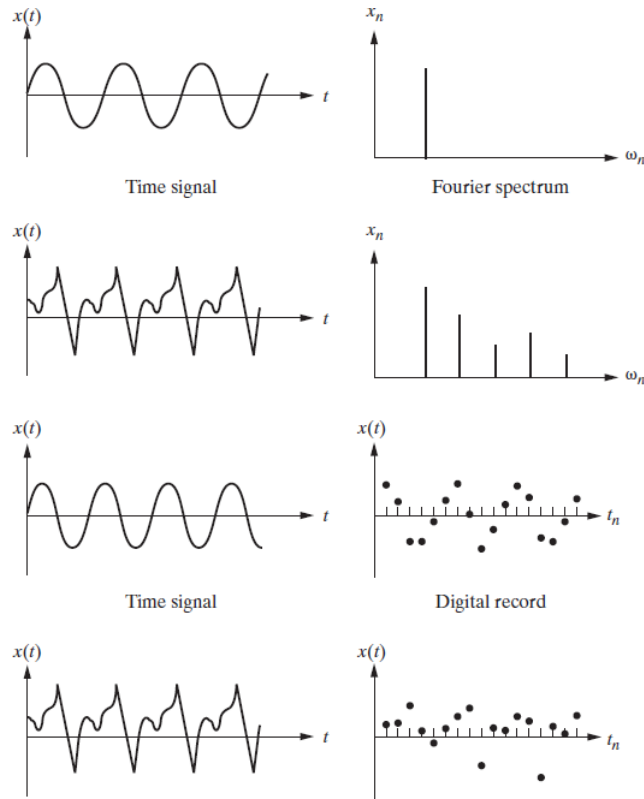


Figure 2.19: Time signal and respective Fourier spectrum and digital record [12, pp. 593]

Once the digital record has been made from the analog signal, the Fourier transform can be performed. This transform provides a series representation of a discrete-time value. This is done using the digital versions of the Fourier transform equations, provided below in equations 2.1 and 2.2:

$$x_k = x(t_k) = \frac{a_0}{2} + \sum_{i=1}^{N/2} \left(a_i \cos \frac{2\pi t_k}{T} + b_i \sin \frac{2\pi t_k}{T} \right) \quad k = 1, 2, \dots, N \quad (2.1)$$

$$\begin{aligned}
a_0 &= \frac{1}{N} \sum_{k=1}^N x_k \\
a_i &= \frac{1}{N} \sum_{k=1}^N x_k \cos \frac{2\pi ik}{N} \\
b_i &= \frac{1}{N} \sum_{k=1}^N x_k \sin \frac{2\pi ik}{N}
\end{aligned} \tag{2.2}$$

Where N is the number of samples, T is the time period, and a_0 , a_i , and b_i are the digital spectral coefficients.

The goal of the analyzer is to calculate these equations given the digital record, or $x(t_k)$. Once the equations have been written out for each N, a matrix of the digital spectral coefficients can be created. Once the matrix is created equations 2.1 and 2.2 can be rewritten as equation 2.3.

$$x = Ca \tag{2.3}$$

Where C is the matrix of coefficients in the equation, x is the vector containing the values of $x(t_k)$, and a is the vector of the spectral coefficients. To solve for a, this equation is rewritten in equation 2.4.

$$a = C^{-1}x \tag{2.4}$$

The task of the analyzer is then to compute C^{-1} and hence a. The most widely used way to find C^{-1} is utilizing a method known as the Fast Fourier Transform (FFT). The FFT is simply a commonly used algorithm that is generally provided in several coding languages.

To make digital analysis feasible, the signal must be sampled over a finite time. This can give rise to a problem known as leakage [12, pp. 595]. To make the signal finite, one can cut it off at any integer multiple of its period. The issue with this is it cannot be done with signals containing a variety of different frequencies. Therefore, the signal can be cut off at mid-period. If this happens, erroneous frequencies will appear in the digital representation of the signal because the digital Fourier transform will assume that the signal is periodic during the entire finite time chosen. This will cause the actual frequency to “leak” into several fictitious frequencies added by the Fourier transform to make the signal periodic. An example of leakage is shown in Figure 2.20. Leakage can be corrected using a window function. Window functions are functions, $w(t)$, that can be multiplied to the original analog signal. The functions force the signal to be zero outside of the sampling period. An example of a window function’s effect on a signal is shown in Figure 2.21.

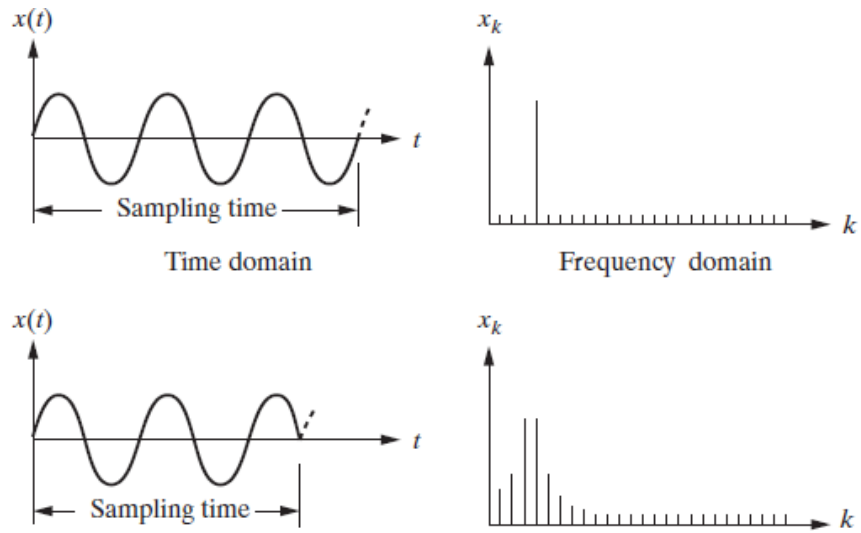


Figure 2.20: Leakage example [12, pp. 596]

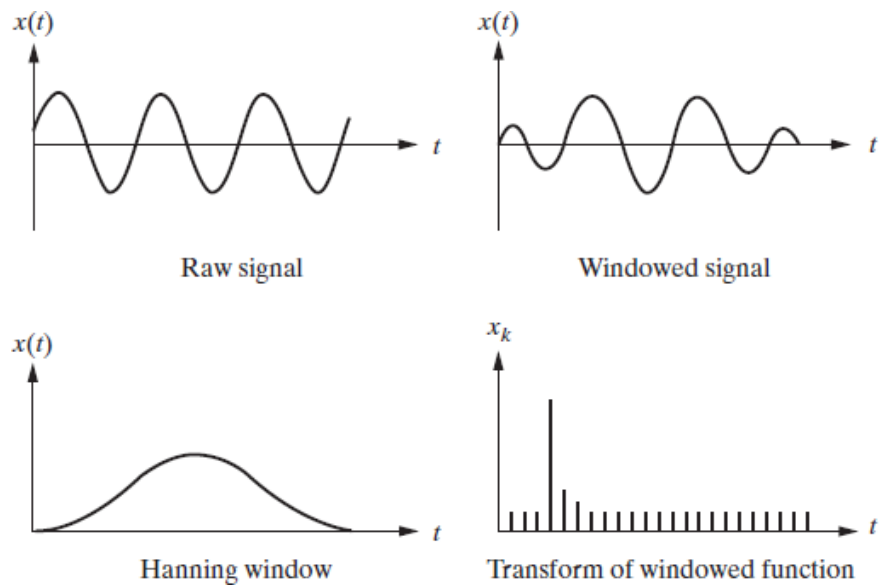


Figure 2.21: The effect of a window function on leakage [12, pp. 596]

3.0 Drop Calibration Experiment

3.1 Calibration

A calibrated sensor is a sensor whose output signals are understood and have a value and unit attached to them. When a sensor is calibrated the voltage change it outputs during a test can be translated into a mechanical quantity as a measurement of force or acceleration. Calibration of any sensor is a necessity prior to the start of its use. This is due to the fact that when sensors are exposed to the natural elements their outputs tend to differ from their factory sensitivity. The factory sensitivity of a sensor comes from calibration tests run in the factory. Over time the sensor loses this calibration and needs to be recalibrated. For example, when sensors are exposed to varying temperature, pressure, or change in ambient conditions their zero reference, the reading the sensor gives when it is not detecting anything, may drift from the original zero reference [45]. Another reason why sensors need to be calibrated is that the operating range of the sensor may need to be adjusted. For example, if the sensor is currently functioning in the range of 0 to 300 pounds per square inch (PSI), but changes in operations require it to run from 0 to 500 PSI, it will need to be recalibrated. Without calibration the output signals given by the sensors have no meaning, and quality measurements cannot be taken.

Accelerometers are no different from any other sensor and require calibration before being used. There are two ways to calibrate an accelerometer, absolute calibration, and relative calibration [46]. Absolute calibration methods involve comparing the measured signal from an accelerometer to a known physical quantity. Examples of this method include inversion and drop calibration. In both of these methods the signal of the accelerometer is compared to the acceleration due to gravity of the Earth. Comparing this signal to a known quantity allows one to calibrate the accelerometer quickly and accurately. Relative calibration methods involve comparing the measured signal from the uncalibrated accelerometer to the measured signal of a calibrated accelerometer. Comparing an uncalibrated accelerometer's signal to a calibrated accelerometer's signal allows one to compare the two signals and thus have a good understanding for what the uncalibrated accelerometer's signal represents, thus calibrating it. Examples of this method include shock and vibration calibration.

Inversion calibration is done by rotating the sensor 180 degrees in the Earth's gravity so that it experiences $-1g$ and $1g$ [46]. First position the accelerometer downwards. Define this output as -9.8 m/s^2 . Next, flip the accelerometer and define this output as $+9.8 \text{ m/s}^2$. This process is shown in Figure 3.1. This test calibrates the accelerometer as it should experience $1g$ of gravity when it is stationary on the face of the Earth. Defining the positive and negative directions also helps ensure that the signs of the final reading will be correct. To perform this calibration correctly the signal conditioning and readout device must be DC coupled, and the readings must be taken for a long time to ensure the curve is flat when the device is stationary. DC coupling allows a device to allow both DC and AC currents to pass through it, however AC coupling only allows AC current to pass through. It is important to differentiate between DC and AC coupled accelerometers for this experiment, as DC coupled accelerometers are very good at measuring a steady signal, whereas AC coupled accelerometers measure time variation of a signal away from a zero value. This makes AC coupled accelerometers bad at measuring a constant signal. Due to the nature of this experiment, DC coupled accelerometers are the correct

choice to use as a constant signal needs to be measured. Figure 3.2 shows a graph of the output signal of the accelerometer during the inversion calibration.

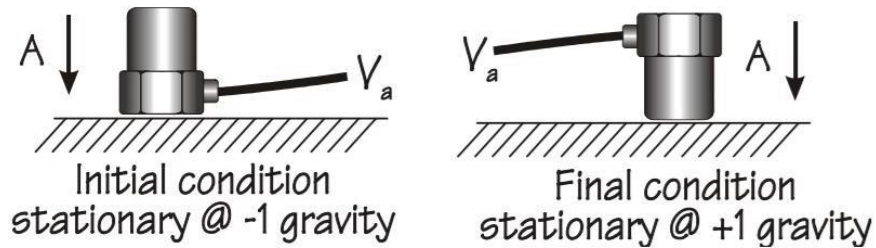


Figure 3.1: Inversion calibration [46]

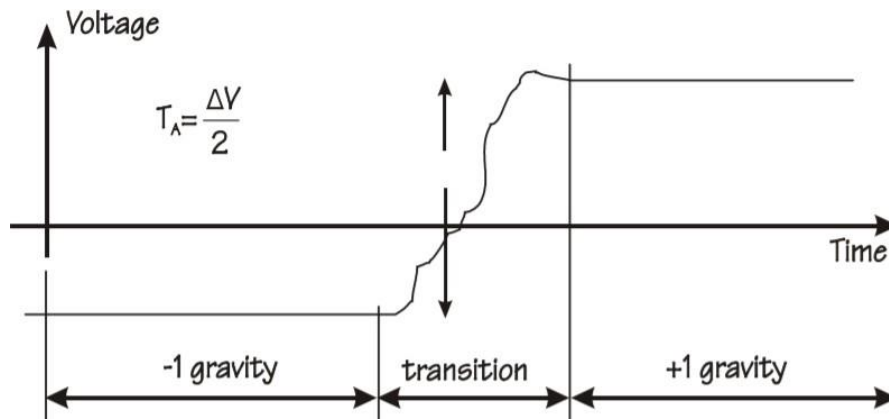


Figure 3.2: Graph of inversion calibration [46]

Another form of calibration is shock calibration. This form of calibration is used for shock accelerometers. To perform this calibration a reference accelerometer must be used [47]. A reference accelerometer is an accelerometer that is already calibrated. The output signal of this accelerometer is then compared with the uncalibrated accelerometer's signal. Based on the discrepancies between the signals the uncalibrated accelerometer can be calibrated. To perform the actual calibration, the uncalibrated accelerometer is mounted onto the reference accelerometer. These accelerometers are then mounted onto an anvil. The anvil is then struck and the resulting waveforms of the output signals of the accelerometers are compared. Figures 3.3 and 3.4 show the setup of the shock calibration, while Figure 3.5 shows a graph of the comparison of the output signals of the accelerometers.

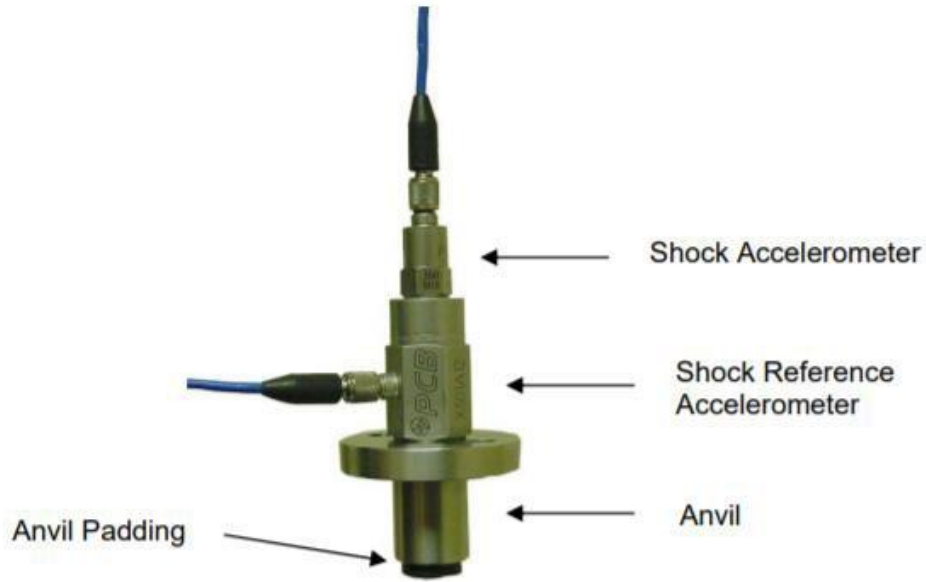


Figure 3.3: Accelerometers and anvil setup [47]

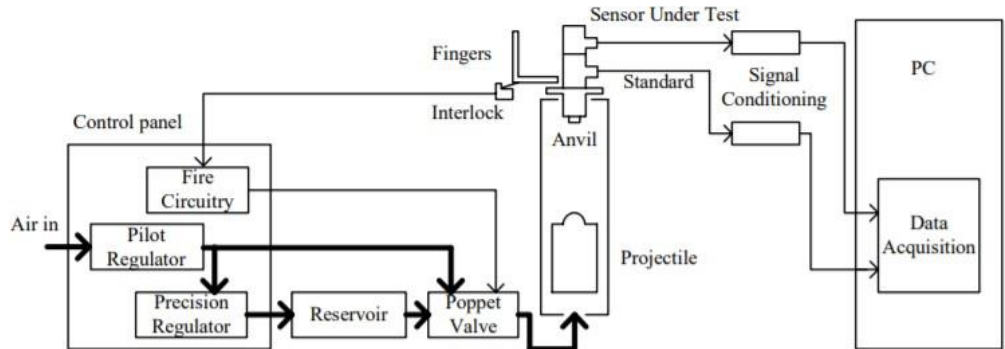


Figure 3.4: Full calibration setup [47]

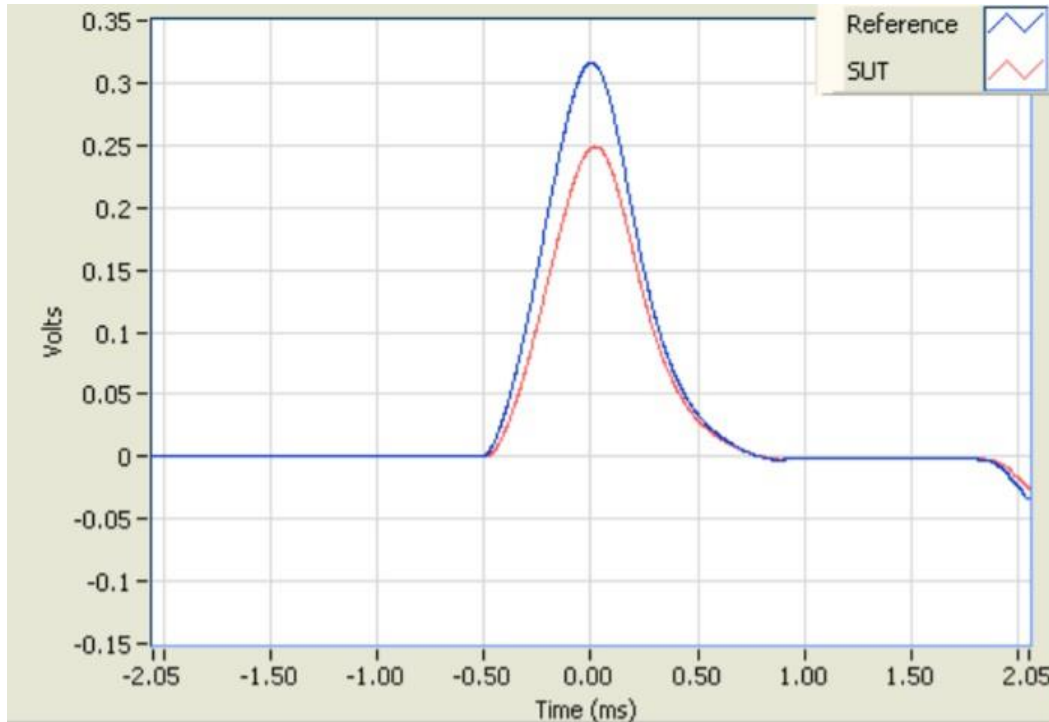


Figure 3.5: Output signal comparison [47]

A similar form of calibration can be used to calibrate standard accelerometers as well. This form of calibration is called vibration calibration. It is similar to shock calibration because it also relies on stacking an uncalibrated accelerometer onto a reference accelerometer [47]. However, these calibration types differ in how the input signal is provided to the accelerometers. In shock calibration this is done by striking the anvil the accelerometers are attached to, whereas in vibration calibration this is done by using an electromagnetic shaker to shake the accelerometers. The shaker is generally driven by a sinusoidal vibration signal. When the shaker shakes the sensors the output signals can be compared similarly to how they are compared in the shock calibration test. The sensitivity of the uncalibrated accelerometer can be measured at a particular frequency or sweeping through the desired range of frequencies generates a frequency response curve of the uncalibrated accelerometer. The most common type of electrodynamic shaker used in this calibration is the air bearing shaker. This is because of the pure single degree of freedom vibration that they can provide, and also because they can minimize transverse motion and distortion othershakers can provide. Figure 3.6 shows the setup of the accelerometers, while Figure 3.7 shows a frequencyresponse curve of an accelerometer. Figure 3.8 shows an air bearing shaker.

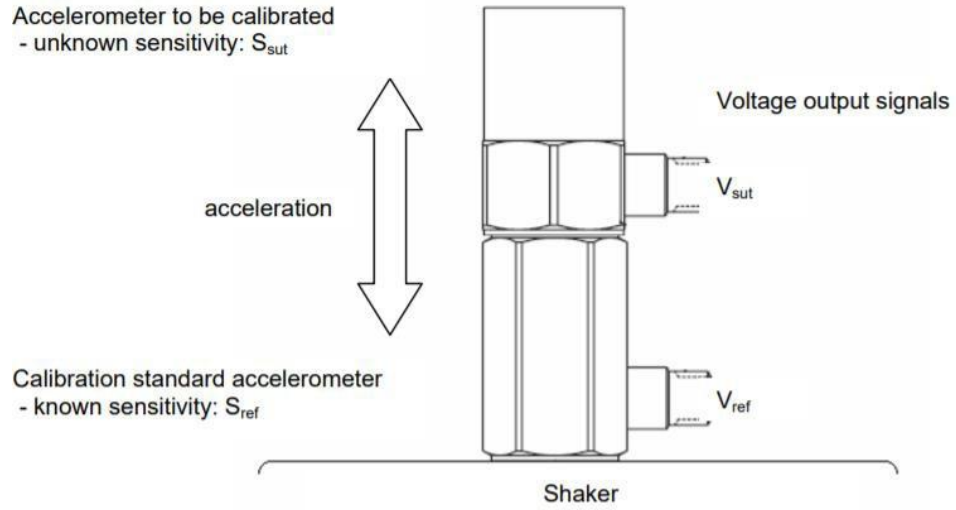


Figure 3.6: Setup of shakers [47]

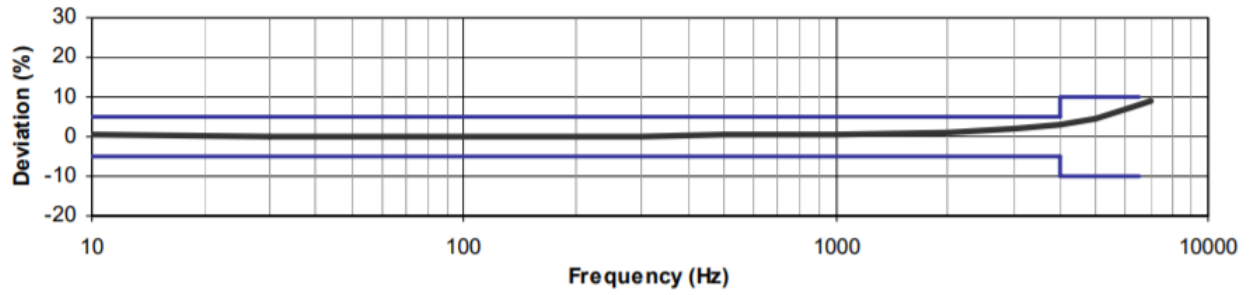


Figure 3.7: Frequency response of an accelerometer [47]

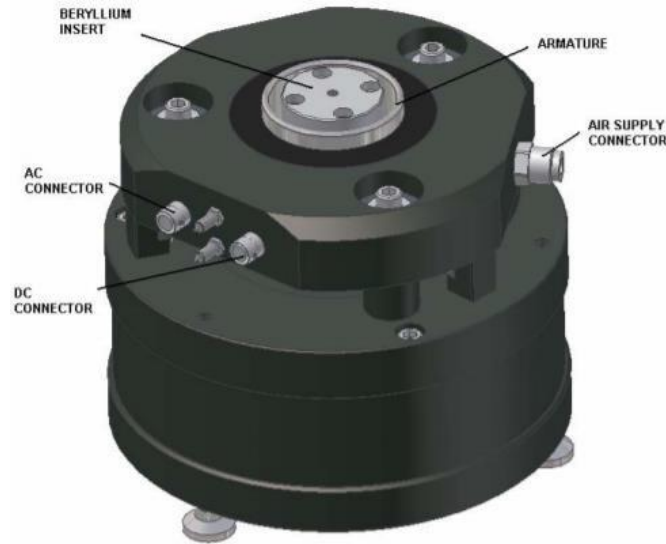


Figure 3.8: Air bearing shaker [47]

The final type of calibration that will be discussed, and the type of calibration this paper will be using to calibrate an accelerometer, is called “drop calibration”. This form of calibration involves allowing an accelerometer to free fall in Earth’s gravity while measuring its output signal [46]. Figure 3.9 shows the setup of a drop calibration test, while Figure 3.10 shows a sample output signal of an accelerometer undergoing free fall. The setup of this experiment is further discussed in Section 3.2. The biggest challenge of this type of calibration is getting the accelerometer into free fall. Several different factors must be considered when attempting to get the accelerometer into free fall. First of all, the height that the accelerometer is being dropped from must be sufficient to get the accelerometer into free fall. Next, the filament connecting the accelerometer to the frame and the wires connecting the accelerometer to the filters and signal analyzers must be light and thin enough that they do not add drag to the accelerometer. Finally, the accelerometer must be heavy enough that it drops straight down and is not influenced by other factors.

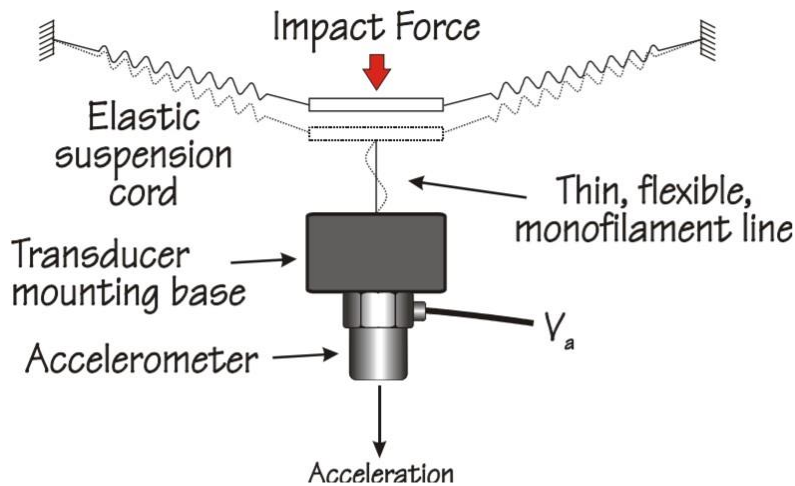


Figure 3.9: Setup of a drop calibration test [46]

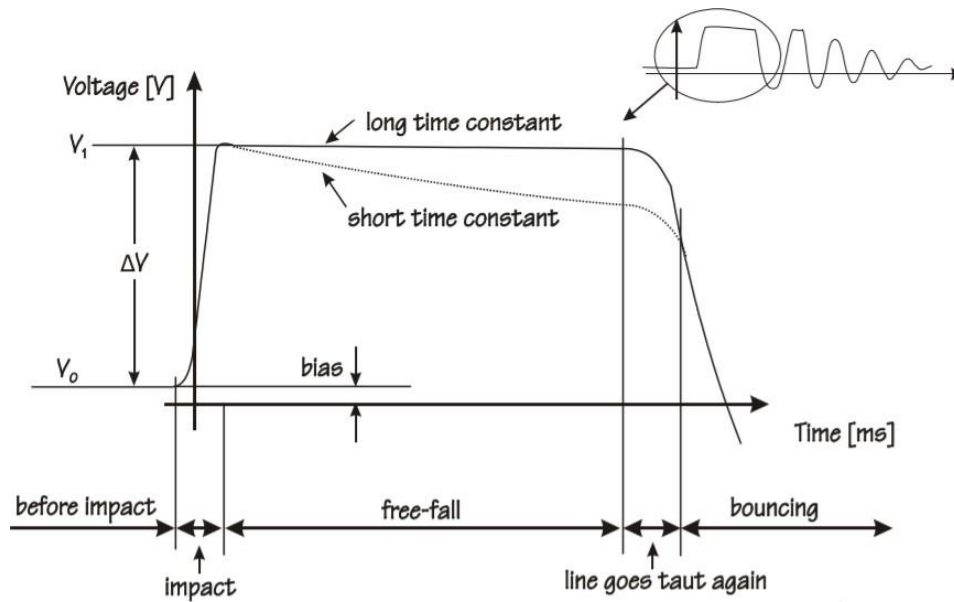


Figure 3.10: Signal of accelerometer during free fall [46]

3.2 Drop Calibration Experiments

A drop calibration experiment is an experiment that involves creating an experimental setup that can properly perform drop calibration of an accelerometer. Most drop calibration experiments have similar setups, but there is some variance to each experiment. Discussed below are two different setups for drop calibration.

The first setup involves a piezoelectric accelerometer. The first step in this setup is attaching drop weights to the accelerometer. The drop weight is used to add weight to the

accelerometer. This makes the accelerometer heavy enough that a substantial drop will occur in the system, and it also makes it more likely to fall straight down and less likely to be influenced by the wires connected to it. These weights are centrally mounted to the accelerometer with either a 0.25 inch thread or a 10-32 thread for a piezoelectric accelerometer or screwed in at each end with a 3 mm screw for a piezoresistive accelerometer [2]. These accelerometers are mounted with a thin film of silicon grease smeared on the bottom of it. This helps to aid in high frequency data transmission. The accelerometer is then connected to a constant current supply, which is also an amplifier, using a microdot cable. Next, the output of the amplifier is connected to a low pass filter using a coaxial cable, which is in turn connected to an oscilloscope, which is a device that displays varying signal voltages. A force sensor is necessary to be used in this experimental setup. The sensor is connected to a charge amplifier using a microdot cable because it is a charge device. The charge amplifier is then connected to the oscilloscope through a low pass filter using a coaxial cable. When the charge amplifier is connected to the oscilloscope the ground button is pressed so that the base amplifier output shows up as zero. This setup is shown visually in Figure 1.1 of this paper. The drops are then performed. The voltage for each drop is shown on the oscilloscope. After each drop the oscilloscope needs to be grounded to disregard any charge that may have been built up in the charge amplifier. This charge can build as a result of the wires creating an electromagnetic field. The expected result of this experiment is a smooth curve with a clear and obvious peak that returns to zero. Errors in this experiment can arise from improper drops, lack of filtering, or unsound cable connections. Figure 3.11 shows what the expected result of this experiment looks like.

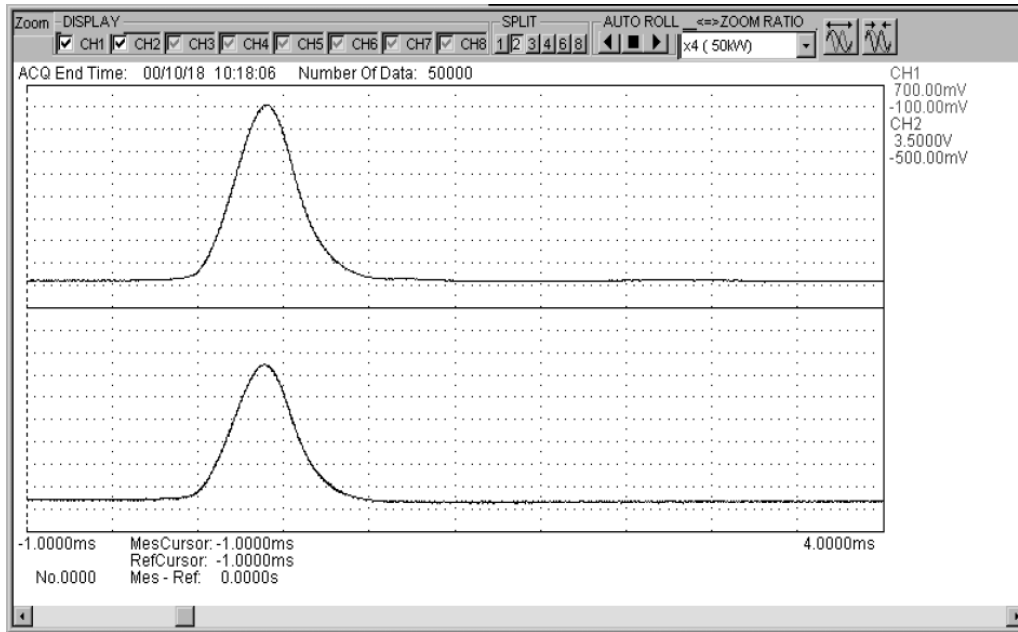


Figure 3.11: Results of first setup drop calibration [2]

One possible setup for this type of calibration involves attaching the accelerometer to a thin, flexible filament and mounting this filament to an elastic suspension cord. Once a force is applied to the cord the accelerometer will drop. The filament is needed to prevent the accelerometer from hitting the ground and breaking. It does not impede the dropping of the accelerometer in any way. The accelerometer will provide an output signal with many peaks and valleys. This is due to the fact that once the filament reaches its full length it will cause the accelerometer to bounce, which in turn will produce an oscillating wave towards the end of the output signal. When the data is analyzed only the first peak will be kept. The sinusoidal waveform will be cut out of the signal as it is not relevant. During free fall the output signal from the accelerometer will be a constant value. This constant value can then be equated to 9.8 m/s^2 because when an object is in free fall the acceleration due to gravity that it experiences is equal to $1g$. The sensitivity of the accelerometer can be determined by dividing this constant value by $1g$. This is the calibration type that will be used in this paper because it is easier to do than vibration calibration, and it provides more data than inversion calibration. The accelerometers used are not shock accelerometers, and therefore shock calibration will not be used.

Continuing with the setup of the experiment, two elastic suspension cords are connected to stable mounting points [46]. They are then connected to a flat metal plate so that the metal plate is suspended between the two cords. The accelerometer is then mounted underneath a transducer mounting base. A filament connects the transducer mounting base to the aforementioned metal plate. When an impact force is provided on the metal plate, the transducer mounting base and accelerometer will drop. The filament prevents the accelerometer from sustaining damage. The accelerometer is then connected to a low pass filter which is in turn connected to an oscilloscope. The result of this experiment will have an oscillating signal after the main curve as the filament will cause the accelerometer to bounce after the initial drop. This sinusoidal signal can be ignored and only the initial curve needs to be considered.

3.3 Design of Drop Calibration Experiment

When designing an experiment, it is important to have a detailed procedure to follow. It is also necessary to have a list of parts that are needed to complete the procedure. The following sections will cover the procedure in depth and also provide a detailed parts list.

3.3.1 Procedure

The procedure for this experiment is based on an explanation and setup of a drop calibration experiment provided by PCB Piezotronics [46]. This experiment is used because it is much easier to follow and overall is a simpler way of conducting a drop calibration experiment. Ideas from Krelle [2] are also used. For this experiment a piezoelectric accelerometer is used.

The first step in this procedure is to create a metal frame that can be used for a drop. The frame will consist of four equal length legs that are connected to one another at their tops by four perpendicular metal rods. After connecting the four legs the top of the frame will look like a rectangle. The legs of the frame will be three feet in length to ensure the height is enough for the accelerometer to reach free fall. Multiple views of this metal frame are shown in Figure 3.12.

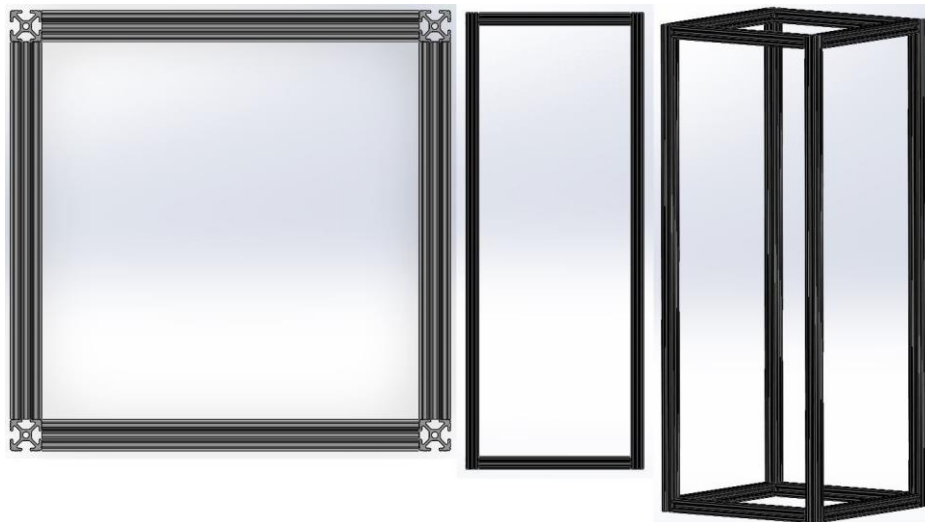


Figure 3.12: Top (left), front (center), and isometric (right) views of metal frame

After the metal frame is complete two springs will be placed into it. The springs will be connected to two corners made in the top plane of the frame using magnetic hooks. A plate will then be put into the middle of the frame and will be suspended by the two springs. After being connected to the springs the plate should be centered in the square that the connecting rods make at the top of the frame. These springs will be strong enough to hold the plate in place, but also not too strong, so that when a force is applied to the plate it will drop. Figure 3.13 shows how the setup should look so far into the experiment.

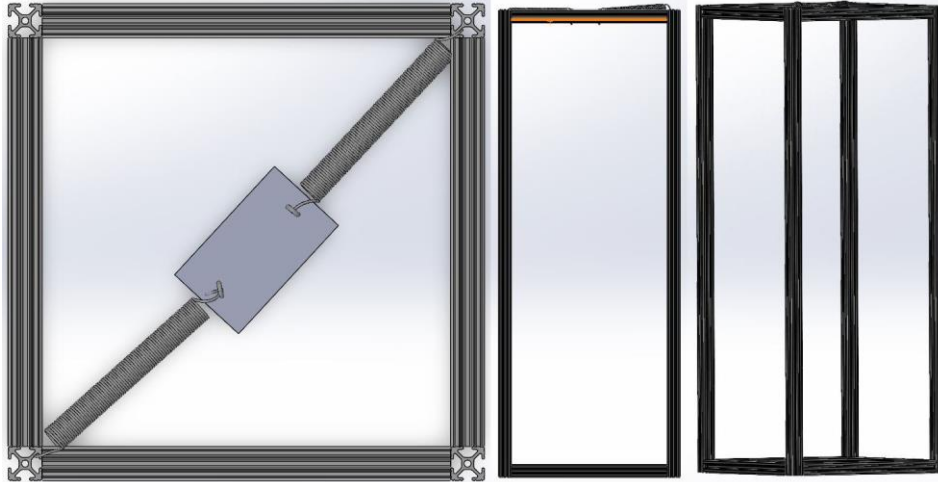


Figure 3.13: Top (left), front (center), and isometric (right) views of metal frame with metal plate and springs

Next, a drop weight and accelerometer combination must be attached to the plate in a way that they do not fall off. In this experiment a drop weight is needed to be attached to the accelerometer. This is because the accelerometer and plate combined are very light, and that makes it so when the plate is struck, the weight may not be enough to cause an actual drop. Attaching a drop weight ensures that when the plate is struck there will be a substantial drop that occurs in the experiment. Figure 3.14 shows the completed setup of the experiment. The bottom view is shown instead of the top because the weight and accelerometer are placed under the plate.

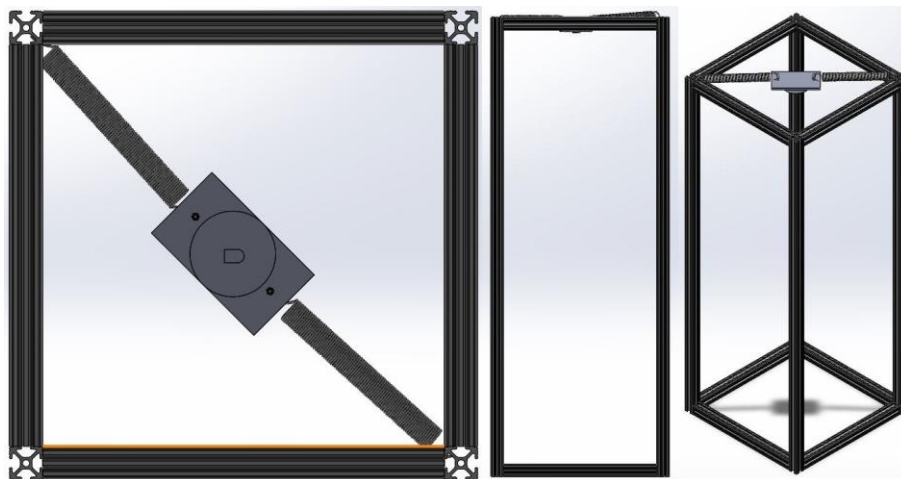


Figure 3.14: Bottom (left), front (center), and isometric (right) views of completed experimental setup

Finally, the accelerometer will be attached to a signal analyzer. This signal analyzer contains a digital low pass filter and a signal conditioner within it. To collect data from the experiment, the metal plate will have to be hit in a way that makes the springs drop it. This will send the metal plate, accelerometer, and mount into free fall. During free fall the signal outputted

by the accelerometer will be filtered, conditioned, and then displayed on LabVIEW. The sensitivity of the accelerometer will be given by Equation 3.1, where S is the sensitivity, V_{peak} is the peak voltage, and g is 9.81 m/s^2 .

$$S = \frac{V_{peak}}{g} \quad (3.1)$$

Figure 3.15 shows the final setup used for this experiment.



Figure 3.15: Drop calibration final setup

3.4 Results

After completing the experiment, the data from the accelerometer will be displayed on LabVIEW in the form of a graph that plots the time vs the signal outputted from the accelerometer in millivolts. This graph then needs to be trimmed so that only the relevant region of the graph, the region where the accelerometer is in free fall, is displayed. This trimming can be done by exporting the data into excel and adjusting the minimum and maximum values on the horizontal axis. Figure 3.16 shows the trimmed graph.

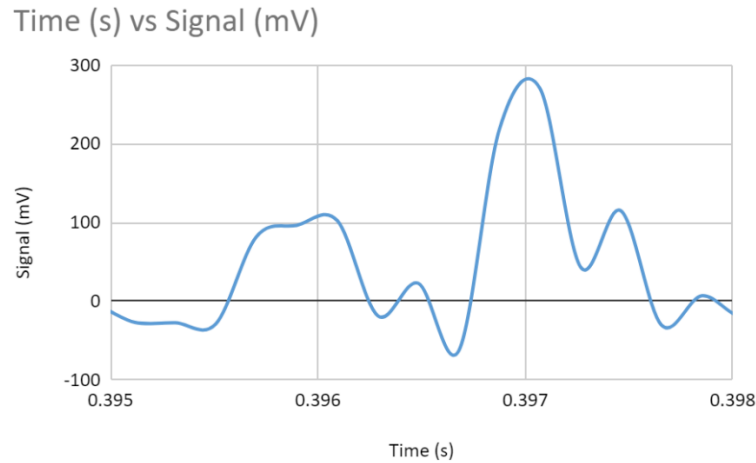


Figure 3.16: Time vs signal graph after drop

This graph starts at 0.395 seconds, because the impact happened 0.395 seconds after the acquisition was started. From this graph it is clear that free fall occurs between around 0.3955 seconds to 0.3963 seconds. The free fall portion of the graph looks different than the expected free fall graph, as shown in Figure 3.10. This error is due to the fact that springs were used to support the plate, unlike the experiment for which the results are shown in Figure 3.10 where suspension cords supported the plate. This creates difference in how the plot will appear in each experiment. The springs used in the experiment conducted in this paper are more elastic than the cords, which cause them to not go taut the way the cords would when the plate reached the end of its drop. The springs would instead try to reset to their original position, and therefore provide a force to the plate when it reaches its final position, which causes the plate to experience a greater acceleration at the end of its fall as it shown in Figure 3.16. A zoomed in graph showing only the free fall portion of the graph is shown in Figure 3.17. The signal shown after this time represents the oscillations of the accelerometer as it continued to bounce after the impact. During the accelerometer's free fall, the output signal is 96.32 mV. Using equation 3.1, this means the sensitivity of the accelerometer is 9.82 mV/m/s^2 , or 96.32 mV/g . This sensitivity differs slightly from the factory sensitivity of the accelerometer which was measured to be 9.94 mV/m/s^2 , or 97.5 mV/g . There were six trials completed of this experiment, and all trials gave a sensitivity similar to the aforementioned determined value. The percentage difference in the determined value for sensitivity and the factory measured sensitivity was 1.21%. This error was probably caused by error in in setup of the experiment or slight decay in the sensor since its shipment.

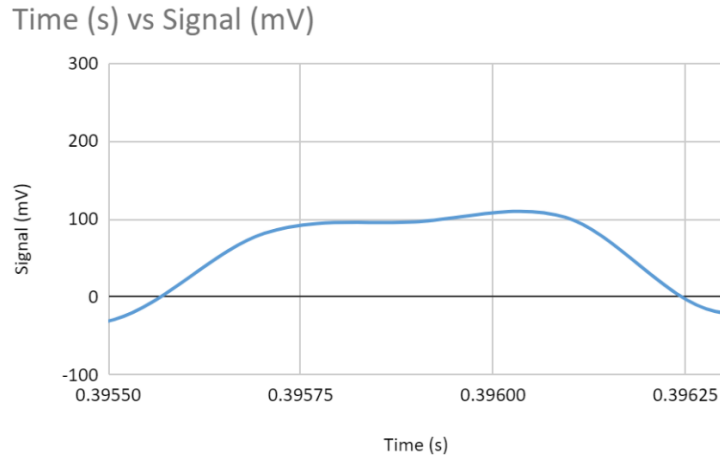


Figure 3.17: Free-fall portion of graph

3.5 Error

There are several sources of error that could have arisen in this experiment. The biggest potential source of error comes from the way in which the plate was mounted to the springs. To ensure that the springs would adequately drop the plate, drop weight, and accelerometer, springs with relatively low stiffnesses needed to be used. As a result, even when the system was at rest the springs were stretched and the plate was hanging lower than the top plane of the frame. Therefore, when the plate was struck and the system began to oscillate, the signal outputted from the accelerometer is even higher than the signal outputted during free fall. This is because after the initial free fall the system bounces to a plane higher than the rest plane of the system. The fact the plate bounces higher than its rest position means that it has gained energy. This added energy comes from the springs. When the springs are fully extended they have the maximum amount of potential energy, so when they compress they will compress fully. Since the rest position of the system occurs at a point where the springs are not fully compressed, the second oscillation will have a higher peak than the first, because it will rise to a plane where the springs are fully compressed. This caused the second oscillation to have a larger output than the initial free-fall. Another source of error could come from the cables used to connect the accelerometer to the data acquisition system. Due to the fact that the cable also underwent a significant amount of oscillation, it is possible it introduced noise into the system. This error is unlikely to have arisen as there is not much noise that is visually evident from looking over the graph.

4.0 Determining Frequencies and Modes of a Beam

4.1 Modal Testing

Modal testing is a form of vibration test that determines natural frequencies, mode shapes, and damping ratios of the object being tested. A natural frequency of an object is a frequency that when an object is exposed to it, the object will tend to deform in a specific way. This specific deformation is called a modal shape. Different modal shapes occur at each natural frequency of an object. The damping ratio is a measure of how oscillations of an object will decay at a specific natural frequency. Modal testing is extremely important as determining natural frequencies, modal shapes, and damping ratios is necessary before launching any aircraft or spacecraft or constructing a building, especially a skyscraper. It is necessary to perform modal tests with aircraft and spacecraft because these craft undergo high degrees of vibration. It is important to find their highest natural frequencies and ensure that the crafts can hold up under those frequencies. If these craft are not properly tested they can result in catastrophic failure after launch which can cost millions of dollars, or even human life. It is also vital to determine modal shapes and natural frequencies of buildings, as taller buildings will be affected greatly by wind. The wind can cause buildings to vibrate at relatively high frequencies, which can cause cracks to form in the building. For this reason, it is important to test the building design before completing construction. If testing is not done properly there is a risk of the building becoming increasingly unstable, which may lead to a future collapse.

There are several ways to conduct a modal test, but they are all founded on the same premise. To perform modal testing, an actuator that can provide a driving force to the tested object is required. Sensors, such as accelerometers, must be placed on the body of the object so that deformation of the object can be properly measured. The sensors are then hooked up to signal conditioners and analyzers so that the signal can be properly seen as the object is excited. A picture of this general setup is shown in Figure 4.1.

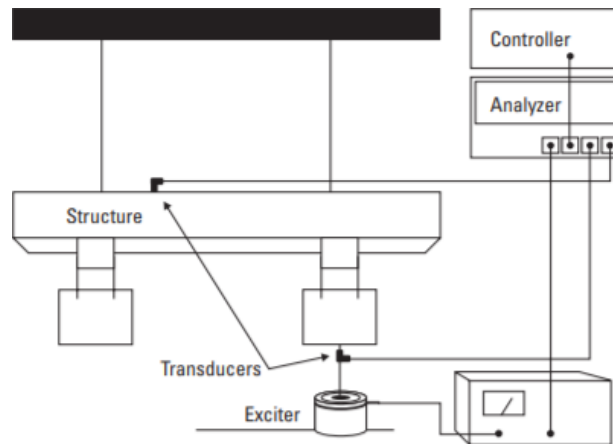


Figure 4.1: General setup of a modal testing experiment [48]

The biggest difference in modal testing experiments is the type of actuator chosen to excite the body. There are two main actuators used shakers, and impact hammers. For each of these actuators the experimental setup looks different.

When a modal test is done by a shaker the biggest change in the experiment is that the shaker needs to be isolated from the system. As previously discussed, the shaker can cause mass loading, which significantly changes the modal shapes and natural frequencies of a system. Therefore, a stinger must be attached to the shaker to prevent this. Using a stinger also prevents motion from occurring in directions different from the one the force is being applied in. The stinger will connect directly to a load cell, which is attached to the body of the object [48]. The placement of the shaker also matters in a modal testing experiment. For the system to truly be able to move freely it needs to be suspended in the air because that is the only way it will have a full range of motion in any direction. The shaker can either be placed on the ground underneath the object, or it can be suspended next to the object. These different setups are shown in Figure 4.2. In experiments involving shakers, power amplifiers are also necessary. They can be used to drive many different forces to the object to get a wide variety of tests done. Generally electromagnetic shakers are the preferred choice of shaker in modal testing experiments.

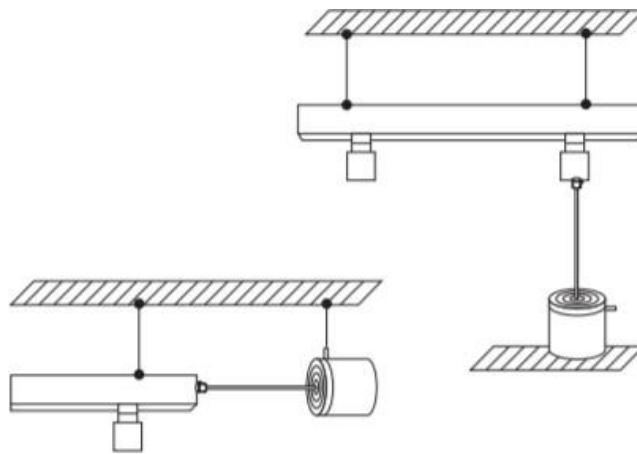


Figure 4.2: Different shaker placement in modal testing [48]

Impact hammers are generally easier to use than shakers in modal testing. These actuators require significantly less setup time. This is because the tip of the hammer prevents mass loading altogether, and impact hammers have a built in load cell in their head. The stiffness of the tip of the hammer and the mass of the hammer determines the maximum excited frequency that can be obtained by the hammer. Potential issues with the impact hammer are a lack of consistency, noise, and leakage [48]. Lack of consistency with the impact hammer is due to the fact that humans cannot make two swings of the hammer exactly the same. This lack of consistency can affect the final results if the experiment is repeated several times. All the results will be close to one other but differ slightly. Noise and leakage can occur based on the time record of the experiment. If the time record is too short leakage will occur, and if it is too long noise will occur. To eliminate these problems windowing is required. Figure 4.3 shows an experimental setup with an impact hammer actuator.

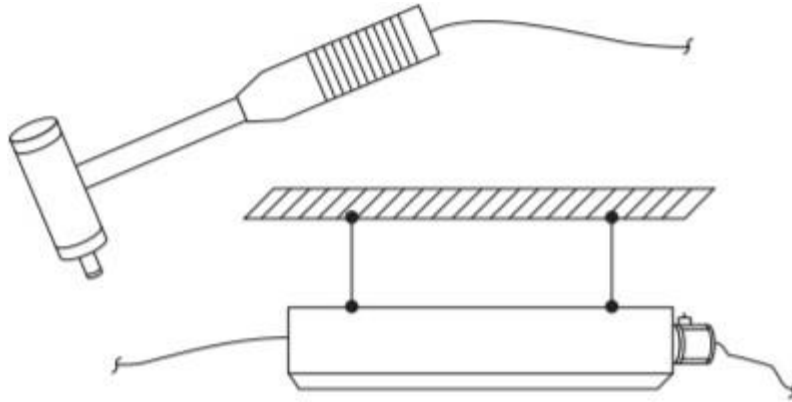


Figure 4.3: Impact hammer modal testing [48]

4.2 Modal Testing Experiments

There are several types of modal testing experiments that can be done. The type of experiment chosen is greatly impacted by the type of actuator used in the experiment. When modal testing big objects, such as aircraft and spacecraft, shakers must be used, however, when modal testing smaller objects, such as a beam, an impact hammer is the actuator of choice.

As previously discussed in section 1.2.3, aircraft vibrational, or modal, testing is done using a process known as ground vibrational testing, or GVT [15]. GVT is a process that requires the use of a phase-resonance method. For this method, the shaker's location and phase relation must be carefully chosen to cause the aircraft to behave as a single-degree-of-freedom system. This method is then complemented by phase separation techniques which find the aircraft's modes using frequency response functions. Spacecraft testing is done in a very different manner. Two types of shakers are used to vibration test a spacecraft, stinger-drive shakers, and base-drive shakers [18]. Stinger vibration tests are conducted with the test craft in a free-free or fixed-interface configuration. These tests are mainly used to verify or update a mathematical model. Base vibration tests are done with a craft mounted to a moving platform that is driven by an electro-dynamic shaker. These tests are primarily used to test workmanship and to verify that flight hardware is working correctly. For both aircraft and spacecraft testing only shakers can be used as an actuator because any other actuator would be unable to provide the necessary vibrations to simulate the environment that these craft will be operated in.

The form of experiment that is more relevant to the experiment that will be conducted in this paper involves modal testing a beam using an impact hammer. To set up an example experiment a steel cantilever beam is first clamped on one end, while the other is left free [4]. The beam is then divided into 11 different sections. This is done so that 12 nodes on the beam can be marked down. These nodes are then labelled from 0 to 11, with 0 being the clamped end and 11 being the free end. Accelerometers are then mounted at nodes 5, 9, and 11 to measure the acceleration at these points when the beam deforms. The accelerometers are placed at these points as points 9 and 11 will undergo a lot of vibration after the impact so they are good points to measure

the acceleration at, while point 5 is selected to give a better understanding of how the impact affects parts of the beam that will undergo little acceleration. This can be seen in Figure 4.4.

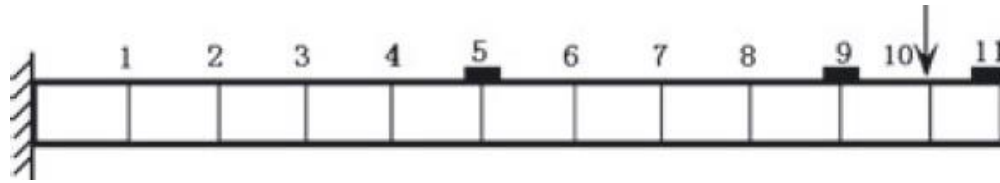


Figure 4.4: Experimental setup with steel cantilever beam [4]

Three different trials are then run. The beam is first struck at node 3 with an impact hammer and results from the accelerometers are noted down. Then the process is repeated with impact hammer strikes at nodes 6 and 10, respectively. These nodes were selected to see if there were any differences in the output of the accelerometers when the beam was struck at a node that barely underwent vibrations, a node that underwent some vibrations, and a node that experienced great vibrations. Graphs of impact of the hammer compared to the combined output of the three accelerometers is shown Figure 4.5. The smaller graph in the top right of each graph is a clearer and more refined version of the larger graph. These graphs show that the combined output of the accelerometers mirror the impact of the hammer, except they show oscillations after the impact, which is due to the fact that the beam will vibrate after the impact. Another observation from these graphs is that all of them are relatively similar despite the impact being on different nodes for each graph.

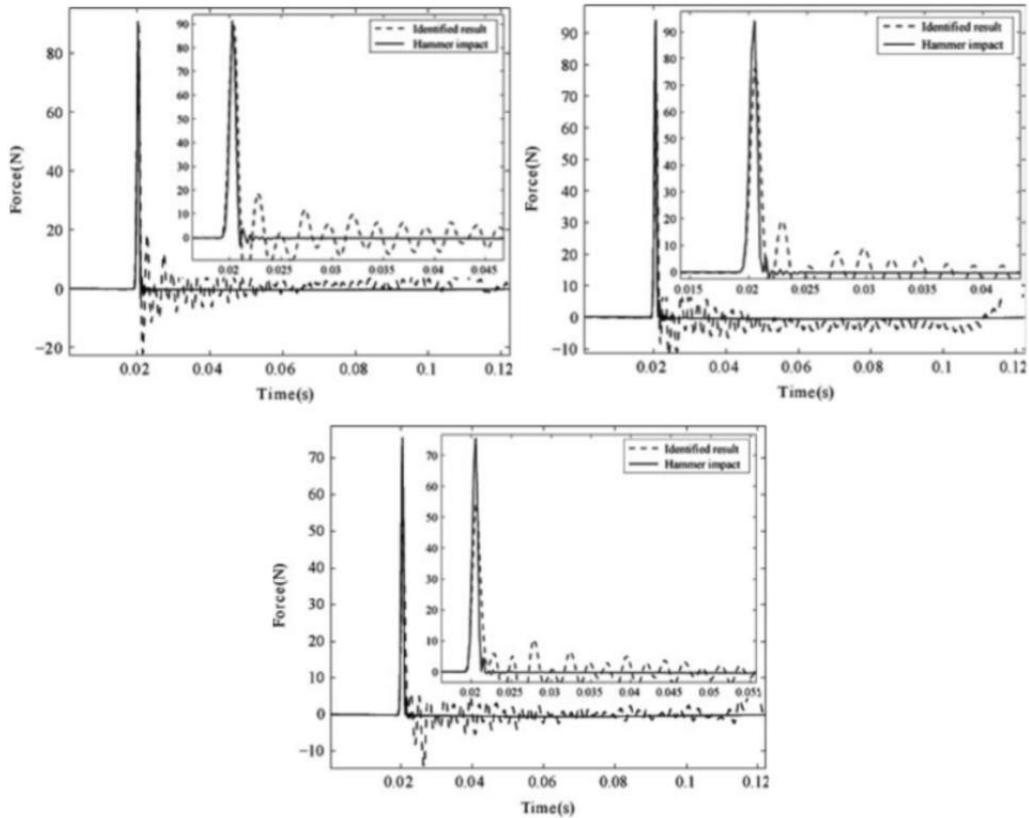


Figure 4.5: Accelerometer results, top left: impact at node 3, top right: impact at node 6, bottom: impact at node 10 [4]

4.3 Design of Modal Testing of Beam Experiment

The following sections will cover the procedure of the experiment and the list of parts necessary to complete the procedure.

4.3.1 Procedure

This procedure is primarily based on Mao et al. [4]. The procedure used by Mao et al. is slightly edited to ensure it fits the equipment available.

The first step in this experiment is to select a beam to test. The beam selected for this experiment is a steel cantilever beam with a thickness of 0.005 m, width of 0.045 m, length of 0.688 m, density of 7850 kg/m³, and young's modulus of 160 GPa. Once the beam is selected it is divided into 11 subsections using a marker. This is done to identify 12 nodes of the system. The beam is then clamped on one end and left free on the other end. The nodes are then labelled so that node 1 is the clamped end and node 12 is the free end. After the beam has been clamped, three accelerometers will be mounted to it. These accelerometers will be placed at nodes 6, 10, and 12. The accelerometer placed at node 6 will be referred to as accelerometer 1, the one placed at node 10 will be accelerometer 2, and the one placed at node 11 will be accelerometer 3. Placing them in these locations helps give a clear picture of the deformation of the beam when it

is struck. These accelerometers are then connected to a low pass filter, which is then connected to a signal conditioner. The signal conditioner is then connected to a data analyzer. Figure 4.6 shows the final setup of the experiment.

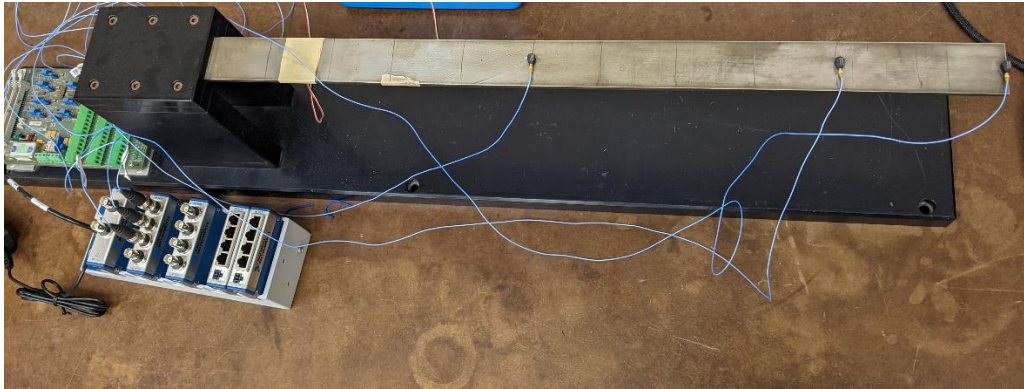


Figure 4.6: Example of setup of beam with marked nodes [4]

After the setup of the experiment is complete, three trials will be run. In the first trial an impact hammer will be used to strike the beam at node 4. The second and third trial involves the beam being struck at nodes 7 and 11, respectively. After the beam is struck the data analyzer will display the data from the accelerometers. Each trial involves striking the beam in a different location because no matter where the beam is struck the beam should still deform in relatively the same way regardless of where it is struck, therefore the data from the accelerometers should be very similar. Striking the beam in different locations ensures that the data that is being taken is accurate. Finally, the data taken by the data analyzer is inputted into LabVIEW. The acquisition frequency should then be set to 0.1 Hz, and the number of averages should be set to 15. The averages will therefore occur every 10 seconds because an acquisition frequency of 0.1 Hz means samples are taken for 10 seconds, therefore, averages should be taken every 10 seconds as the sampling from the previous hit will end. This means that the beam will need to be impacted every 10 seconds for 150 seconds. The averages need to be taken in this fashion as the data acquisition system used in this experiment does not support triggering. LabVIEW then outputs graphs from which the exact natural frequencies, and modal shapes of the beam can be determined.

4.4 Results

Prior to beginning the experiment, it is necessary to find theoretical values of the natural frequencies and mode shapes of the beam. To find these values, ANSYS was used. To calculate accurate values, the beam geometry and specific material parameters of the beam were added into ANSYS. ANSYS then calculated the first six natural frequencies of the beam and provided a modal shape at each frequency. Figures 4.7-4.12 show the modal shapes and the natural frequency they correspond to. The accelerometers in this experiment were placed in the center of the beam which affected the results as axial bending modes were unable to be detected.

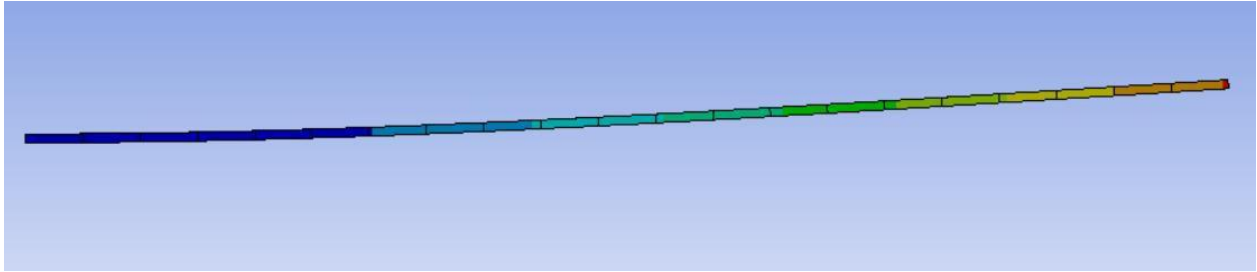


Figure 4.7: First vertical bending mode

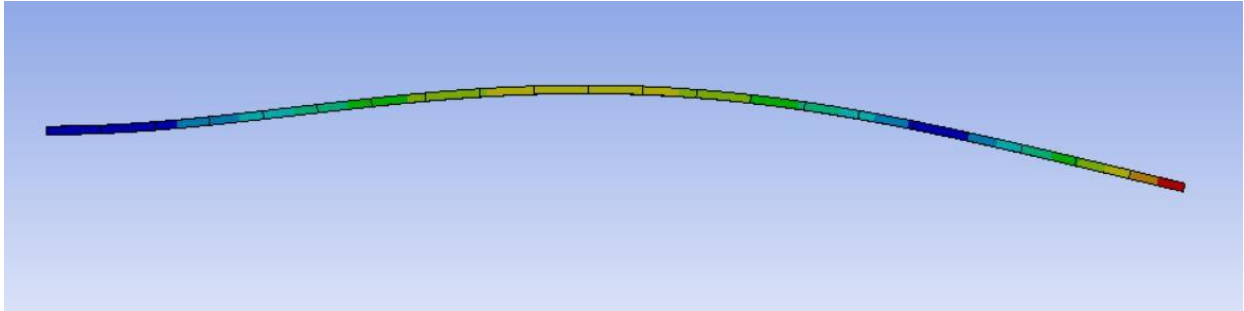


Figure 4.8: Second vertical bending mode

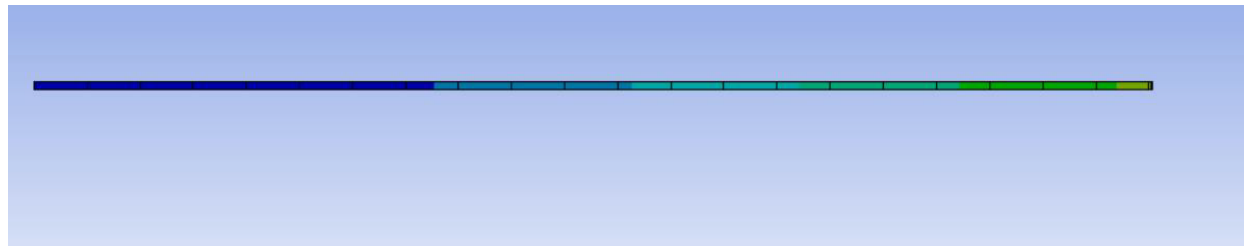


Figure 4.9: First axial bending mode

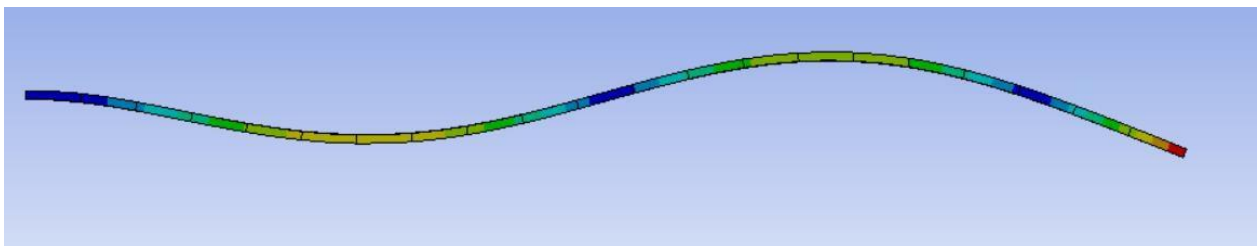


Figure 4.10: Third vertical bending mode

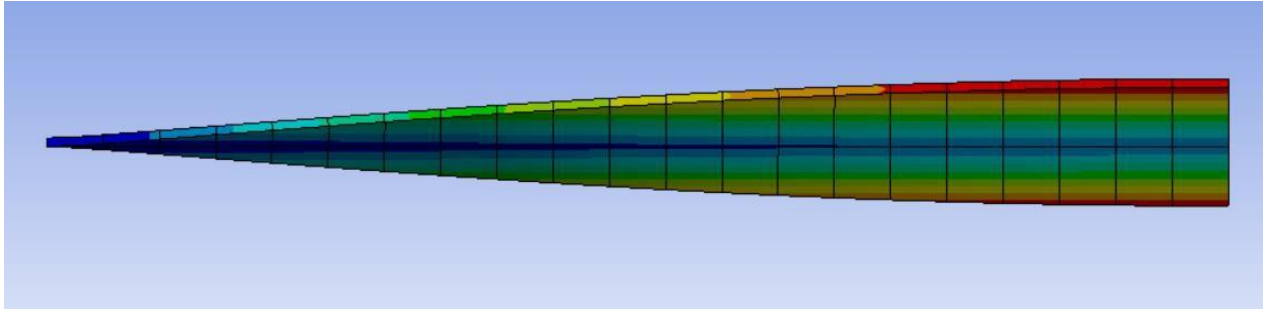


Figure 4.11: First torsional mode

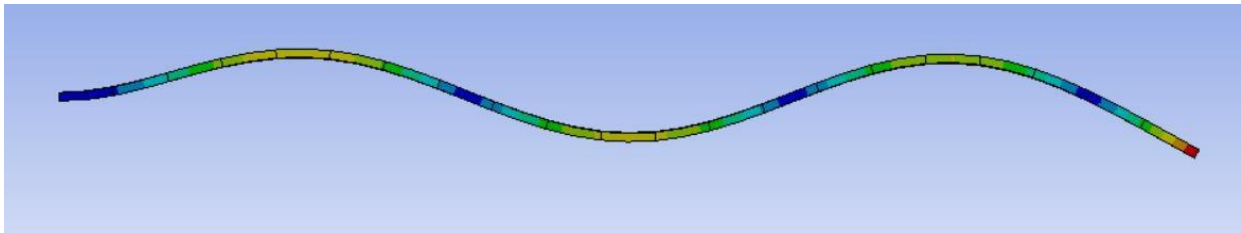


Figure 4.12: Fourth vertical bending mode

After conducting the experiment, nine graphs were obtained, three for each accelerometer, one for each impact location. These graphs were plotted by LabVIEW in Frequency vs Decibels. The plots were in decibels as this helps determine the peaks of the graph much more easily. Figures 4.13, 4.14, and 4.15 show the graphs in Frequency vs Decibels for each accelerometer.

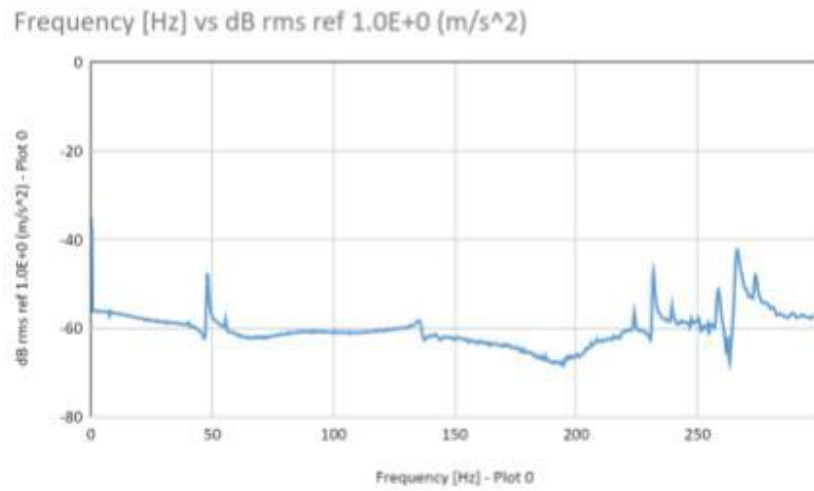
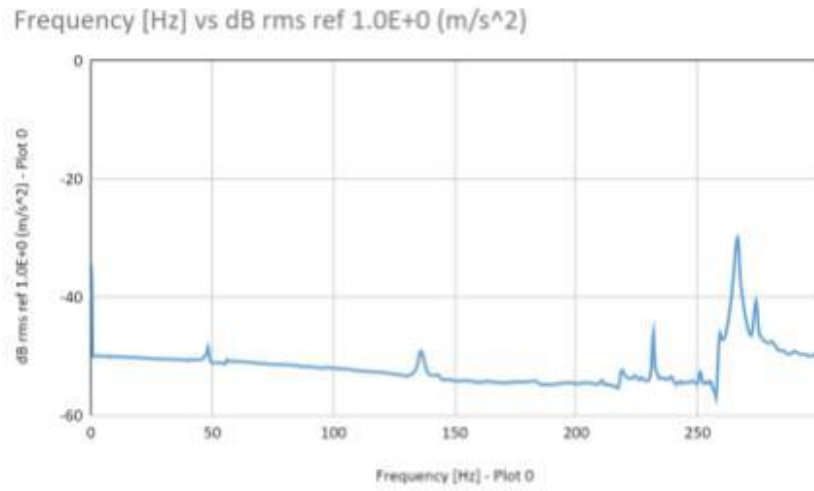
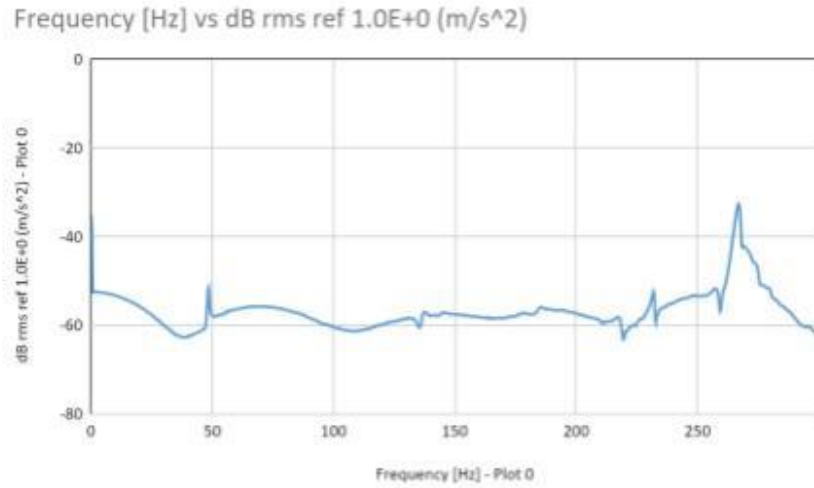


Figure 4.13: Graphs of accelerometer 1; Strike at node 4 (top), strike at node 7 (center), strike at node 11 (bottom)

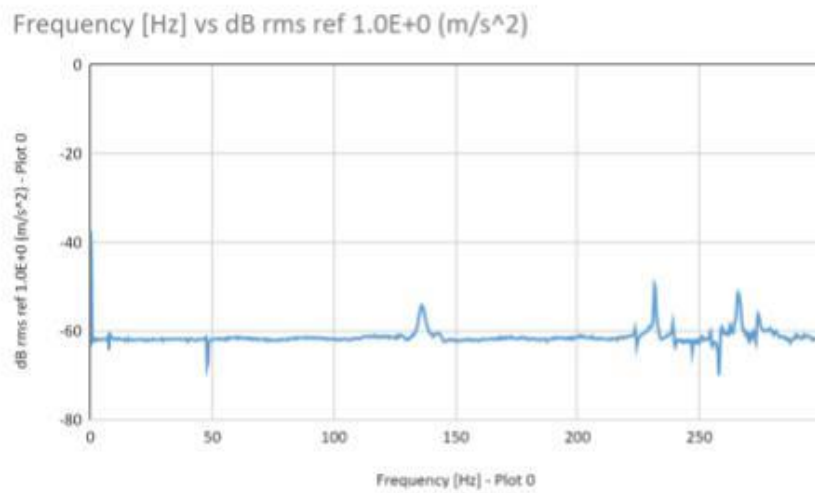
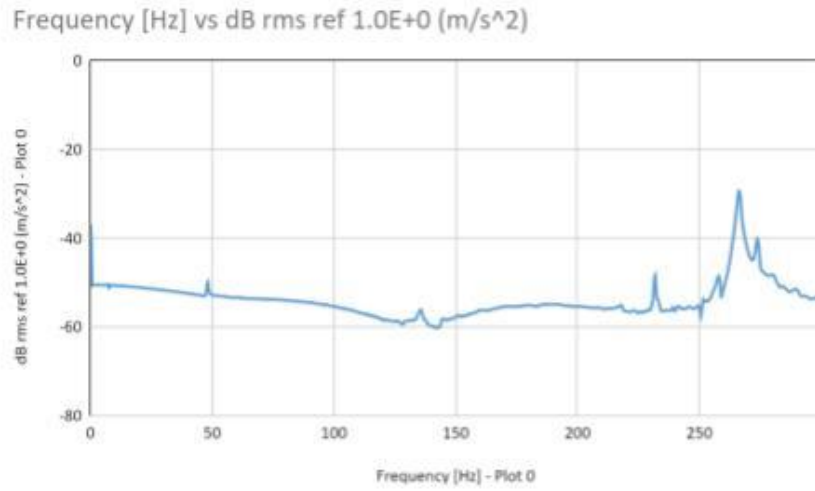
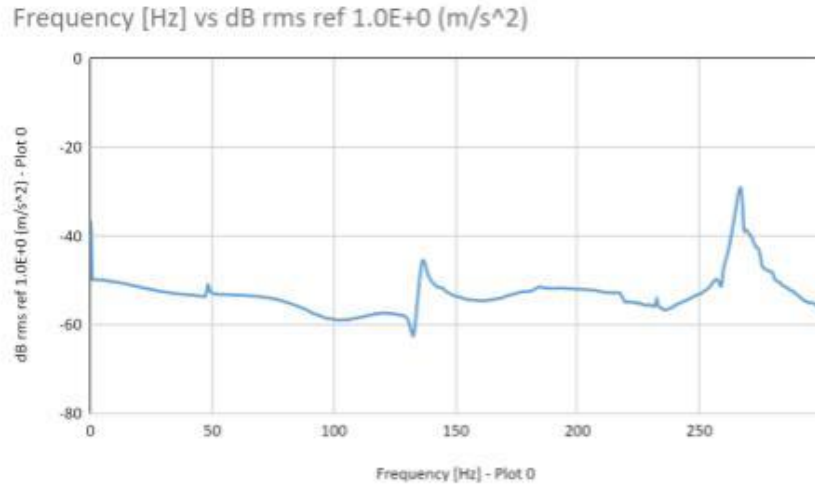


Figure 4.14: Graphs of accelerometer 2; Strike at node 4 (top), strike at node 7 (center), strike at node 11 (bottom)

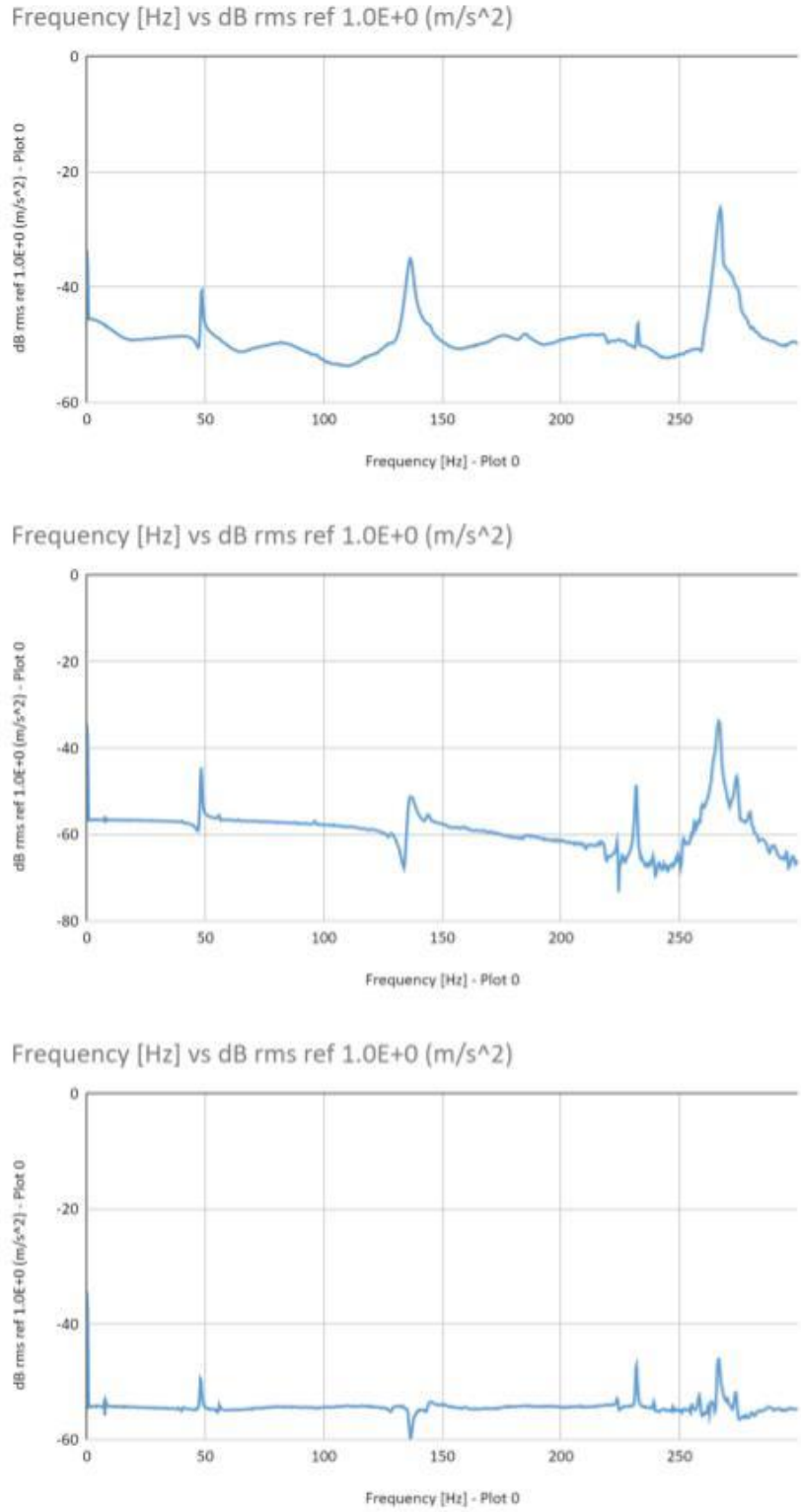


Figure 4.15: Graphs of accelerometer 3; Strike at node 4 (top), strike at node 7 (center), strike at node 11 (bottom)

By analyzing the data from these graphs, it is possible to determine the first five natural frequencies of the beam. This can be done by simply determining which frequencies correspond to the values of the highest peaks and lowest peaks. Through this information it can be deduced that the first five experimental natural frequencies of this beam are: 7.27 Hz, 47.9 Hz, 136.09 Hz, 231.89 Hz, and 266.24 Hz. These natural frequencies differ from the theoretical frequencies that were calculated by using ANSYS. As seen in Table 4.1, the biggest difference is that the frequency near 71.37 Hz that was calculated by ANSYS is not represented in the graphs for the experimental data. This is because at this frequency the beam has an axial bending mode, which causes the beam to move in a plane perpendicular to the direction that the accelerometers measure. If the accelerometers were placed on the lateral face of the beam instead of on the top face, they could better detect the motion at this natural frequency. The first five experimental and theoretical natural frequencies are expressed in Table 4.1 along with the percent error difference.

Table 4.1: Theoretical vs experimental natural frequency comparison

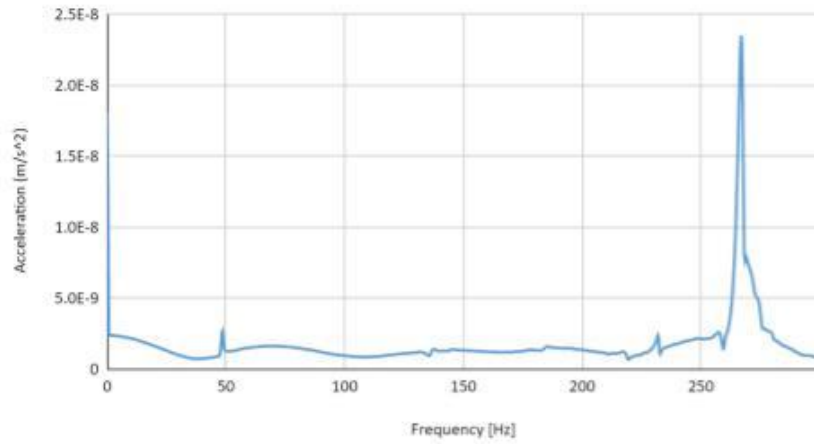
Theoretical Natural Frequency [Hz]	Experimental Natural Frequency [Hz]	Error [%]
8.011	7.27	9.25
50.193	47.9	4.57
71.37	N/A	N/A
140.54	139.09	1.03
230.71	231.89	0.51
275.47	266.24	3.35

From this table it is evident that the experimental natural frequencies line up with what they were predicted to be by ANSYS. The next step in analyzing the data is to determine the mode shapes of the beam. To determine mode shapes, the units of decibels are no longer relevant. Instead, decibels need to be converted back into units of acceleration. This can be done by using equation 4.1 provided below:

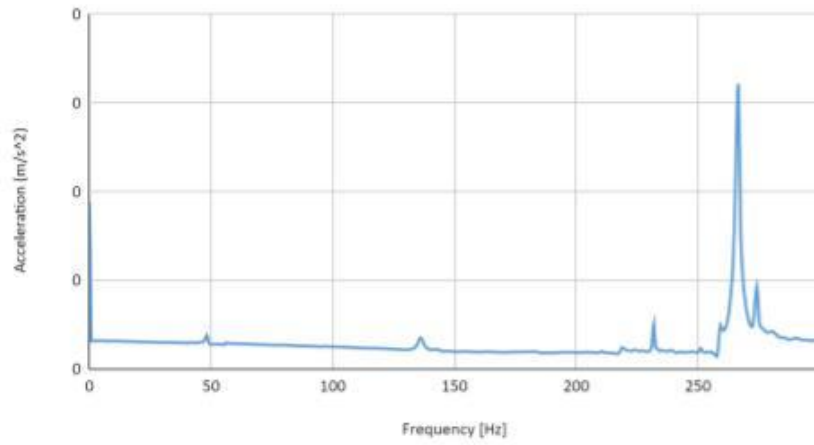
$$a_1 = a_{ref} * 10^{(db/20)} \quad (4.1)$$

Where a_1 = Acceleration, $a_{ref} = 1e-6$, and db = Decibels. Using this equation all values with decibel units can be converted to values with units of acceleration. Applying this equation to the graphs above the graphs for frequency vs acceleration can be obtained. Figures 4.16, 4.17, and 4.18 show these graphs.

Frequency [Hz] vs Acceleration (m/s²)



Frequency [Hz] vs Acceleration (m/s²)



Frequency [Hz] vs Acceleration (m/s²)

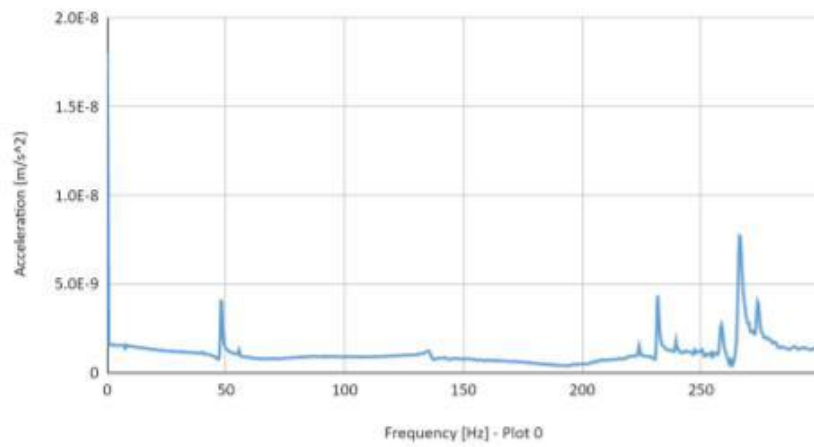


Figure 4.16: Frequency vs acceleration graphs of accelerometer 1; Strike at node 4 (top), strike at node 7 (center), strike at node 11 (bottom)

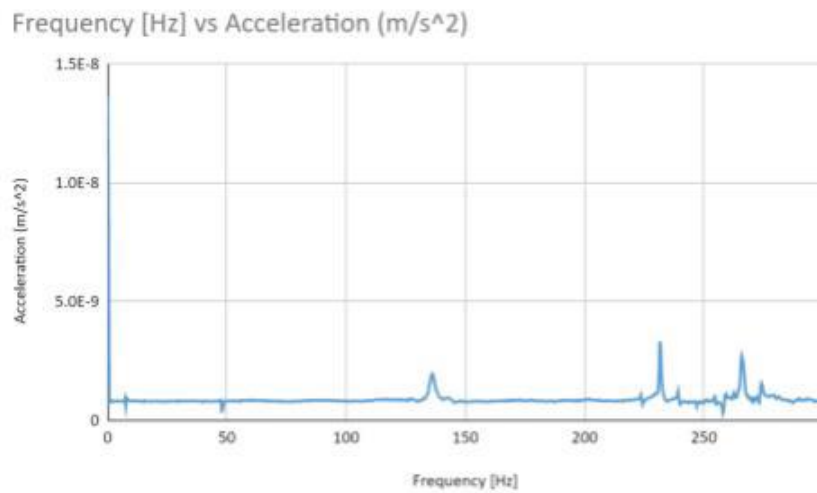
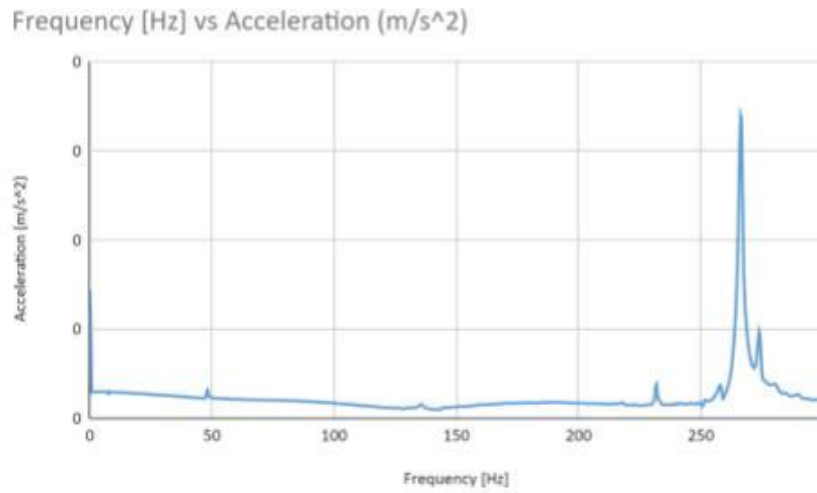
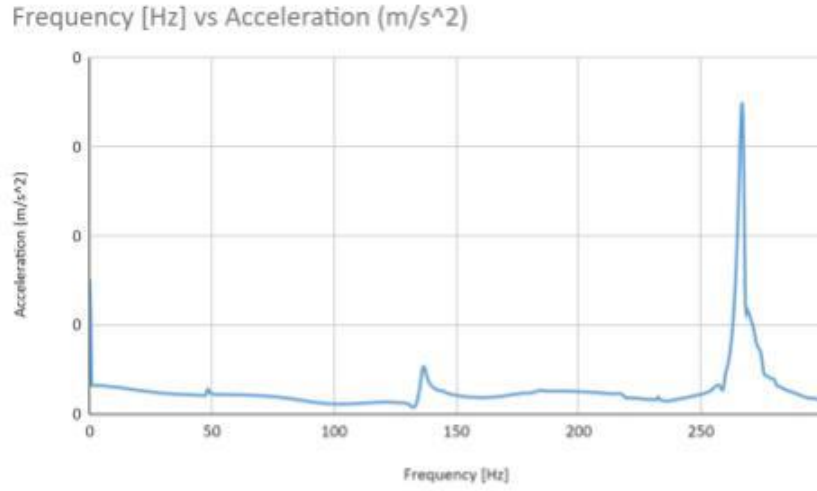
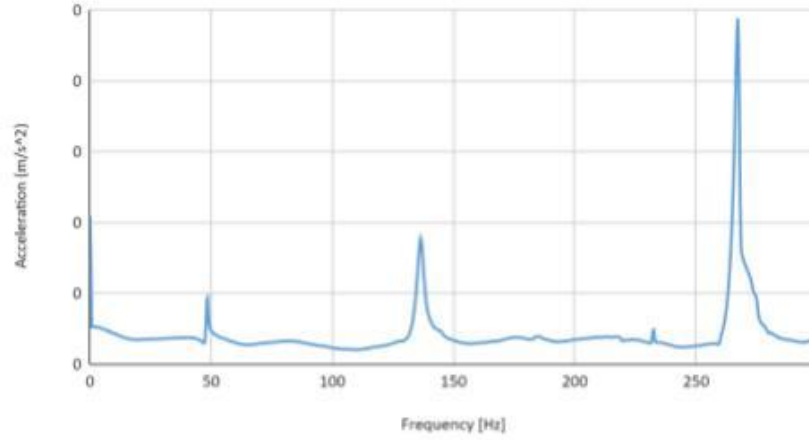
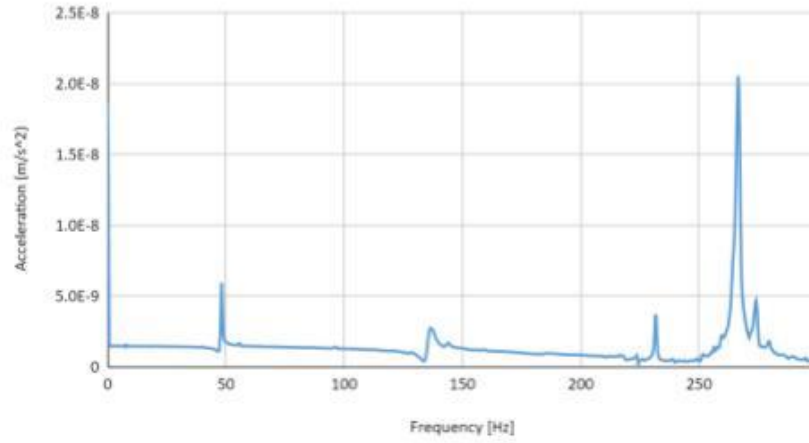


Figure 4.17: Frequency vs acceleration graphs of accelerometer 2; Strike at node 4 (top), strike at node 7 (center), strike at node 11 (bottom)

Frequency [Hz] vs Acceleration (m/s²)



Frequency [Hz] vs Acceleration (m/s²)



Frequency [Hz] vs Acceleration (m/s²)

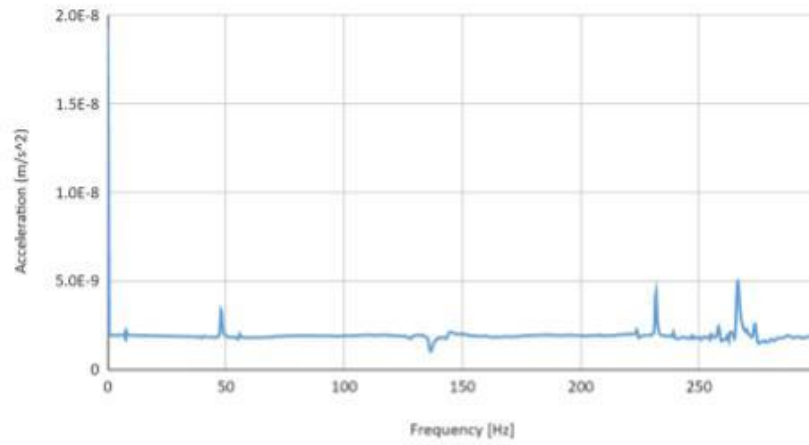


Figure 4.18: Frequency vs acceleration graphs of accelerometer 3; Strike at node 4 (top), strike at node 7 (center), strike at node 11 (bottom)

From these frequency vs acceleration graphs, the absolute value of the acceleration for each accelerometer at each natural frequency needs to be determined. To get the signs associated with each value the raw voltage data needs to be analyzed. These values then need to be plotted against the displacement of each accelerometer from the fixed end of the beam. This will result in five different graphs for each strike. Each graph will have four points, one at representing the acceleration at the fixed end of the beam, one representing the acceleration at Node 6, one representing the acceleration at Node 10, and one representing the acceleration at Node 12. Each graph will show the shape of the beam at a single natural frequency. For the purposes of this paper only the strikes at Node 11 are considered to make the graphs. This is because the Strikes at Node 11 provided the most vibrations to the beam and thus provided clearest results. Figures 4.19-4.23 show the mode shapes at each natural frequency, while tables 4.2-4.6 represent the numerical data graphed.

Table 4.2: Distance from fixed end vs acceleration at first vertical bending mode

Length (m)	Acceleration (m/s ²)
0	0
0.375	9.12e-10
0.563	1.56e-9
0.688	2.07e-9

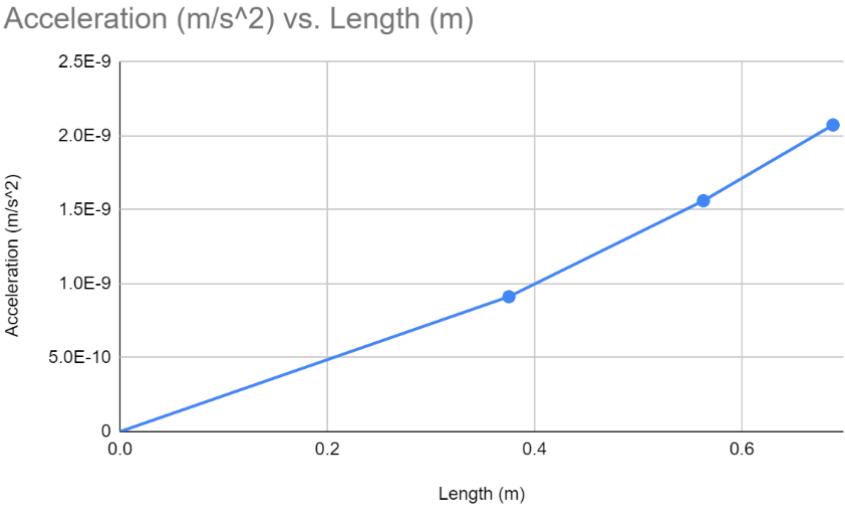


Figure 4.19: Modal shape at first vertical bending mode

Table 4.3: Distance from fixed end vs acceleration at second vertical bending mode

Length (m)	Acceleration (m/s ²)
0	0
0.375272727	4.06e-9
0.5629090905	4.05e-9
0.688	-3.34e-9

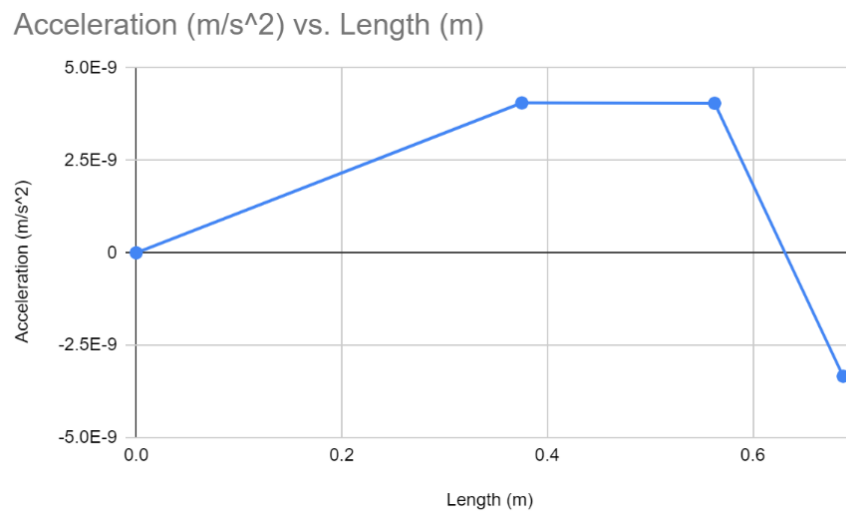


Figure 4.20: Modal shape at second vertical bending mode

Table 4.4: Distance from fixed end vs acceleration at third vertical bending mode

Length (m)	Acceleration (m/s ²)
0	0
0.375272727	-1.06e-10
0.5629090905	1.96e-9
0.688	-1.20e-9

Table 4.6: Distance from fixed end vs acceleration at fourth vertical bending mode

Length (m)	Acceleration (m/s ²)
0	0
0.375272727	-7.71e-9
0.5629090905	2.59e-9
0.688	-4.97e-9

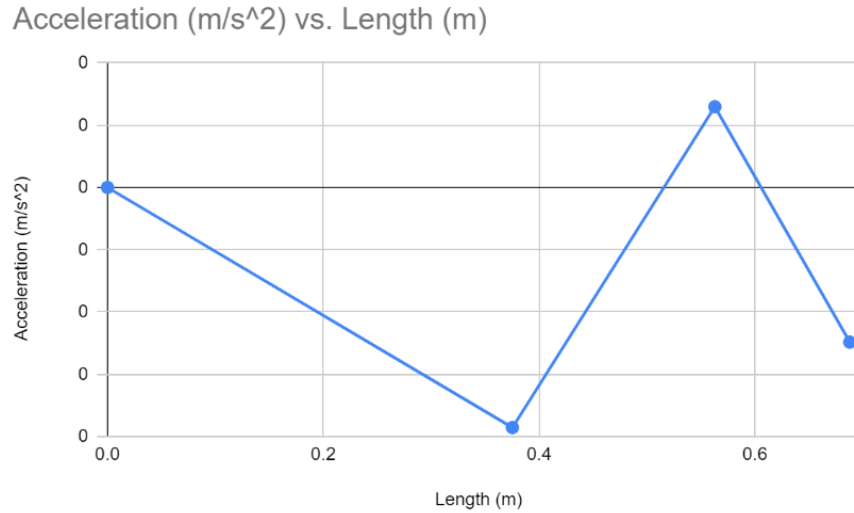


Figure 4.23: Modal shape at fourth vertical bending mode

From these results, it is difficult to tell if the experimental mode shapes are similar to the ones given by ANSYS. Despite the disparity between the results for most of the graphs the individual points on the graph appear to be in the right place.

4.5 Error

In this experiment there are several sources of error, but the two primary ones are human error and error caused by the lack of accelerometers used. Human error played a role in this experiment due to the actuator being an impact hammer. When collecting data to graph LabVIEW used averaging, which means that multiple hits at equally spaced time intervals were required to obtain accurate graphs. Due to the imperfection of human hand-eye coordination hitting the beam in the exact same location every time is near impossible, which could cause slight variations in the final graph outputted by LabVIEW. However, this was potentially mitigated by selecting a high number of averages, 15. Due to this number of averages human error played a much less significant role in the final results. Another key source of error was the number of total accelerometers used. This impacted the experiment by only providing the deflection of the beam at 4 points. If more accelerometers were used, the deflection of the beam could have been seen at more points, which would help to give a more accurate picture of the overall deflection of the beam. With only the 3 accelerometers that were used in this experiment,

only the first three modes can be reasonably determined. The other modes have too much aliasing error, due to the lack of accelerometers along the length of the beam. Other potential sources of error include improper signal filtering and added noise due to faulty components. These sources of error are a lot less impactful than the previously discussed ones, as from the graphs outputted by LabVIEW it is clear that there is hardly any impactful noise added to the system.

5.0 Building a Vibration Absorber

5.1 Vibration Absorber

A vibration absorber is a device that is attached to a system to prevent that system from vibrating. It accomplishes this by absorbing the vibrations imposed on the system, and thus vibrating instead of it. Vibration absorbers are necessary as they prevent a system from being damaged due to excessive vibrations. This is particularly important for systems where the vibrations imposed are variable and change frequently. An example of a system that requires a vibration absorber is a skyscraper. These buildings are so large that any amount of wind can cause vibrations throughout the building. Wind also frequently changes direction and strength, which then cause inconsistent vibration throughout the building. These vibrations can then cause cracks in the support beams of the building which will eventually weaken it enough to cause a collapse. To prevent vibrations from making an impact on the stability of the building a large vibration absorber is used, which prevent major vibrations caused by the wind or disturbances on the ground. An example of a prominent vibration absorber in a skyscraper is the one located within Taipei 101. Another system where vibration absorbers are important are power lines. Wind can cause power lines to vibrate to the point where they can begin to oscillate. This is dangerous as if power lines begin to oscillate a flashover, an electrical discharge over the surface of an insulator, can occur. Due to the large amount of electricity that power lines carry, a flashover can cause serious problems such as forest fires. The oscillations can also cause mechanical failure, leading to the powerlines dropping from the electricity poles that hold them up. This can also lead to fires. Vibration absorbers are also used in machinery. The vibrations that are imposed on a machine by an action that it must perform repetitively can eventually degrade the machine. A vibration absorber can help take the stress off of the parts of the machine and extend its lifetime.

A basic vibration absorber that can operate within a specific bandwidth can also be designed. This form of vibration absorber can be used in machinery that always runs at a constant speed, or a system that has a constant excited frequency [49]. Due to the narrow bandwidth of frequencies that the system is exposed to it is easier to design a vibration absorber in these cases. The principle that a vibration absorber is created on is that the primary system will have force applied on it by the disturbance, which will in turn cause motion. The motion of the system will in turn apply a force to the absorber. As determined by Newton's third law of motion, when the absorber moves it will also apply a force on the primary system. Thus, the system will have two forces acting on it, one force caused by the disturbance, and the other caused by the absorber. These two forces must have a net sum of zero to prevent the primary system from moving. A system with and without a vibration absorber is shown in Figure 5.1.

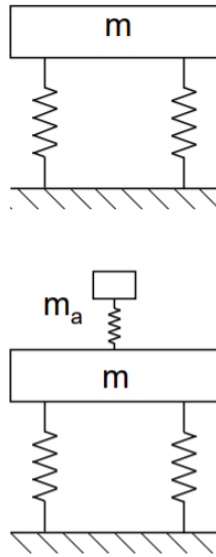


Figure 5.1: System without vibration absorber (top), System with vibration absorber (bottom)

5.2 Vibration Absorber Designs

As discussed in the previous section there are several types of vibration absorbers. There are two types of vibration absorbers, one which are used to absorb vibrations in systems that experience vibrations that occur in a larger bandwidth, and the second which are used to absorb vibration in systems that experience vibrations in a narrow bandwidth. Figure 5.2 and 5.3 show vibration absorbers that fall under the first category, while Figure 5.1 shows an absorber that falls under the second category.

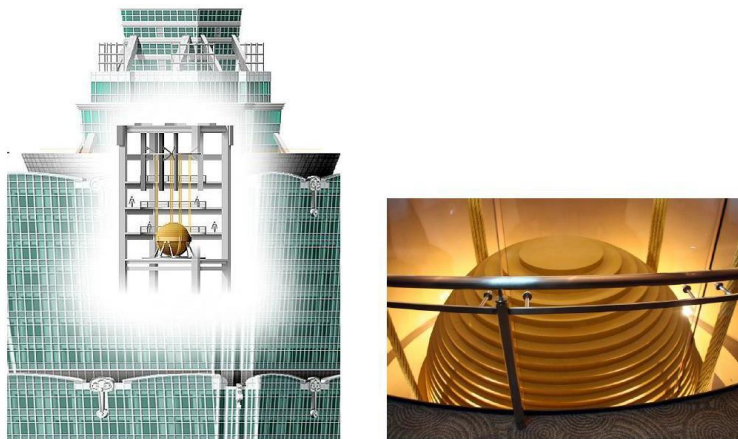


Figure 5.2: Taipei 101 vibration absorber [49]



Figure 5.3: Power line vibration absorber [49]

This paper will focus on designing a vibration absorber that can be used for a system that is exposed to a narrow bandwidth of frequencies. An example of a design of an absorber that can accomplish this is discussed in Bobrovnikskii et al. [3]. This design consists of a primary system represented by a single mass referred to as M_1 . The absorber is also a single mass referred to as M_2 . Both M_1 and M_2 are mounted on rubber gaskets. M_1 and M_2 are then attached by a spring, which has a force sensor attached to it, and M_1 is connected to a shaker. Both M_1 and M_2 then have accelerometers mounted to them. This design is shown in Figure 5.4. 1 is the shaker and M_1 which is referred to as the oscillatory system, 2 is referring to the absorber, 3 is referring to the rubber gaskets, 4 is the shaker, 5 is the accelerometers, and 6 is the force sensor.

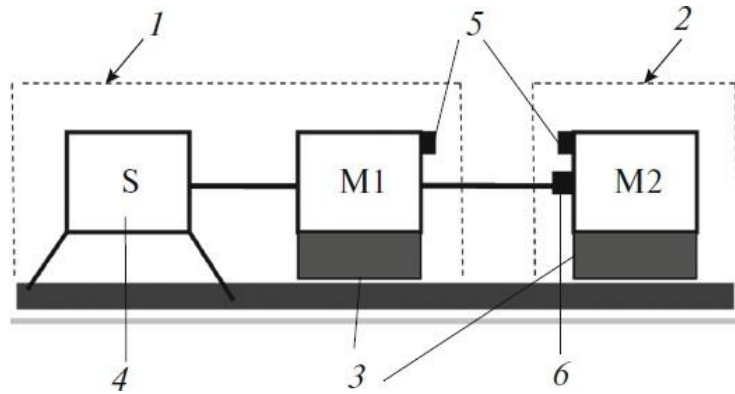


Figure 5.4: Experimental setup of vibration absorber [3]

To ensure that this experiment goes smoothly, one must ensure certain parameters are met[49]. The most important parameter to determine is the frequency at which the amplitude of displacement of the primary system, M1, will be zero. The next parameter to meet is to ensure that the ratio of the mass of the absorber, M2, to the mass of the primary system, M1, is between 0.05 and 0.25. If the ratio is below this range the absorber will be too light to impact the primary system and if the ratio is above this number than the mass of the absorber will be too great and can cause stress and fatigue problems to the primary structure.

5.3 Procedure

The procedure utilized in this paper draws inspiration from several sources but is a unique design.

The first step in this procedure is to obtain two masses, a primary mass, and a mass to act as an absorber. The values for these masses must be chosen in a way where the ratio of the absorber mass to the primary mass is between 0.05 and 0.25.

For the next step of this experiment the same frame designed for the drop calibration experiment that was discussed in Section 3.3.1 is used. The primary mass is mounted to a plate that is then suspended from the frame used suspension cords. Below this mass a spring is attached, from which the second mass dangles. Each mass will have an accelerometer connected to it so that the vibrations of each individual mass can be seen. To cause the masses to vibrate the frame will be manually shaken. A spring was used instead of a rigid support to make the results of the experiment easier to see visually. If a rigid support was connected the experiment would still function the same, however, the results would not be as visually apparent. Figure 5.5 shows a 3-D modeled version of the setup using SolidWorks.

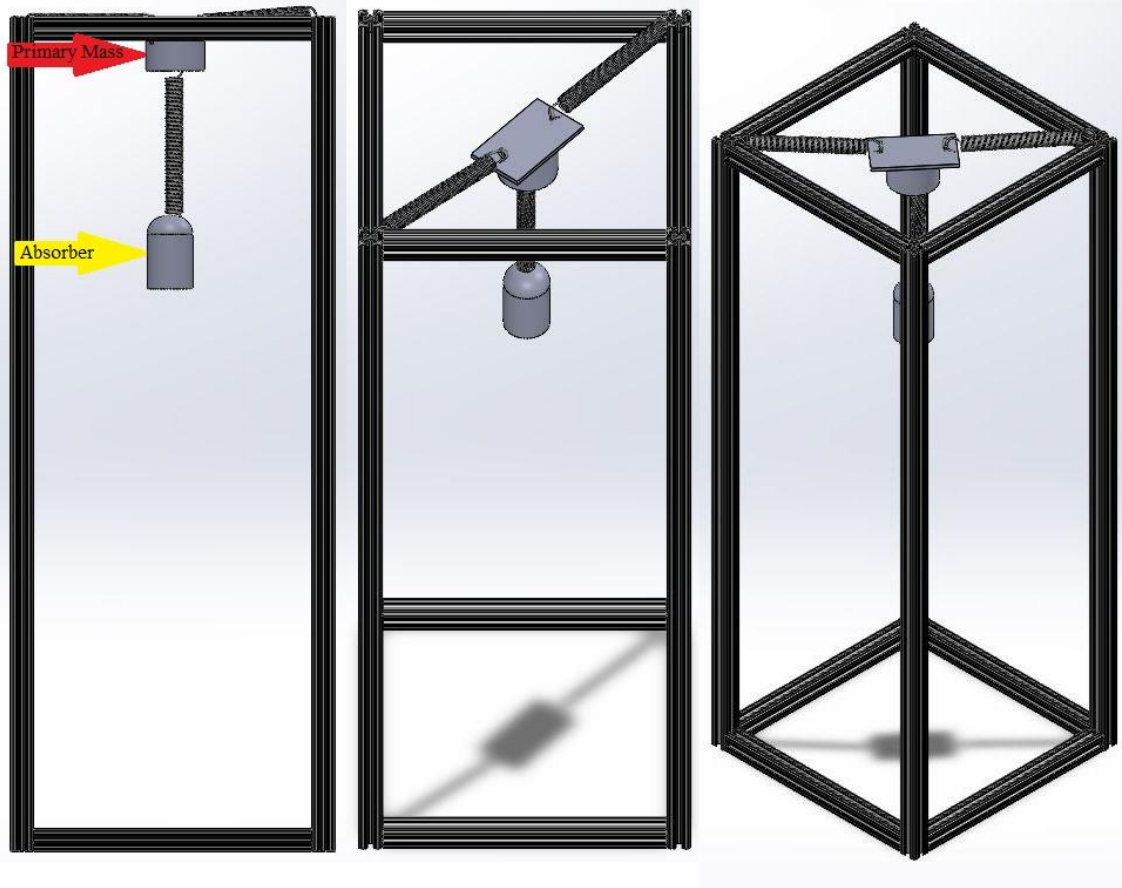


Figure 5.5: Front (left), and two isometric (center, right) views of completed experimental setup

To take measurements of how well the absorber works, first the experiment will be run without the absorber mass connected. After clear data is taken, the absorber mass will be reconnected, and the experiment will be run again. A comparison of the data taken for each experiment will reveal how effective the vibration absorber truly is. This experiment should allow a visual observation of how well the vibration absorber is working, as well as analytical proof.

Figure 5.6 shows the final setup of this experiment.



Figure 5.6: Vibration absorber experiment final setup

5.4 Results

The first part of this experiment was conducted by removing the secondary mass, or vibration absorber, from the system. After removing the absorber, the frame was shaken and the signal from the accelerometer on the primary mass was recorded. Visually, it was evident that the mass was experiencing significant vibration, and the data recorded by LabVIEW confirmed this. The signal of the accelerometer was converted from voltage to acceleration by dividing the output signal by the listed sensitivity. Figure 5.7 shows the graph of the acceleration of the primary mass without the vibration absorber.

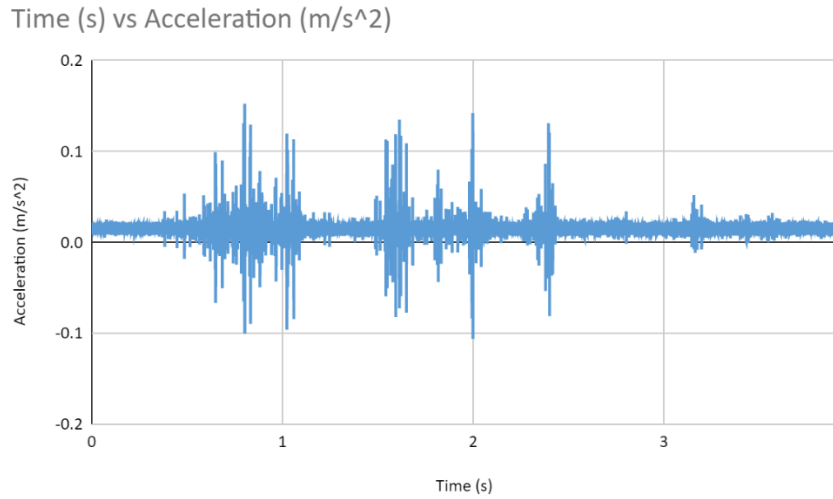


Figure 5.7: Acceleration of primary mass before vibration absorber

Once the results were obtained, the absorber was connected with a spring to the primary mass. The frame was shaken again and the readings from the accelerometers on both the primary mass and absorber were taken. Visually, it was clear that the primary mass was experiencing less vibration than the absorber. Figures 5.8 and 5.7 show the acceleration readings of the primary mass and the absorber respectively.

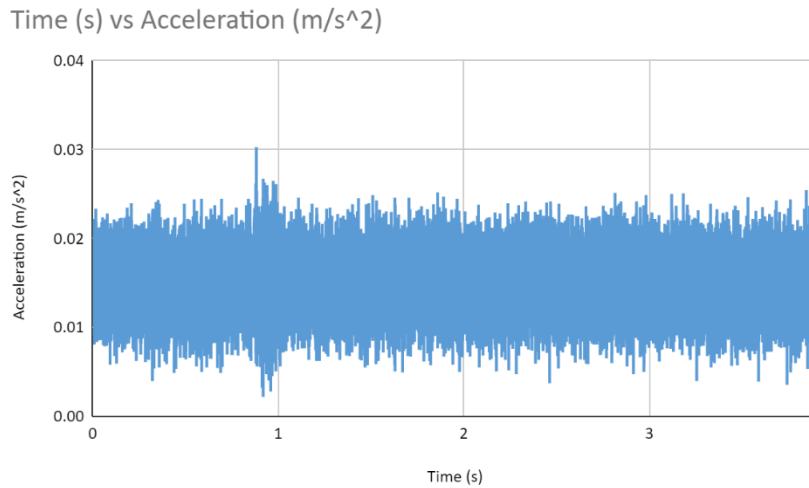


Figure 5.8: Acceleration of primary mass with vibration absorber

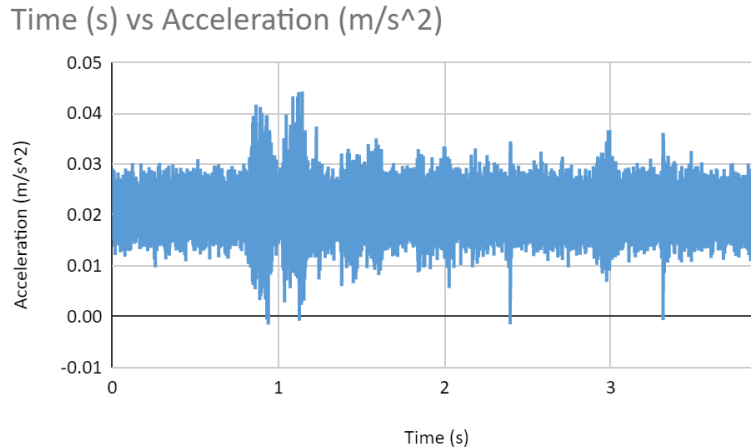


Figure 5.9: Acceleration of vibration absorber

From these graphs it can be observed that in the system with the vibration absorber the primary mass undergoes less acceleration than the absorber undergoes more acceleration. Upon further calculation, there is a 46.27% difference in peak acceleration of the primary mass versus the peak acceleration from the absorber mass, which makes it clear that the absorber is undergoing significantly more acceleration than the primary mass. From these results, it can be confidently seen that the vibration absorber is indeed absorbing vibrations from the primary mass.

5.5 Error

The biggest potential source of error in this experiment is the fact that tape was used to combine two masses. This needed to be done due to the fact that there was no available combination of masses that fit the necessary mass ratio of between 0.05 and 0.25 because all of the available masses were too close in weight. To combat this, the two heaviest masses were combined with tape, and that joined mass was used as the primary mass, while the smallest available mass was used as the absorber. These masses provided a mass ratio of 0.25, which was perfect for the experiment. The reason tape can introduce error, however, is that it restricts vibrations. For this reason, it is possible that the measured accelerations were not entirely accurate. Despite this error, the success of the vibration absorber was still valid as even with the tape the experiment functioned as expected. Another source of potential error comes from the fact that the shaking was not consistent between trials. Because the shaking was done manually, there was no way to ensure the vibrations being imposed on the system were equal each and every time. One way to combat this gap in knowledge in the future is to add a third accelerometer which measures the frame's acceleration. This addition will make it so the differences in the shaking can be seen by analyzing the results of this third accelerometer. This way if there is a 20% reduction in shaking between the two experiments a 20% reduction in vibration will be expected in the primary mass. If the vibration reduction is greater than 20% it will be clear that the vibration absorber is working. Luckily, it was visually clear that despite these inaccuracies the absorber was clearly working.

6.0 Conclusion

6.1 Summary

In this paper three different vibration experiments were designed and conducted. The three experiments were conducting drop calibration of an accelerometer, measuring frequencies and modes of a beam, and building a vibration absorber. The experiments were designed for students returning to campus after the Covid-19 pandemic. Experiments are an important way of supplementing school teaching because they allow students to apply what they have learned in a more real world setting. These specific experiments were chosen as they provide a great deal of understanding about how to apply theoretical knowledge about vibrations, and they also introduce students to several key pieces of equipment that they will need to utilize in future careers.

While working on and conducting these experiments, there were several lessons to be learned. The most prominent lesson learned was that even though an experimental design may appear to work on paper, when in the lab there are several factors that can cause the design to change. For example, if a piece of equipment that was used in a design fails to work correctly, the entire design may need to be changed on the spot. For this reason, flexibility, and the ability to adjust on the fly is very important when designing one's own experiments. Another key lesson learned was to always find several research papers on a subject. This is important as when designing an experiment, it is not usually possible to completely follow a paper due to equipment constraints, budget restrictions, or unclear steps in the design. As a result, having several papers to refer to is important so that gaps in a design can be more easily filled and an experiment that is possible to conduct with the resources available can be designed.

6.2 Future Work

Future work that builds off of what was done in this paper, includes refining the design of the experiments, and implementing them in a classroom setting. As discussed, for each experiment there were a few sources of error that may have caused results that were slightly incorrect. An example of this error can be found in the design of the determining frequencies and modes of a beam experiment. In Section 4.5 it is mentioned that the number of accelerometers used in the experiment is too few. This is a good example of a design flaw that needs to be changed before the experiments can be conducted by students. The lack of accelerometers on the beam gives a very unclear picture of the modes of the beam, so the results from this experiment are flawed. Another example of a design flaw is seen in the vibration absorber experiment. Due to the masses provided not fitting the mass ratio, two masses needed to be combined with tape. Tape can cause several errors in vibration based experiments because it reduces vibration across the body that it is on. In the future this experimental design needs to be edited by either obtaining masses that fit the mass ratio required or by combining the masses in a different way. An aspect that can be incorporated into the drop calibration experiment in the future is measuring the length of the springs at the resting point of the system. This would be helpful as with this length calculations can be done to determine if the jump in the signal during the second oscillation corresponds to what one would theoretically expect or not. This would help decrease the error in the experiment. Finally, in the vibration absorber experiment an accelerometer must be placed on

the frame in order to measure the acceleration of the manual shake. As touched upon previously, this would help indicate the difference in the shaking done with and without the absorber. Having a numerical indication of the difference between these two shakes can help more reliably determine if the absorber is working correctly. Without being certain of the difference in the shakes it is difficult to determine if the reduction in vibration of the primary mass is because of the difference in shaker or the vibration absorber.

After optimizing each design to either reduce or completely remove the error discussed for each experiment, these experiments need to be implemented in a classroom setting. This means the finalized designs need to be conducted in a way that several students can work on an experiment simultaneously and complete each experiment within a reasonable time. To accomplish this, several versions of each design need to be built and tested to ensure each is working properly. Once this is accomplished, the experiments can be easily integrated into the class syllabus.

6.3 Lab Guidelines and Procedure

This section will give a brief introduction to each experiment and a more simplified procedure for the students.

6.3.1 Drop Calibration

Drop calibration is a way to calibrate accelerometers by measuring the signal they output while they are in free-fall. This outputted signal can be divided by the acceleration due to gravity of Earth, which will provide the sensitivity of the accelerometer. In this experiment an apparatus will be used to conduct the drop calibration.

- I. Screw the screw eyes into the provided plate.
- II. Attach the provided drop weight to the plate.
- III. Mount the magnetic hooks onto the apparatus.
- IV. Attach one end of the spring to the hook and the other to a screw eye. Repeat for both springs.
- V. Attach one end of a coaxial cable to the acquisition system and other to the accelerometer being calibrated.
- VI. Use the provided wax to mount the accelerometer to the drop weight hanging from the plate.
- VII. Set up LabVIEW to record the output signal from the accelerometer in mV.
- VIII. Hit the top of the plate with an impact hammer to initiate the drop.
- IX. After LabVIEW is done taking the data, trim the graph so that only the free-fall portion is visible.

- X. Export the data to Excel and find the numerical value of the outputted signal.
- XI. Finally, divide the value by either 9.81 m/s^2 or 1 g. The resulting value is the sensitivity of the accelerometer.

6.3.2 Obtaining Frequencies and Modes of a Beam Experimentally

While it is possible to calculate the frequencies and modes of a beam theoretically, it is important to find the true frequencies and modes. This is necessary because there will be subtle differences between the theoretical and true values. While these subtle differences do not impact much in the classroom, in a real world setting these differences may be enough to cause serious errors. The only way to determine the true frequencies and modes of a system is to do so experimentally. The beam selected for this experiment is a steel cantilever beam with a thickness of 0.005 m, width of 0.045 m, length of 0.688 m, density of 7850 kg/m^3 , and young's modulus of 160 GPa. The beam is clamped on one end and free on the other.

- I. Divide the beam into 11 equal subsections using measuring tape.
- II. Label the 12 resulting nodes from 1-12 in order, 1 being the fixed end and 12 being the free end
- III. Use the provided wax to add an accelerometer to all nodes except nodes 1, 4, 7, and 11. Place each accelerometer at varied positions on each node. This is done so that torsional nodes can be seen more clearly.
- IV. Connect each accelerometer to the acquisition system using a coaxial cable.
- V. Setup LabVIEW using the sound and vibration toolkit to acquire signals from all three accelerometers simultaneously.
- VI. Setup LabVIEW to have an acquisition frequency of 0.1 Hz and to take 15 total averages. Set it so that each average is taken every 10 seconds.
- VII. Ensure that for each accelerometer a graph is being taken in raw voltage and in dBs.
- VIII. Conduct a trial where an impact hammer is used to strike node 4. Strike node 4 every 10 seconds 15 times.
- IX. Save the resulting graphs outputted for each accelerometer to Excel.
- X. Conduct a trial where an impact hammer is used to strike node 7. Strike node 7 every 10 seconds 15 times.
- XI. Save the resulting graphs outputted for each accelerometer to Excel.
- XII. Conduct a trial where an impact hammer is used to strike node 11. Strike node 11 every 10 seconds 15 times.

- XIII. Save the resulting graphs outputted for each accelerometer to Excel.
- XIV. For each of the nine resulting graphs with dBs as their y-axis use the formula: $a_1 = a_{ref} * 10^{(db/20)}$ to convert the graphs y-axis from dBs to acceleration. These graphs will provide the natural frequencies of the beam.
- XV. Using these graphs of frequency versus acceleration find the absolute values of acceleration at each natural frequency for each accelerometer.
- XVI. Next use the nine graphs of raw voltage to determine the signs of these values.
- XVII. Finally, plot the values of acceleration of each accelerometer at each natural frequency versus the distance away from the fixed point of each accelerometer. This should provide the modes of the beam.

6.3.3 Building a Vibration Absorber

A vibration absorber is a device used to absorb vibrations from a structure. Vibration absorbers work by taking the vibration from a structure and vibrating instead of the structure. These devices are used in structures that tend to be exposed to serious vibrations, such as skyscrapers and telephone wires. They prevent damages and failures by ensuring that the structures themselves do not vibrate excessively. In this experiment a basic vibration absorber will be constructed to show how they work in the real world.

- I. Screw the screw eyes into the provided plate.
- II. Select a primary mass and an absorber mass that have a ratio of absorber mass to primary mass of around 0.25.
- III. Attach a screw eye to the bottom of the primary mass and another to the top of the secondary mass.
- IV. Attach the primary mass to the plate.
- V. Attach a suspension cord to both screw eyes in the plate and hang each from the top of the frame.
- VI. Use wax to attach an accelerometer to the primary mass and the frame.
- VII. Attach each both accelerometers and a third one to the acquisition system using coaxial cables.
- VIII. Setup LabVIEW to display the output signal, in acceleration, graphically of three accelerometers.
- IX. Shake the frame.
- X. Export the graphs of the accelerometer attached to the frame and the accelerometer

attached to the primary mass to Excel.

- XI. Attach a spring to the screw eye on the bottom of the primary mass.
- XII. Attach the other end of the spring to the screw eye on the top of the absorber.
- XIII. Shake the frame.
- XIV. Export the graphs of the accelerometer attached to the frame, the accelerometer attached to the primary mass, and the accelerometer attached to the absorber to Excel.
- XV. Compare the graphs of the accelerometer attached to the frame and determine the difference in maximum acceleration.
- XVI. Compare the difference between the maximum acceleration in the graphs of the accelerometer attached to the primary mass. See if this change in acceleration is comparable to the result from the previous step or if it is much different. If it is different, that is proof that the absorber is working.
- XVII. Finally, compare the maximum acceleration of the absorber to the maximum acceleration of the primary mass when the absorber is attached. The absorber's acceleration should be significantly higher.

References

- [1] Lu, N., Lu, C., Yang, S., and Rogers, J., “Highly Sensitive Skin-Mountable Strain Gauges Based Entirely on Elastomers,” *Advanced Functional Materials*, vol. 22, no. 19, 2012, pp. 4044–4050.
- [2] Krelle, A., “Drop Calibration of Accelerometers for Shock Measurement,” *Defense Science and Technology Organisation*, Aug. 2011.
- [3] Bobrovnitskii, Y. I., Morozov, K. D., and Tomilina, T. M., “Impedance approach to designing efficient vibration energy absorbers,” *Acoustical Physics*, vol. 63, 2017, pp. 141–147.
- [4] Mao, Y.-M., Guo, X.-L., and Zhao, Y., “Experimental Study of Hammer Impact Identification on a Steel Cantilever Beam,” *Experimental Techniques*, vol. 34, no. 3, 2009, pp. 82–85.
- [5] Magee, C. L., and Frey, D. D., “Experimentation and its Role in Engineering Design: Linking a Student Design Exercise to New Results from Cognitive Psychology,” *Int. J. Engng Ed.*, vol. 21, no. 3, 2006.
- [6] Magin, D., and Kanapathipillai, S., “Engineering students' understanding of the role of experimentation,” *European Journal of Engineering Education*, vol. 25, no. 4, 2000, pp. 351–358.
- [7] Frederick, P. J., “Student involvement: Active learning in large classes,” *New Directions for Teaching and Learning*, vol. 1987, no. 32, 1987, pp. 45–56.
- [8] Taras, L. B., “Promoting Student Involvement with Environmental Laboratory Experiments in a General Microbiology Course,” *Microbiology Education*, vol. 4, no. 1, May 2003, pp. 23–29.
- [9] Winkler, R. L., and Murphy, A. H., “Experiments in the laboratory and the real world,” *Organizational Behavior and Human Performance*, vol. 10, no. 2, 1973, pp. 252–270.
- [10] Onyema, E. M., Eucheria, N. C., Obafemi, F. A., Sen, S., Atonye, F. G., Sharma, A., and Alsayed, A. O., “Impact of Coronavirus Pandemic on Education,” *Journal of Education and Practice*, vol. 11, no. 13, May 2020.
- [11] Lundstedt, T., Seifert, E., Abramo, L., Thelin, B., Nyström, A., Pettersen, J., and Bergman, R., “Experimental design and optimization,” *Chemometrics and Intelligent Laboratory Systems*, vol. 42, 1998, pp. 3–40.
- [12] Inman, D. J., and Singh, R. C., *Engineering Vibrations*. Harlow, Essex: Pearson Education Limited, 2014.
- [13] Damjanovic, D., “Ferroelectric, dielectric and piezoelectric properties of ferroelectric thin films and ceramics,” *Reports on Progress in Physics*, vol. 61, no. 9, 1998, pp. 1267–1324.

- [14] Lin, H.-C., and Ye, Y.-C., “Reviews of bearing vibration measurement using fast Fourier transform and enhanced fast Fourier transform algorithms,” *Advances in Mechanical Engineering*, vol. 11, 2019, p. 168781401881675.
- [15] Peeters, B., Debille, J., Climent, H., and Hendricx, W., “Modern Solutions for Ground Vibration Testing of Small, Medium and Large Aircraft,” *SAE International Journal of Aerospace*, vol. 1, no. 1, 2008, pp. 732–742.
- [16] Göge, D., “Automatic updating of large aircraft models using experimental data from ground vibration testing,” *Aerospace Science and Technology*, vol. 7, no. 1, 2003, pp. 33–45.
- [17] Govers, Y., Sinske, J., Schwochow, J., Jelcic, G., Buchbach, R., Springer, J., and Boeswald, M., “Efficient ground vibration testing of aircraft based on output-only modal analysis during taxi,” *58th AIAA/ASCE/AHS/ASC Structures, Structural Dynamics, and Materials Conference*, 2017.
- [18] Kolaini, A. R., Tsuha, W., and Fernandez, J. P., “Spacecraft vibration testing: Benefits and potential issues,” *Advances in Aircraft and Spacecraft Science*, vol. 5, no. 2, 2018, pp. 165–175.
- [19] Poncelet, F., Kerschen, G., and Golinval, J. C., “In-orbit vibration testing of spacecraft structures,” *University of Liège, Aerospace and Mechanical Engineering Department*, 2008.
- [20] Mulkey, H. W., Maynard, A. P., and Anflo, K., “Green Propulsion Advancement and Infusion,” *2018 Joint Propulsion Conference*, 2018.
- [21] Ali, A., Sandhu, T., and Usman, M., “Ambient vibration testing of a pedestrian bridge using low-cost accelerometers for SHM applications,” *Smart Cities*, vol. 2, no. 1, 2019, pp. 20–30.
- [22] Love, J. S., Haskett, T. C., and Morava, B., “Effectiveness of dynamic vibration absorbers implemented in tall buildings,” *Engineering Structures*, vol. 176, 2018, pp. 776–784.
- [23] Fuller, C. R., Maillard, J. P., Mercadal, M., and von Flotow, A. H., “Control of Aircraft Interior Noise Using Globally Detuned Vibration Absorbers,” *Journal of Sound and Vibration*, vol. 203, no. 5, 1997, pp. 745–761.
- [24] Banerjee, J. R., “Modal analysis of sailplane and transport aircraft wings using the dynamic stiffness method,” *Journal of Physics: Conference Series*, vol. 721, 2016, p. 012005.

- [25] *Home*. Harga Electrolab Sieve Analysis Shaker - Buy Harga Sieve Shaker, Electrolab Sieve Shaker, Sieve Analysis Shaker Product on Alibaba.com. (n.d.). https://www.alibaba.com/product detail/Harga-electrolab-sieve-analysis-shaker_62519861524.html.
- [26] Tiwari, N., Puri, A., and Saraswat, A., “Lumped parameter modelling and methodology for extraction of model parameters for an electrodynamic shaker,” *Journal of Low Frequency Noise, Vibration and Active Control*, vol. 36, no. 2, 2017, pp. 99–115.
- [27] Lee, C. K., Lin, C. T., Hsiao, C. C., and Liaw, W. C., “New Tools for Structural Testing: Piezoelectric Impact Hammers and Acceleration Rate Sensors,” *Journal of Guidance, Control, and Dynamics*, vol. 21, no. 5, 1998, pp. 692–697.
- [28] Gil, P., and Strzelczyk, P., “Performance and efficiency of loudspeaker driven synthetic jet actuator,” *Experimental Thermal and Fluid Science*, vol. 76, 2016, pp. 163–174.
- [29] “Piezo actuators: Types and applications,” *Types And Applications - Piezo Actuators / APC International*. [Online]. Available: <https://www.americanpiezo.com/piezo-theory/actuators.html>. [Accessed: 26-Nov-2021].
- [30] Montalvão, D., “Introduction to sensors and Signal Processing,” *Mechatronics*, 2015, pp. 125–220.
- [31] “Measuring Strain with Strain Gages,” *NI*, 15-Jul-2020. [Online]. Available: <https://www.ni.com/en us/innovations/white-papers/07/measuring-strain-with-strain-gages.html>. [Accessed: 30-Jun-2021].
- [32] *What is a Strain Gauge Rosette?* HBM. (2020, October 7). <https://www.hbm.com/en/7330/what-is-a-strain-gauge-rosette/>.
- [33] *45°/90° Strain Gages, 3-Element*. Omega Engineering. (n.d.). https://in.omega.com/pptst/SGD_3-ELEMENT45-90.html.
- [34] Cimballa, J. M., “Stress, Strain, and Strain Gages.” Penn State University, University Park, 24-Oct-2013.
- [35] Engineering, O., “Load Cells & Force Sensors,” <https://www.omega.com/en-us/>, 14-Oct-2020. [Online]. Available: <https://www.omega.com/en-us/resources/load-cells>. [Accessed: 30-Jun-2021].

- [36] Khan, G. A., “Strain Gauge Load Cell,” *Inst Tools*, 19-May-2019. [Online]. Available: <https://instrumentationtools.com/strain-gauge-load-cell/>. [Accessed: 30-Jun-2021].
- [37] Beberniss T. J., and Ehrhardt, D. A., “High-speed 3D digital image correlation vibration measurement: Recent advancements and noted limitations,” *Mechanical Systems and Signal Processing*, vol. 86, 2017, pp. 35–48.
- [38] *Digital Image Correlation (DIC)*. Analytical Technologies AGOC. (n.d.). <https://analyticalonline.com/digital-image-correlation-dic.html>.
- [39] Chen, D.-M., Xu, Y. F., and Zhu, W. D., “Identification of damage in plates using full-field measurement with a continuously scanning laser Doppler vibrometer system,” *Journal of Sound and Vibration*, vol. 422, 2018, pp. 542–567.
- [40] Swenson, E. D., Sohn, H., Olson, S. E., & Desimio, M. P. (2010). A comparison of 1D and 3D laser vibrometry measurements of Lamb waves. *Health Monitoring of Structural and Biological Systems 2010*. <https://doi.org/10.1117/12.847362>
- [41] “Scanning Vibrometers,” *Laser Doppler Vibrometers*. [Online]. Available: <https://www.optomet.com/products/scanning-vibrometers/>. [Accessed: 30-Jun-2021].
- [42] Venugopal, S. K. (2018). *Robot assisted 3D vibrometer measurements with one vibrometer* (thesis). Technische Universitat Braunschweig, Braunschweig.
- [43] Poore, M., “Why Low Noise Cables?,” *New England Wire Technologies*, 19-Oct-2017. [Online]. Available: <https://www.newenglandwire.com/why-low-noise-cables/>. [Accessed: 30-Jun-2021].
- [44] Smith, S. W., in *The scientist and engineer's guide to digital signal processing*, San Diego, CA: California Technical Pub., 1997, pp. 261–276.
- [45] “What is Sensor Calibration and Why is it Important?,” *RealPars*, 11-Nov-2020. [Online]. Available: <https://realpars.com/sensor-calibration/>. [Accessed: 16-Jul-2021].
- [46] “The Basics of Accelerometer Calibration.” PCB Piezotronics, 07-Sep-2012. [Online]. Available: <http://modalshop.com/filelibrary/Basics%20of%20Calibration.pdf>
- [47] Peres, M. A., and Sill, R. D., “A New Solution for Vibration Calibration of Accelerometers,” *SAE Technical Paper Series*, 13-November-2006.

[48] Reynolds, G., "Fundamentals of Modal Testing." Agilent Technologies, 01-Aug-2005.
[Online]. Available:
<https://www.modalshop.com/techlibrary/Fundamentals%20of%20Modal%20Testing.pdf>

[49] Chanat, D., "Design of vibration absorbers," *Design of Vibration Absorbers* Available:
<http://pioneer.netserv.chula.ac.th/~anopdana/433/ch62.pdf>.